SORPTION AND DIFFUSION OF ORGANIC PENETRANTS THROUGH STYRENE BUTADIENE RUBBER/ POLY(ETHYLENE-*CO*-VINYL ACETATE) BLENDS

Thesis submitted to

UNIVERSITY OF CALICUT

in partial fulfilment of the requirements for the award of the degree of

DOCTOR OF PHILOSOPHY

in

CHEMISTRY
under the

FACULTY OF SCIENCE

by

PADMINI M.

forwarded

HEAD OF THE DEPARTMENT
DEPARTMENT OF CHEMISTRY
UNIVERSITY OF CALICUT

DEPARTMENT OF CHEMISTRY
UNIVERSITY OF CALICUT

MAY 2007

Certificate

This is to certify that the thesis entitled **'Sorption and Diffusion of Organic Penetrants through Styrene Butadiene Rubber/Poly(ethylene-*co*-vinyl acetate) Blends'** is an authentic record of the research work carried out by **Ms. Padmini M.** under our joint supervision and guidance in partial fulfilment of the requirements for the award of the degree of **Doctor of Philosophy** in **Chemistry** under the Faculty of Science, University of Calicut, Kerala. The work presented in this thesis has not been submitted for any other degree or diploma of any University or Institute. It is also certified that **Ms. Padmini M.** has fulfilled the course requirements and passed the qualifying examination for the Ph.D. degree of the University of Calicut.

Dr. E. Purushothaman

Dr. G. Unnikrishnan

05- 05-2007

Declaration

I hereby declare that the thesis entitled **'Sorption and Diffusion of Organic Penetrants through Styrene Butadiene Rubber/Poly(ethylene-*co*-vinyl acetate) Blends'** is an authentic record of the research work carried out by me under the joint supervision and guidance of **Dr E. Purushothaman**, Professor, Department of Chemistry, University of Calicut, Kerala and **Dr G. Unnikrishnan,** Assistant Professor, Polymer Science and Technology Laboratory, Department of Science and Humanities, National Institute of Technology Calicut, Kerala and that no part of this work has been presented/ reported earlier for any degree or diploma of any University/ Institute.

University of Calicut
05- 05-2007

Padmini M.

Acknowledgements

I offer my prayers before **God Almighty** for giving me the opportunity to undertake this research programme and for the blessings showered upon me.

I express my immense gratitude and indebtedness to my supervising teachers, **Dr. E. Purushothaman,** Professor, Department of Chemistry, University of Calicut, Kerala and **Dr. G. Unnikrishnan**, Assistant Professor, Polymer Science and Technology Laboratory, Department of Science and Humanities, National Institute of Technology, Calicut (NITC), Kerala for suggesting the topic of my research work, for their cordial and inspiring guidance and, the constant encouragement offered to me without which I could not have completed this work. I am also grateful to **Prof. (Dr.) Sabu Thomas**, School of Chemical Sciences, Mahatma Gandhi University, Kottayam for his valuable suggestions.

I extend my sincere thanks to **Prof. (Dr.) K. Krishnankutty**, Head of the Department of Chemistry, University of Calicut, Kerala for providing me with the facilities and co-operation during the course of this work. I take this opportunity to thank the former Heads of the Department of Chemistry, University of Calicut, **Prof. (Dr.) K. K. Aravindakshan**, and **Prof. (Dr). M. P. Kannan** for their inordinate enthusiasm and support during this programme.

I have great pleasure to express my sincere gratitude to **Dr. G. R. C. Reddy**, Director, NITC, Kerala, India. Thanks are also due to the former Directors of NITC **Prof. (Dr.) M. P. Chandrasekharan** and **Prof. (Dr.) S. S. Gokhale** for providing me with the facilities to carry out the work.

I convey my gratitude to **Prof. (Dr.) P. Meenakshikutty**, former Head, DSH, NITC, **Dr. Lisa Sreejith** and **Dr. Soney Varghese,** Lecturers, DSH, NITC, for their support and encouragement given to me.

I am highly thankful to **Dr. Z. A. Zoya**, Principal, Government Engineering College, Calicut, Kerala and to the former Principals, **Dr. K. V. Narayanan**, and **Prof. Rani Thomas** for their co-operation.

I am extremely grateful to my Professors **Dr. S. Madhavan Kutty Nair** and **Dr. Geetha Parameswaran,** former Professors of Department of Chemistry, and **Prof. (Dr.) V. S. Krishnan Nair**, Department of Zoology, University of Calicut, Kerala, for their advice and encouragement given to me during this programme. I also offer my heartfelt thanks to **Prof. A. Parvathy**, former Head, Department of Chemistry, Government Arts and Science College, Calicut, **Prof. C. P. Valsala**, former Principal, Government College, Pattambi, and **Dr. Omana. P. Perumpully**, Head, Applied Science Department, Government Engineering College, Calicut for their sincere and inspiring support extended to me through out my work.

I am thankful to my colleagues, friends and all well wishers for the keen interest they have shown in this work. I am also thankful to **Mr. Hassan Mubbin**, and **Mr. M. Jayachandran**, for their valuable assistance.

I express my thanks to **Ms. M. Louly**, Deputy Director, **Mr. Arjunan Pillai**, JSO, and other members of Common Facility Service Centre, Manjeri, Kerala for providing me with their facilities and help.

My work could not have been completed without the help of my co-researchers, **Dr. A. Sujith, Dr. C. K. Radhakrishnan, Dr. A. P. Haseena, Dr. Priya Dasan,**

Ms. Prajitha Kumari, Mr. B. Ganesh, Ms. Shyla George, Mr. Habeeb Rahiman, Mr. P. A. Sreekumar, Mr. K. C. Manoj, Mr. P. Aneesh and Mr. Suraj Varma, NITC, Kerala, and **Mr. C. Rajesh,** and **Mr. K. Pramod,** Department of Chemistry, University of Calicut, Kerala.

I remember with gratitude the laboratory staff of Applied Science Department, GEC, Calicut and DSH, NITC, Kerala.

I am also thankful to **Mr. V. K. Harish Kumar** for the skill and labour expended in the preparation of this thesis.

Finally, the moral support and constant encouragement extended to me by my husband **Mr. Sreedharan** and my children **Sreekanth, Sreenath, Sreeraj** and **Sithara** are also acknowledged with love and affection.

University of Calicut

05 - 05 -2007

Padmini M.

Glossary of Terms

A_s	Weight of solvent in swollen sample
BIIR	Brominated isobutylene isoprene rubber
C	Concentration of diffusing molecule
CR	Chloroprene rubber
D	Diffusion coefficient
D*	Intrinsic diffusion coefficient
d	Deswollen weight of polymer blend
DCP	Dicumyl peroxide
DSC	Differential scanning calorimetry
DMTA	Dynamic mechanical thermal analysis
DCSBR	Dichlorocarbene modified styrene butadiene rubber
ENR	Epoxidised natural rubber
EPDM	Ethylene propylene diene terpolymer
EPR	Ethylene propylene monomer rubber
EV	Efficient vulcanization
EVASH	Poly(ethylene-*co*-vinyl alcohol-*co*-vinyl mercaptoacetate)
EVA	Poly(ethylene-*co*-vinyl acetate)
E_D	Activation energy
EVOH	Ethylene vinyl alcohol
E	Young's modulus
F	Volume fraction of filler
f	Functionality of a junction in polymer network

FTIR	Fourier transform infrared spectroscopy
ΔG	Gibbs free energy
ΔH	Enthalpy change
HAF	High abrasion furnace
h	Initial thickness of sample
ISAF	Intermediate superabrasion furnace
*i*PP	Isotactic poly(propylene)
*i*PS	Isotactic poly(styrene)
J	Diffusive flux
K_s	Equilibrium sorption constant
k'	First order rate constant
LDPE	Low density poly(ethylene)
MBTS	Mercaptobenzothiazyl disulphide
MEK	Methyl ethyl ketone
M*i*PK	Methyl *iso* propyl ketone
M*n*PK	Methyl *n*-propyl ketone
M_c	Molar mass between crosslinks
$M_{c(aff)}$	Molar mass between crosslinks for affine limit
$M_{c(ph)}$	Molar mass between crosslinks for phantom limit
MPA	Modified poly(amide)
NF	Nanofiltration
NR	Natural rubber
NBR	Acrylonitrile butadiene rubber
N_A	Avogadro number
n_1	Number of solvent molecules

n_2	Number of polymer molecules
P	Permeation coefficient
p	Pressure
PBD	Poly(butadiene)
PC	Bisphenol A poly(carbonate)
PCL	Poly(ε-caprolactone)
PE	Poly(ethylene)
PMMA	Poly(methyl methacrylate)
PP	Poly(propylene)
PPO	Poly(2, 6-dimethyl phenylene oxide)
PS	Poly(styrene)
PVC	Poly(vinyl chloride)
Q_t	Moles of solvent sorbed by 0.1 kg of polymer blend at time 't'
Q_∞	Moles of solvent sorbed by 0.1 kg of polymer blend at equilibrium
R	Universal gas constant
rPS	Recycled expanded poly(styrene)
sPS	Syndiotactic poly(styrene)
S	Sorption coefficient
SAN	Styrene acrylonitrile copolymer
SBR	Styrene butadiene rubber
SEBS	Poly (styrene-b-(ethylene-*co*-butylene)-b-styrene)
SEBS-g-MA	Maleic anhydride grafted poly (styrene-b-(ethylene-co-butylene)-b-styrene)

SEM	Scanning electron microscopy
SMR L	Standard Malaysian rubber light
SDS	Sodium dodecyl sulphate
SRF	Semi-reinforcing furnace
S	Sorption coefficient
ΔS	Entropy change
T	Temperature
TPE	Thermoplastic elastomer
THF	Tetrahydrofuran
t	Time
t_{90}	Optimum cure time
t_{s2}	Scorch time
UF	Ultrafiltration
ULDPE	Ultralow density poly(ethylene)
V_r	Volume fraction of blend in fully swollen sample
V_{rF}	Volume fraction of blend in fully swollen filled sample
V_s	Molar volume of solvent
V_0	Volume of solvent plus polymer
V_{0s}	Volume fraction of solvent
W_1	Initial weight of sample
W_2	Weight of sample at equilibrium swelling
X	Degree of crystallinity
α	Swelling coefficient
β	Lattice constant

χ	Interaction parameter
δ_P	Solubility parameter of polymer
δ_S	Solubility parameter of solvent
ϕ	Volume fraction of polymer blend
γ	Number of effective chains
μ	Number of junctions
ν	Crosslink density
θ	Slope of initial portion of plot of Q_t versus $\sqrt{t}$
ρ_p	Density of matrix
ρ_s	Density of solvent

Contents

Preface

Molecular transport of organic solvents through polymeric materials has been a subject of both technological and fundamental interest for a variety of applications such as food packaging, controlled drug release, reverse osmosis, electrodialysis and mixture separation. A deep knowledge of the behaviour of different polymeric systems in liquid environment is highly essential for developing suitable products for all these applications. The investigation of the transport characteristics of different macromolecular systems such as polymer blends, composites and interpenetrating networks is thus an extremely fascinating field of research.

Styrene butadiene rubber (SBR) is a general purpose multitalented synthetic rubber having high filler loading capacity, good flex resistance, crack-initial resistance and abrasion resistance, which make it useful for several engineering and industrial applications. However, it has poor ageing characteristics. In order to minimize the oxidative degradation of SBR during service at high temperature, it is advisable to blend it with a saturated or lesser unsaturated polymer. Poly(ethylene- *co*- vinyl acetate) (EVA), a semi crystalline polymer, may be considered as a good partner for this purpose as it offers excellent ageing resistance, weather resistance, toughness, chemical resistance and processability. A blend of amorphous SBR and semi-crystalline EVA can give many desirable transport characteristics and mechanical properties. The goal of the present work is to evaluate the transport features of SBR/EVA blends, using different organic liquids, with special reference to the effects of blend ratio, crosslinking systems, fillers and a compatibilizer. The

background, objectives and the results of the investigation have been presented in nine chapters in this thesis.

Chapter 1 gives an overview of the fundamentals of transport phenomena, factors affecting the transport process in polymeric systems, characteristics of polymer blends and the transport features of blend systems. It also presents an account of the earlier reports on the transport features of polymeric systems, especially of polymer blends, and the scope of the present investigation. The details of the materials used and experimental techniques adopted are given in Chapter 2.

Chapter 3 summarises the transport characteristics of SBR/EVA blends, with aliphatic hydrocarbons as penetrants. The sorption and diffusion processes have been examined in terms of blend ratio and penetrant size. The results have been complemented with the observations on the morphology of the blends by using scanning electron microscopy (SEM).

Chapter 4 describes the results of the investigation on the interaction of SBR/EVA blends with chlorinated hydrocarbons. This chapter also deals with the stress-strain properties of the blends under dry, swollen and deswollen conditions.

The effect of a physical compatibilizer viz. dichlorocarbene modified styrene butadiene rubber (DCSBR) on the transport characteristics of the blend systems has been described in Chapter 5. Special attention has been given to the effect of compatibilizer loading. The mechanical properties and the surface morphology of the blends have also been given to support the observations on the transport process.

The barrier properties of SBR/EVA blends reinforced with three different carbon black fillers viz. semi-reinforcing furnace (SRF), high-abrasion furnace (HAF) and intermediate super abrasion furnace (ISAF) have been described in Chapter 6. The extent of reinforcement of fillers in the matrix, which significantly controls the transport phenomenon, has been discussed in terms of Kraus equation.

A comparison between a black filler (intermediate super abrasion furnace, ISAF) and a white filler (silica; Ultrasil VN3), of the same loading, on the transport features of SBR/EVA blends has been discussed in Chapter 7. The results have been explained in terms of the differences in the interaction between the blend components and the filler particles.

A study of the transport behaviour through SBR/EVA filled with a bio- degradable filler viz. chitin has been presented in Chapter 8. A comparison of the sorption behaviour of the samples, with and without chitin, has been done using polar and non-polar solvents viz. de-ionized water, pentane, hexane, and kerosene.

The major findings of the present investigation and the scope of future work have been given in Chapter 9.

Chapter 1

Introduction

Summary

This chapter gives an account of the theory and the factors affecting the sorption and diffusion of small molecules through polymeric systems. The general features of mass transport through polymer blends are presented. Earlier works on the sorption and diffusion of penetrants through macromolecular systems have been highlighted. The aim and scope of the present investigation are also discussed.

1.1 Diffusion through Polymers

The examination of the diffusion and permeation properties of polymers is a topic of immense practical importance in designing food packaging materials [1], solvent reservoirs [2], pervaporators [3], and controlled release devices [4, 5]. Another interesting application where the diffusion characteristics of polymers play a major role is the use of selective permeation through membranes to effect separations. The first systematic description of the permeation process through polymers dates back to 1831, when Mitchell [6] noted that natural rubber membranes allowed the passage of CO_2 faster than H_2 under equivalent conditions.

Significant attention has now been focussed on membrane separation technology, which necessitates the study of sorption, diffusion and permeation of various penetrants through polymeric systems. The advantages of this technology over conventional separation processes are reduced capital cost, lower energy consumption, use of smaller and light weight materials, and lower installation costs due to modular design and simple operations. Another growing area in membrane filtration is nanofiltration (NF). Nanofilters are usually prepared as thin film composite membranes consisting of a thin separating layer containing negatively charged hydrophilic groups attached to ultrafiltration (UF) membrane support. Applications using NF membranes include the demineralization of water and the removal of lignin and related impurities from wood-pulp streams. Membranes can also be used effectively to separate liquid mixtures (water-organic and organic-organic) in competition with the traditional processes such as filtration, adsorption, liquid-liquid extraction, and fractional crystallization. One important membrane operation termed pervaporation uses a pressure drop to separate components from a

liquid mixture on the basis of preferential solubility and diffusivity [7]. Membranes for pervaporation may be dense (homogeneous), asymmetric, or composites consisting of a thin permselective polymeric layer covering a microporous support.

In the medical field, polymeric membranes are used for haemodialysis and controlled drug delivery. Typically, they serve, by selective diffusion, to remove toxins of low to moderate molecular weight from blood, when a damaged kidney can no longer do so. An ideal material for this purpose is cellophane, which can be prepared in the form of small diameter hollow fibres [8]. Controlled drug delivery provides two important applications for the use of polymers in the effective management of medical drugs in the body. First is controlled release thereby a steady therapeutic concentration of the drug is maintained and second is site-directed drug delivery where polymer serves as a carrier to bring the drug to a specific site in the body. The rate of drug release can be controlled by the diffusion reaction. Polymers commonly used for this purpose are polydimethyl siloxane and poly(ethylene- *co*- vinyl acetate) [8].

Many other interesting applications of the transport phenomena through polymers can be cited from literature [9-11]. All these applications highlight the importance of the investigation of the sorption and diffusion processes through macromolecular networks.

1. 2 Fundamentals of Transport Phenomena

Transport of penetrants through a polymer matrix can be explained in terms of sorption, diffusion and permeation phenomena. The diffusion of small molecules through a polymer membrane occurs due to the random motions of individual

molecules [12]. If a concentration gradient is established across some arbitrary reference section in the polymer, a net transport of the penetrant occurs in the direction of decreasing concentration. This phenomenon can be described in terms of Fick's first law of diffusion according to which the flux J (the amount of penetrant passing through a plane of unit area normal to the direction of flow during unit time) in the x-direction of flow is proportional to the concentration gradient $\frac{\partial c}{\partial x}$ as :

$$J = -D\frac{\partial c}{\partial x} \qquad \text{.....1.1}$$

where D is the diffusion coefficient and c the concentration of the diffusing molecule. This equation is applicable when the diffusion is in the steady state.

On the other hand, Fick's second law describes the unsteady state transport process, which is given by the rate of change of the penetrant concentration at a plane within the membrane as:

$$D\frac{\partial^2 c}{\partial x^2} = \frac{\partial c}{\partial t} \qquad \text{.....1.2}$$

This is an ideal case in which the membrane is isotropic and D is independent of distance, time and concentration. Depending on the boundary conditions, there are many solutions available for Equation 1.2.

When the diffusion rate J achieves a steady value (no longer varies with time) a material balance requires that it also be independent of x, in which case Equation 1.1 can be integrated to give,

$$\int_0^h J dx = -\int_{c=c_1}^{c=c_2} D(dc) \qquad \text{.....1.3}$$

$$J = -\frac{1}{h}\int_{c=c_1}^{c=c_2} D(dc) \qquad \text{.....1.4}$$

Equation 1.4 indicates the steady-state diffusion rate which is inversely proportional to the overall membrane thickness h for a given set of boundary conditions. To complete the integration, the variation of D with c must be known. In some systems, the diffusion coefficient does vary with concentration because the van der Waals forces are high between the diffusing molecules themselves and between the diffusing molecules and the polymer chains.

When there are relatively weak intermolecular forces of attraction between the diffusing molecules and the polymer chains, the solubility is low and the polymer structure is not significantly altered. Under these circumstances c can vary without affecting D, and Equation 1.4 then becomes:

$$J = -\frac{D}{h}(c_2 - c_1) \qquad \text{.....1.5}$$

where c_2 and c_1 are the concentrations of the diffusing molecules dissolved at the downstream and upstream polymer-membrane faces respectively. In many cases, it is the pressures or partial pressures p of a gas or vapour above the faces of the polymer film, rather than the surface concentration, which are known. These quantities are related by Henry's law, which states that:

$$C = Sp \qquad \text{.....1.6}$$

where S is the solubility constant for a given penetrant-polymer system.

The combination of Equations 1.5 and 1.6 gives the well-known permeation equation:

$$J = DS\left[\frac{p_1 - p_2}{h}\right] \qquad \text{.....1.7}$$

The product DS is called the permeability coefficient, P, so that

$$P = D.\mathrm{S} \qquad \text{.....1.8}$$

1.3 Factors Affecting Transport Phenomena

The important factors which influence the transport process are briefly discussed in the following sub-sections.

1.3.1 Nature of Polymers

In order to study the transport phenomena through polymeric materials, it is important to understand the features of two principal microstructural conditions of polymers viz. the rubbery and glassy states. In the rubbery state, larger chain segments participate in the diffusion process due to the internal micro-motion of chain rotation and translation as well as vibration. A larger free volume is readily accessible for diffusion in this state. On the other hand in the glassy state, there is restricted chain mobility. Rotation about the chain axis is limited and the motion within the structure is largely vibratory within a frozen quasi-lattice. Polymers of these types are very dense structures, with very little internal viod space. Hence penetrant diffusivities through such a structure are low. In both rubbery and glassy states, these properties can be further modified by the presence of crystalline phase, or by stress induced crystallization. Both crystallization and orientation tend to place additional constraints on the mobility of the amorphous phase through which

diffusion takes place. Also the crystalline phase is usually impermeable, which results in longer and more tortuous diffusion path [13].

The glass transition temperature (T_g) of the polymer has a very marked influence on the transport properties. Polymers with low glass transition temperature possess greater segmental mobility and will have higher diffusivity. For example, the T_g values of polyethylene (PE) and polypropylene (PP) are -125°C and -20°C respectively. PE has a flexible backbone, but in the case of PP, there are $-CH_3$ groups to inhibit the freedom of rotation. Bulky substituent groups hinder chain rotation and therefore raise the T_g. Comparably sized substituent groups with increase in polarity, which may enhance intermolecular interaction, can also elevate T_g. This is illustrated by the T_g data for vinyl polymers given in Table 1.1 [8,14].

Table 1.1 Effect of substituent groups on T_g

Polymer	Substituent group	T_g° (C)
Poly(ethylene)	-H	-125
Poly(propylene)(atatic)	$-CH_3$	-20
Poly(vinyl chloride)	-Cl	89
Poly(acrylo nitrile)	-CN	100
Poly(styrene)	$-C_6H_5$	100

Increasing flexibility of the side group can lower T_g as is evident by the comparison of the chemical structure of poly(methyl methacrylate) (T_g=105 °C), poly(ethyl methacrylate) (T_g= 65 °C) and poly(propyl methacrylate) (T_g= 35 °C). Van Amerongen [15] studied the diffusion and permeability of hydrogen, helium, nitrogen, oxygen, acetylene and cyclopropane through a series of natural and

synthetic rubbers and observed that samples containing larger number of substituent methyl groups had lower diffusion and permeability coefficients. Excellent reports on the diffusion process through many plastics [16-20] and elastomers [21- 25] are available in literature.

1.3.2 Polymer Molecular Weight

The effect of polymer molecular weight on the transport properties is generally found to be very low. Several experimental studies revealed that the diffusion and permeability coefficients were not strongly dependent on the molecular weight of the polymers [26-28].

1.3.3 Crystallinity and Orientation

In crystalline polymers, the crystalline areas act as impermeable barriers to permeants and they force permeant molecules to diffuse along longer path length. Van Amerongen [29] noted a reduction in diffusion, solubility and permeability coefficients with increasing crystalline content for gutta-percha. Brown et al. [30] investigated the diffusion and sorption of small molecules through amorphous and crystalline polybutadienes. They found that, for amorphous polymers (*trans* content less than 70-80 %), the diffusion coefficient at zero penetrant concentration decreased with increase in *trans* content and at *trans* content above 80%, a sudden drop in the diffusion coefficient occured due to the onset of crystallinity. Orientation of the polymer may also affect the permeation behaviour. However, the overall effect is highly dependent upon crystallinity.

1.3.4 Nature of Crosslinks

An uncrosslinked polymer will dissolve in a suitable solvent whereas crosslinked polymer will not. This is due to the covalent chemical bonds formed between the macromolecular chains during vulcanization. However, a crosslinked polymer may admit significant amount of solvents to pass through it and become soft and swell in contact with them. Such swelling is generally reversible and the samples return to their original size on drying [31]. Unnikrishnan and Thomas [32] investigated the effect of nature of crosslinks on the diffusion and transport of aromatic hydrocarbons through natural rubber membranes, vulcanized by four vulcanizing systems viz. conventional, efficient, dicumyl peroxide and a mixture consisting of sulphur and peroxide. It was found that natural rubber crosslinked with CV system absorbed the highest amount of solvent whereas those crosslinked by peroxide system took the lowest, and samples crosslinked by mixed and EV systems exhibited an intermediate behaviour. Poh et al. [33] studied the sorption behaviour of bulk and solution crosslinked natural rubber networks prepared by the irradiation with γ rays. They found that, in benzene solution, crosslinked networks swell more than the corresponding bulk crosslinked networks having the same crosslink density.

1.3.5 Effect of Plasticizers

The addition of plasticizers can result in the neutralization of a part of the intermolecular forces of attraction between the macromolecules of a polymer. Thus they can impart higher freedom of movement between the polymeric macromolecules thereby increasing the flexibility and plasticity of the compounded polymer and hence enhanced penetrant transport. The CO_2 and water vapour

permeabilities of chitosan /poly(vinyl alcohol) blends plasticized with sorbitol and sucrose were investigated by Arvanitoyannis et al [34]. They found that the permeability values increased with increase in plasticizer content. Barrer et al.[35] reported the increase in diffusion coefficients for the transport of hydrogen and neon through poly(vinyl chloride) upon the addition of tricresyl phosphate as a plasticizer. Kazarian et al. [36] observed the diffusion of azo dyes in glassy polymers plasticized by supercritical carbon dioxide. The plasticization increased the polymer free-volume and caused the swelling of the polymer matrix.

1.3.6 Nature of Fillers

The addition of inert fillers may either increase or decrease the permeability depending on their degree of adhesion and compatibility with the polymer. An inert filler which is compatible with the polymer matrix will be impermeable to the penetrant molecules due to the reduction in the free volume and this would create a tortuous path of the penetrant molecule [37]. The measurement of free volume hole property by positron annihilation lifetime spectroscopy (PALS) was carried out for polymer-clay nanocomposite materials, consisting of styrene butadiene rubber (SBR) and layered silicate clay of rectorite and a conventional composite material SBR/N326 (carbon black), by Wang et al. [38]. The PALS, together with differential scanning calorimetry (DSC), results showed that the layered rectorite had a stronger effect on restraining polymer chain mobility, which resulted a decreased fractional free volume and gas permeation than the carbon black fiiler. Lowering of equilibrium swelling in filled samples indicates an excellent filler-matrix adhesion [39]. The effect of the type of carbon black on the interaction between polychloroprene rubber and motor oil was examined by Lawandy and

Botros [40].They found that the interaction constants were not affected by the type of carbon black as long as the mixes contained the same filler concentration and category, whereas the mixes containing the same filler type but different concentrations showed different interaction constants. Many interesting works describing the influence of different types of fillers on the transport process through polymeric systems have been found in literature [41, 42].

1.3.7 Nature of Penetrant

The size and shape of the penetrant molecules also influence the transport behaviour through polymers. An increase in size in a series of chemically similar (homologous series) penetrants generally lead to a decrease in diffusion coefficient due to the increased activation energy needed for diffusion. The decrease in diffusion with increase in penetrant size has been reported by many investigators [43-45]. Hong [46] studied the effect of solvent size on the diffusion process for various solvents with natural rubber and polybutadiene, in terms of free volume theory. Kim et al [47] reported a decrease in equilibrium penetrant uptake with increasing penetrant chain length for the transport of alkanes, from heptane to dodecane, through crosslinked polystyrene. The penetrant's shape also has a noticeable effect on permeability. For instance, flattened or elongated molecules have higher diffusion coefficients than spherical molecules of equal molecular volume [48].

1.3.8. Effect of Temperature

The temperature dependence of transport coefficient such as permeation and diffusion coefficient generally follows the Arrhenius type relation:

$$P = P^* \exp\left[-\frac{E_p}{RT}\right] \quad \text{.....1.9}$$

and

$$D = D_0 \exp\left[-\frac{E_D}{RT}\right] \quad \text{.....1.10}$$

where E_P and E_D denote the activation energy of permeation and diffusion respectively. Likewise, the sorption coefficient follows the analogous Van't Hoff's form for equilibria:

$$S = S_0 \exp\left[-\frac{\Delta H_S}{RT}\right] \quad \text{.....1.11}$$

where ΔH_S is the standard enthalpy change for the sorption process. The E_P and E_D are interrelated as follows:

$$E_p = E_D + H_S \quad \text{.....1.12}$$

The enthalpy of sorption ΔH can be computed by using Van't Hoff's relation as:

$$\log K_s = \frac{\Delta S}{2.303R} - \frac{\Delta H_S}{2.303RT} \quad \text{.....1.13}$$

In this equation, K_S is the thermodynamic sorption constant and ΔS the entropy of sorption.

1.4 Transport Properties of Different Polymeric Systems

1.4.1 Rubbery Polymers

The important characteristics of rubbery polymers are high segmental mobility, and the related availability of free volume between molecules. The presence of free volume and moving chains are favourable for diffusion through them. Garcia et al. [49] gave a correlation between transport properties and free volume through a positron annihilation study in a high barrier polymer and showed that transport

properties could be improved by means of antiplasticizers' addition. Lawandy and Helaly [50] investigated the permeation rate of chloroform in a chloroprene rubber vulcanizate with different carbon black type and loading. They observed an increase in the penetration rate with increase in filler loading. An inverse relationship was noticed between the particle size of carbon black and the penetration rate, at higher degree of equilibrium. This was attributed to the wrinkles formed at the surface of the rubber at high equilibrium swelling. Molecular transport of *n*-alkanes through diol chain-extended polyurethane (PU) membranes in the temperature interval 25-60°C was investigated by Swamy et al.[51]. Sorption experiments were performed gravimetrically and the related coefficients were calculated from Fick's equation. The results showed that the nature and size of interacting *n*-alkane molecules as well as the morphology of the chain-extended PUs played a significant role in the transport process. The activation energy was also calculated using Arrhenius equation.

The interactions of a wide range of organic liquids having a variety of structural/functional groups with polyurethane membranes have been reported [52]. In this study, the effects of temperature, molecular size and the polarity of the solvent on the interactions were examined. Among the solvents used, chlorobenzene exhibited a stronger affinity for polyurethane. Hexane, a symmetrical nonpolar solvent, showed a lower interaction with the PU membrane. Chiang and Sefton [53] used diffusion analysis to investigate the morphology of styrene-butadiene-styrene (SBS) triblock copolymer. Unlike the diffusion process in conventional rubber, they found that the diffusion of cyclohexane vapour in SBS thermoplastic elastomer

exhibited the non- Fickian time-dependent characteristics. The transport behaviour of penetrants through different rubbery polymers has been reported by several other research groups [54-57]. Thomas et al. [58-62] investigated the molecular transport of organic liquids through a number of rubber membranes with special reference to the effects of the nature of crosslinks, penetrant size and temperature.

1.4.2 Glassy Polymers

Glassy polymers are characterized by the presence of hard and brittle moiety with restricted chain mobility and have very little void space (0.2-10 %). Therefore, diffusion in glassy polymers is more complex compared to that in rubbery polymers. The review by Stannet and Hopfenberg [63] described the various glassy state transport anomalies, which include: (a) dual sorption modes even for inert gases; (b) time-dependent boundary conditions for vapour transport; (c) diffusion coefficient characterized by an apparent time dependence; (d) polymer relaxations that provide the rate determining transport step; (e) polymer fracture or micro fracture (crazing) accompanying polymer relaxation. Orchard and Ward [64] reported that when polyethylene tubes were immersed in toluene, a change in weight was obtained. They estimated the diffusion rates from these values and compared the drawn and undrawn tubes of isotopic homopolymer and copolymer feed stocks. The equilibrium uptake values of the drawn tubes were at least three times lower than those of the feed stock with diffusion coefficient reduced by a factor of twelve or more. Later Vrentas and Vrentas [65] evaluated the predictive capabilities of a sorption equation for describing the sorption behaviour of three glassy polymer/penetrant systems.

1.5 Polymer Blends

The blending of two or more polymers has become an increasingly important technique for improving the cost- performance ratio of many commercial products. Polymer blends are physical mixtures of two or more structurally different polymers or co-polymers with no covalent bonds between them. The blending of different polymeric materials is quite attractive due to the fact that some already existing polymers can be used for it to meet a specific requirement and thus the costly development of new polymers via polymerization or by the copolymerization of new monomers can be avoided. The ultimate properties of the blends can be manipulated by the proper selection of component polymers. Blending technique also provides attractive opportunities for the reuse and recycling of polymer wastes. Over the last several years researchers around the world have been trying to get new polymeric materials through blending with specific properties for different applications [66-70]. The major fields of use are automotive, electrical and electronic, packaging, building and household industries.

1.5.1 Reasons for Blending

Historically, polymer blends were developed to improve the impact strength of rigid polymers [71]. It is now one of the main topics of international polymer research. There are a number of reasons why researchers turned their attention towards blends. Typically, a polymer blend can offer a set of properties which are not possible with the component polymers alone. By simply varying the concentrations of the constituents of a blend, an innumerable variety of materials, each with a unique set of properties can be obtained. Generally, the following reasons are cited for blending [72].

a) Developing materials with a full set of desired properties,

b) Extending engineering resins' performance by diluting them with low cost commodity polymers,

c) Improving a specific property, e.g., impact strength, rigidity, ductility, chemical-cum-solvent resistance, barrier properties, abrasion resistance, flammability, gloss, etc.,

d) Adjusting the material performance to fit customer specifications at lowest price,

e) Recycling industrial/municipal wastes.

1.5.2 Classification

Blends are broadly classified on the basis of miscibility between the constituents and their nature.

1.5.2.1. Based on miscibility

On the basis of miscibility, blends are of three types.

a) Completely miscible blends: For completely miscible blends, $\Delta Hm < 0$ due to specific interactions. In this case, homogeneity is observed at least on a nanometer scale, if not on the molecular. This type of blends exhibit only one glass transition temperature (T_g), which is in between the glass transition temperatures of the individual components, in a close relation to the blend composition.

b) Partially miscible blends: The partially miscible blends, with a part of one component dissolved in the other, exhibit generally a fine morphology and satisfactory properties. Both the blend phases are homogeneous, and have their own T_g. Both T_g values are shifted from that of the pure component towards the other

component. In this case, the interface is wide and the interfacial adhesion is relatively good.

c) Completely immiscible blends: In this case, the interface is sharp with coarse phase morphology and there is only poor adhesion between the phases. This leads to a weak and brittle mechanical behaviour [73].

1.5.2.2 Based on constituents

Polymer blends can be categorized as plastic/plastic, rubber/plastic and rubber/rubber systems, based on the constituents.

a) Plastic-plastic systems

Blends of thermoplastics play an increasingly important role in industry. The primary aim of developing engineering plastic blends is to replace metals. Their use has proliferated in automobile, aerospace and business machine/appliance markets. Polyethylene/polystyrene (PE/PS) system has been the most thoroughly investigated of all polymer blends [74]. Huarng et al. [75] reported the immiscible behaviour of polyvinyl chloride/styrene acrylonitrile (PVC/SAN) blends. They suggested that for most of the compositions, PVC/SAN blends had two distinct glass transition temperatures. Blends of high molecular weight PS and polymethyl methacryalate (PMMA) exhibit a two phase morphology and have been found to be incompatible by different techniques [76, 77]. Many other blends of thermoplastics have also been reported by several researchers [78, 79].

b) Rubber-plastic systems

The rubber-plastic blends, which are commonly known as thermoplastic elastomers (TPE), are the most familiar ones in this catagory. Among the different types of

thermoplastic elastomers, those prepared by physical blending of an elastomer and a thermoplastic material under high shearing action have gained considerable attention due to the simple method of their preparation and easy attainment of the desired physical properties [80]. A large number of articles are available in literature on thermoplastic-elastomer blends. Properties of EPDM/polypropylene (PP) blends with partial crosslinking of the elastomer phase were reported by Fisher [81]. Campbell et al. [82] described the method of preparation, injection moulding conditions and physical properties of NR/PE and NR/PP blends. Rheology, morphology, mechanical properties and failure mode of various thermoplastic-elastomer blends have been reported by De and co-workers. [83-86] Coran and Patel [87-90] published a series of articles on rubber-thermoplastic blends. Thomas and co-wokers [91-93] also reported the development and characterization of different TPEs.

c) Rubber-rubber systems

The rubber-rubber blends have drawn considerable attention due to their wide range of properties and applications. The most pertinent properties of them are homogeinity of mixing and cure compatibility. Many of the rubber blends are immiscible since the mixing of the components is endothermic and the entropic contribution is small because of the high molecular weights. Blends of two or less incompatible rubbers are commonly used in the automobile tyre industry inorder to improve processability. These materials combine the excellent ageing and flex crack resistance of one component and good mechanical properties of the other. Oliveira and Soares [94] investigated the effects of a curing system and curing parameters on the mechanical properties, ageing resistance and crosslink density of

NBR/EPDM blends. The curing characteristics of the blends were found to be affected by the accelerator type and the sulphur concentration. The mercaptobenzothiazyl disulphide (MBTS) single accelerator system was able to crosslink the EPDM phase effectively and consequently the blends exhibited better mechanical performance than the other systems based on tetramethyl thiuram disulphide (TMTD). Several researchers have developed blends of NR with other rubbers such as EPDM [95] and polychloroprene (CR) [96]. Tanrattanakul and Udomkichdecha [97] did the development of novel elastomeric blends containing NR and ultra-low-density polyethylene (ULDPE). Blends were prepared on a two-roll mill for three ratios (70/30, 60/40, and 50/50 NR/ULDPE). They found that the tensile properties, tear resistance, and ageing of the blends were superior to those of NR/ SBR blends. Saad et al. [98] studied the compatibility of NR with different types of synthetic rubbers such as SBR, BR, EPDM, and CR. A systematic study, done by them on the electrical and mechanical properties of the blends, indicated that NR/SBR and NR/BR were compatible while others were incompatible. Kim and Hamed [99] developed a 50/50 blend of NR and *cis*-polybutadiene rubber. The blend found application in tyre sidewalls as it had resistance to fracture over a range of conditions covering rapid as well as slow crack growth.

1.5.3 Polymer-Polymer Miscibility

The polymer-polymer miscibility is primarily due to negative heat of mixing, resulting from specific interactions between the two types of macromolecules. The criteria for polymer/polymer miscibility are embodied by the equation for the free energy of mixing:

$$\Delta G_m = \Delta H_m - T\Delta S_m \quad \text{.....1.14}$$

where G_m is the Gibbs free energy, H_m is the enthalpy, S_m is entropy and T is the absolute temperature of mixing respectively. The necessary conditions for miscibility are:

(a) $\Delta Gm < 0$ and 1.15

(b) $$\left(\frac{\partial^2 \Delta G_m}{\partial \phi_1^2}\right)_{T,P} > 0 \quad \text{.....1.16}$$

where ϕ_i is the mole fraction of the i^{th} component.

Since the entropy of mixing of the polymers is very low, it would be required that the enthalpy of mixing ΔH_m be negative for polymer-polymer miscibility.

1.5.4 Interface

The interface is an important component which decides the properties of an immiscible blend. A poor chemical and/ or physical interaction between the two components usually implies a high interfacial energy and low interfacial thickness. These parameters have significant influence on the performance of multiphase materials. However, the highest degree of miscibility does not always give the best engineering properties. In some cases, some amount of phase separation is necessary to obtain the desired properties. The mechanism and dynamics of phase separation in polymer blends has been a research subject, to obtain high performance materials by controlling the morphology [100].

1.5.4.1 Role of compatibilizer

A compatibilizing agent permits the effective blending of otherwise incompatible polymers to yield compositions with unique properties generally not attainable from

either of the components. A variety of additives can be used to promote miscibility by reducing the interfacial tension.

Liu and Baker [101] discussed several methods for compatibilization such as introduction of non-reactive graft or block copolymers, addition of functional polymers, low molecular weight coupling agents, and reactive polymers. Non-reactive compatibilizers are typically block and graft copolymers of the partners and are more specific in their action. They can be useful in improving interfacial coupling. A typical example for the addition of functional polymers is the grafting of maleic anhydride or similar compounds to polyolefins [102]. Maleic-modified polyethylene and phenolic-modified polyethylene have been reported to be effective compatibilizers for HDPE/NBR blend. A completely different strategy for polymer blend compatibilization occurs by the addition of a mixture of low molecular weight chemicals such as peroxide and multifunctional chemicals. Reactive compatibilizers chemically react with blend components and are, therefore, effective for many systems. For example, Baker et al. [103] used azide crosslinking agents that attach PP chains to PS chains in a PP/PS blend. The azide group upon heating loses nitrogen, to form highly reactive nitrene species that gets inserted into C-H bonds in the polymer chains.

1.5.4.2 Role of fillers

Many polymers are not miscible and the blends usually consist of microdispersions of one in the other or have intermingled microregions often having dimensions around 0.1 to 1.5 μm. Fillers have an important direct action on the physico-mechanical properties of polymer blends. For example, Ahmed and EI-Sabbagh [104] examined the physico-mechanical properties and thermal ageing of rubber

vulcanizates (NR/SBR) containing white fillers, such as calcium, zinc, strontium, calcium-zinc, strontium-zinc, and strontium-calcium-zinc molybdate, so as to get white rubber vulcanizates with better properties than rubber vulcanizates containing carbon black. In general, fillers act as modifiers in polymer blends, as attested by several reports [105-108].

1.6 Transport through Polymer Blends

The synthesis of a particular polymer blend membrane is being motivated by the desire to superimpose the requisite properties upon the basic transport properties of a base polymer. Alternatively, the preparation of a truly miscible blend permits the continuous alteration of membrane properties as a function of blend composition. Many interesting studies have been reported based on the transport characteristic of polymer blends. Cates and White [109-111] were among the first to report the sorption behaviour of water in blends of poly acrylonitrile (PAN) and cellulose, silk and cellulose acetate. The sorption of water in PAN/cellulose acetate and PAN/cellulose varied linearly with blend composition. For the transport of water in PAN/silk blend, a complex sorption behaviour was observed. Merrobian and Ammondson [112] investigated the permeability of *n*- heptane and methyl salicylate through polyethylene- nylon blends. Subramanian and Mehra [113-115] found a substantial improvement in the barrier properties of polyolefine by the incorporation of small amounts of nylon or polyester into it. The diffusion and sorption of methyl substituted benzenes through cross-linked nitrile rubber/poly(ethylene-*co*-vinyl acetate) (NBR/EVA) blend membranes have been studied by Joseph et al.[116] with special reference to the influence of blend composition, cross-linking systems, temperature and size of penetrants. Dhoot et al. [117] followed the equilibrium sorption and kinetics of acetone, methyl ethyl ketone (MEK), methyl *n*-propyl ketone (M*n*PK), and methyl *i*-propyl ketone (M*i*PK) uptake in uniform, biaxially

oriented, semicrystalline polyethylene terephthalate(PET) films at 35 °C and low penetrant activity. Sorption isotherms for all penetrants were well described by the dual-mode sorption model. Sorption and desorption kinetics were described either by Fickian diffusion or by a two-stage model incorporating Fickian diffusion at short times and protracted polymer structural relaxation at long times. Diffusion coefficients and equilibrium solubility at fixed relative pressure decreased in the following order: acetone>MEK>M*n*PK>M*i*PK. Diffusion coefficients for each penetrant increased with increasing penetrant concentration. Marais et al.[118] analysed the transport of water vapour and gases (oxygen and carbon dioxide) through poly(ethylene-*co*-vinyl acetate) (EVA) films of different VA content, poly(vinyl chloride) (PVC) and EVA/PVC blend films. The increase in water absorption with the VA content leads to a steady increase in the permeability coefficients of EVA copolymers. For gas permeation, practically all the experimental curves were characterized by a constant diffusion coefficient, whatever the VA content of the copolymer used. The mixing of the glassy PVC polymer with EVA copolymer (in a rubbery state) resulted in a reduction in water and gas permeability. This was due to the low segment mobility of the dense PVC material which could form hydrogen bonds between the hydrogen atoms and the chlorine-substituted carbon of PVC with VA carbonyl groups. Compared to EVA copolymers, the EVA/PVC blends with equivalent VA contents were better in terms of selectivity.

Diffusivity and solubility data for toluene and *n*-heptane in semi-crystalline PE were obtained from gravimetric experiments by Lutzow et al. [119]. The results indicated that both diffusivity and penetrant solubility in the polymer amorphous phase decreased with increasing crystallinity. Harding and Gladden [120] studied the diffusion of liquid alkanes into a variety of semi-crystalline PE samples. The

results highlighted the importance of the crystalline phase in controlling the diffusion process in terms of both the geometric impedance imposed by the presence of impenetrable crystals and their effect on the mobility of the polymer chains comprising the amorphous material through which the penetrants migrate.

Siddaramaiah et al. [121] analysed the sorption and diffusion of halogenated hydrocarbon penetrants through different (EPDM) blends, such as EPDM/natural rubber, EPDM/bromobutyl rubber, and EPDM/styrene butadiene rubber (50/50 w/w), and observed that the transport data were affected by the nature of the interacting solvent molecule rather than its size and also by the structural variations of EPDM blends. The temperature dependence of the transport coefficient was used to estimate the activation parameters, such as the activation energy of diffusion (E_D) and the activation energy of permeation (Ep) from Arrhenius plots. The activation parameters E_D for aliphatic chlorinated organic penetrants were in the range 7.27-15.58 kJ/mol. These values fell in the expected range for rubbery polymers, well above their T_g. Also, the thermodynamic parameters such as enthalpy and entropy were calculated and were found to be in the range of 2-15 kJ/mol and 3-54 J/mol/K, respectively. Low density polyethylene (LDPE) and either isotactic polypropylene (*i*PP) or a copolymer of isotactic polypropylene with 3% of ethylene (CPP) have been blended, and characterized by Barra et al.[122], with X-ray, DSC, dynamic mechanical analysis, and transport studies. The observed sorption properties were in agreement with the additivity of sorption of the two amorphous phases.

Sorption and diffusion of toluene in LDPE/PVC blends, in the form of powders prepared by elastic-strain grinding, were investigated by Markevich et al.[123] who found that LDPE was active, while PVC inactive towards toluene vapour. It was observed that the first cycle of toluene vapour sorption in films of polymer blends proceeded considerably slowly than the second and subsequent sorptions; attributed to the slow relaxation of the non-equilibrium polymer structure formed during sample preparation. The limiting values of sorption increased with increasing content of PVC in the blend, evidently owing to the growing size of microvoids. The diffusion coefficient of toluene in LDPE-PVC blends decreased with increasing content of PVC. In polymer blends toluene was sorbed in the form of clusters. Wang et al. [124] performed diffusion experiments with xylene and toluene through different high-density polyethylene/modified polyamide (HDPE/MPA) blends at different temperatures. The results showed that the logarithm of the diffusion flux decreased linearly with the reciprocal of temperature. Our research group also reported the transport characteristics of different rubber based systems [125-129].

1.6.1 Blends Based on Styrene Butadiene Rubber

SBR is a general purpose synthetic rubber which has many applications. The high filler loading capacity, good flex resistance, crack-initiation resistance and abrasion resistance make it useful in several engineering and industrial areas. Basfar and Silverman [130] investigated the ozone resistance of styrene butadiene rubber (SBR) cured by a combination of sulphur and ionizing radiation. FTIR studies indicated that the high ozone resistance of SBR formulations, cured by a combination of sulphur and ionizing radiation, was associated with unusually high

vinyl concentration. Mechanical properties of SBR and NR were investigated by Findik et al.[131]. They prepared twelve rubber compounds by blending SBR and NR in different proportions, and reported that the tensile, hardness, and wear properties of the blends increased with an increment in NR percentage. Popovic et al. [132] studied the mechanical properties, crosslink density and surface morphology of SBR/silicone(MQ) rubber blends, cured with sulphur, peroxide and combinations of both systems. The best results were obtained with SBR/MQ 80/20 blends. Zhou et al. [133] analysed the rheological behaviour of a series of blends of PVC with different contents of SBR, by means of capillary rheometry, and reported that SBR/PVC blends had better processability by injection molding. George et al. [134-137] reported the morphology, dynamic mechanical properties and transport behaviour of NR/SBR blends. The effect of blend ratio on the dynamic mechanical properties of the blends was investigated at different temperatures. The storage modulus was found to be decreased with an increase in temperature. The effect of γ radiation on the morphological and physical properties of styrene-butadiene rubber (SBR) and ethylene-propylene-diene monomer (EPDM) blends was investigated by Dubey et al. [138]. The probability of spur overlap increased with the increase in EPDM content in the blends, which in turn resulted in a significant improvement in the mechanical properties of the irradiated SBR-EPDM blends with higher EPDM fraction. The efficiency of four multifunctional acrylates as crosslinking aids for the radiation-induced vulcanization of SBR-EPDM blend was also studied. The results established the lower efficiency of methacrylates over acrylates in the process and indicated that among the crosslinking agents studied trimethylol propane triacrylate was the most efficient one. El -Nashar [139] studied the compatibilization of

EPDM/SBR blends by EPDM-graft-styrene copolymer. The compatibilizer was prepared by the γ ray irradiation induced grafting of EPDM with styrene monomer. The compatibilized blends were examined by scanning electron microscopy and and in terms dielectric properties. The results revealed that the addition of a small per cent of graft copolymer to EPDM/SBR blends improved the physico-mechanical properties of the blend vulcanizates and this could be due to the enhancement of the blend compatibility.

Many interesting reports on the transport properties of SBR and its blends exist in literature. George et al. [140] investigated the effects of different vulcanizing systems on the transport of aromatic hydrocarbons through SBR membranes. Ismail and Suzaimah [141] studied the swelling of SBR/ epoxidized natural rubber (ENR) and found that at room temperature (23 °C) and 100 °C the swelling degree of SBR/ENR blends decreased with increase in the ENR content. Botros and Tawfik [142] synthesized styrene butadiene rubber-g-acrylic acid (SBR-g-AA), and characterized by Raman IR spectroscopy. This was incorporated into SBR/CR blend with different blend ratios. The homogeneity of the blends was examined with SEM, DSC, and in terms of their dielectric properties. The scanning electron micrographs illustrated the improvement of the morphology of SBR/CR rubber blends as a result of the incorporation of SBR-g-AA. Swelling behaviour in toluene, motor oil, and brake fluid, of the blend vulcanizates was also assessed. Siddaramaiah et al. [143] examined the interaction of crosslinked EPDM/SBR blends with carbonyl penetrants. They observed that the transport data were affected by the nature of interacting solvent molecule rather than its size and also by the

structural variation of the blends. In addition, our research group also reported the transport characteristics of SBR based systems [144,145].

1.6.2 Blends based on Poly(ethylene-*co*-vinyl acetate)

EVA is a polymer that approaches elastomeric materials in softness and flexibility, yet can be processed like other thermoplastics. The material has good clarity and gloss, barrier properties, low-temperature toughness, stress-crack resistance, hot-melt adhesive and heat sealing properties and resistance to UV radiation. EVA has little or no odour and is competitive with rubber and vinyl products in many electrical applications. These peculiar characteristics of EVA have generated significant interest in the development of its blends with other polymeric materials so as to improve some specific properties or to enlarge its range of useful temperatures. The semi-crystalline nature and polarity enable EVA to form compatible blends with many other polymers.

Physical properties EVA/NR blend based foam were investigated by Kim and co-workers [146]. EVA was blended with NR, and the EVA/NR blends were subsequently foamed at 155 °C, 160 °C, and 165 °C. The physical properties of the foams were then measured as a function of foaming temperatures and blend compositions. EVA/NR (90/10) blend, foamed at 165 °C, showed lower density, better rebound resilience, and higher tear strength than EVA foam. The mechanical properties of EVA/PE blends have been reported by Kovacs and Kallo [147]. The compatibility of these blends was studied by scanning electron microscopy. An optimum composition in terms of mechanical properties was established. Blends of EVA with PE have been extensively studied by several researchers [148-150]. The

mechanical properties of blends of PA6 and EVA have been studied by Bhattacharyya et al.[151]. The tensile strength and the tensile modulus of the blends were found to be decreased steadily with increase in EVA content. Tang et al.[152] examined the effect of EVA having different VA content as an impact modifier in PS/EVA blends. There are several works in the literature concerning the studies on the blends of EVA with polychloropene [153,154], nitrile rubber [155-160], natural rubber [161-163] etc. Kundu et al. [164] examined the solvent resistance of blends of CR and EVA. The retention in tensile properties was found to be the maximum for CR and high CR content samples after solvent ageing.

Interesting studies based on the transport features of EVA and its blends with various polymers are available in literature. For example, Lee et al. [165] examined the permeability of nine steroids through EVA as a function of both permeant and membrane properties. Steroids with higher melting points permeated more slowly. Sorption and diffusion of methyl substituted benzenes through cross-linked nitrile rubber/poly(ethylene-*co*-vinylacetate) (NBR/EVA) blend membranes were reported by Joseph et al.[166]. They analysed the influence of blend composition, cross-linking systems, temperature and size of penetrants on the transport behaviour, and observed that as the EVA content increased in the blends, the solvent uptake decreased. The diffusion and transport of cyclohexanone through crosslinked NBR/EVA blends have been studied by Varghese et al. [167] with special reference to blend composition, crosslinking systems, fillers, filler loading, and temperature. At room temperature the mechanism of diffusion was found to be Fickian for cyclohexanone-NBR/EVA blend systems. However, a deviation from the Fickian mode of diffusion was observed at higher temperature. The transport coefficients,

namely, intrinsic diffusion coefficient (D*), sorption coefficient (S), and permeation coefficient (P) increased with an increase in NBR content. The sorption data have been used to estimate the activation energies for permeation and diffusion. Foldes [168] studied the transport properties of various additives in EVA by measuring their diffusion rate and solubility. A correlation was found between the diffusion rate and the fractional free-volume of the non-crystalline phase of the polymer, as well as the specific volume of the diffusant.

Present Work

There are reports on many blends based on SBR and EVA separately, while blends of EVA and SBR have not been well exposed in the scientific literature, except a few [169,170], eventhough both the polymers and their blends find extensive applications in industry. No systematic study has yet been carried out on the transport behaviour of SBR/EVA blends with special reference to the effects of blend ratio, different croslinking systems, compatibilizer and different types of fillers.

The aim of the present work is to carry out a systematic investigation on the transport characteristics of the blends of SBR and EVA. Three vulcanizing systems viz. sulphur (S), dicumyl peroxide (DCP) and a mixed system (S+DCP) have been used to crosslink the matrix. A compatibilizer viz. dichlorocarbene modified SBR (DCSBR) has been used. The fillers used are semi-reinforcing furnace (SRF), high abrasion furnace (HAF), intermediate super abrasion furnace (ISAF), silica and chitin. The results have been explained in terms of different kinetic and sorption parameters.

The following are the objectives of the present investigation:

i) To examine the transport properties of unfilled but crosslinked SBR/EVA blends with:

   a) Aliphatic hydrocarbons viz. pentane, hexane, heptane and octane,

   b) Chlorinated hydrocarbons viz. dichloromethane, chloroform and carbon tetrachloride,

ii) To study the effect of a compatibilizer, dichlorocarbene modified SBR (DCSBR), on the transport properties of SBR/EVA blends,

iii) To evaluate the interaction of three fuels with carbon black filled SBR/EVA blends,

iv) To compare the influence of carbon black and silica fillers on the sorption and diffusion properties of SBR/EVA blends,

v) To investigate the water absorption features of SBR/EVA blends filled with chitin whisker.

References

[1]. J. Landois-Garza and J. H. Hotchkiss, *ACS Symp. Ser.*, **365**, 42 (1988).

[2]. R. B. Seymour, *Engineering Polymer Source Book*, McGraw-Hill Publishing Co., New York, 1990.

[3]. R.Y. M. Huang (Ed.), *Pervaporation Membrane Separation Processes*, Elsevier, New York, 1991.

[4]. P. V. Kulkarni, S. B. Rajur, P. Antich, T. M. Aminabhavi and M. I. Aralaguppi, *J. Macromol. Sci. Rev. Macromol. Chem. Phys.*, **C30**, 441 (1990).

[5]. N. A. Peppas and R.W. Korsmeyer, *Hydrogels in Medicine and Pharmacy*, N. A. Peppas (Ed.), CRC Press, Boca Raton, FL, 1987.

[6]. J. K. Mitchell, R. *Inst. J.* **2**, 101 (1831).

[7]. J. Neel, *Pervaporation Membrane Separation Processes*, R. Y. M. Huang (Ed), Elsevier Science, New York, 1991.

[8]. J. R. Fried, *Polymer Science and Technology*, Prentice-Hall, Englewood Cliffs, N.J., USA, 1995.

[9]. M. Alger and T. Stanley, *Polym. Prepr.*, **30**, 24 (1989).

[10]. W. R. Vieth, *Diffusion in and through Polymers, Principles and Applications*, Haser Publishers: New York, 1990.

[11]. C. J. Guo and D. De Kee, *Chem. Eng. Sci.*, **46**, 2133 (1991).

[12]. M. Chainey, *Hand Book of Polymer Science and Technology*, Vol.4, Composites and Speciality Applications (Ed. N.P. Cheremisinoff) Marcel Dekker, INC, New York, p.499 1989.

[13]. S. A. Saleem, V. M. Shah, and B. J. Hardy, *J. Polym. Sci., Polym. Phys. Ed.*, **25**, 1293 (1987).

[14]. T. Nakagawa, Y. Fujiwara and N. Minoura, *J. Membr. Sci.*, **18**, 111 (1993).

[15]. G. J. Van Amerongen, *J. Polym. Sci.*, **62**, 2215 (1996).

[16]. K. S. Kwan, C. N. P. Subramaniam and T. C. Ward, *Polymer*, **44**, 3071 (2003).

[17]. T. M. Aminabhavi, H. T. S. Phayde, J. D. Ortego and W. E. Rudzinski, *J. Hazard. Mater.*, **49**, 125 (1996).

[18]. K. E. Fagelman and J. T. Guthrie, *Surf. Coat. Intern. Part B: coat. Transa.*, **89**. 1 (2006).

[19]. S. Berten and J. J. Robin, *Eur. Polym. J.*, **38**, 2255 (2002).

[20]. J. Zhang, Y. Yao, X. L. Wang and J. H. Xu, *J. Appl. Polym. Sci.*,**101**, 436 (2006).

[21]. Siddaramaiah, S. Roopa, U. Premakumar, and A. Varadarajulu, *J. Appl. Polym. Sci.*, **67**, 101 (1998).

[22]. S. H. Botros and H. L. Tawfic, *Polym. Plast. Technol. Eng.*, **44**, 209 (2005).

[23]. K. A. Dubey, Y. K. Bhardwaj, C. V. Chaudhari, S. Bhattacharya, S. K. Gupta and S. Sabharwal, *J. Polym. Sci., Part B: Polym. Phys.*, **44**, 1676 (2006).

[24]. H. Ismail and Supri, *Polym. Test.*, **25**, 318 (2006).

[25]. J. Sharif, W. M. Z. W. Yunus, K. H. Dahlan and M. H. Ahmad, *J. Appl. Polym. Sci.*, **100**, 353 (2006).

[26]. A. R. Berens and H. B. Hopfenberg, *J. Membr. Sci.*, **10**, 283 (1982).

[27]. G. S. Park, *J. Polym. Sci.*, **11**, 97 (1953).

[28] W. W. Brandt, *J. Polym. Sci.*, **41**, 403 (1959).

[29]. G. J. Van Amerongen, *Rubber Chem. Technol.*, **37**, 1065 (1964).

[30]. W. R. Brown, R. B. Jenkins and G. S. Park, *J. Polym. Sci. Symp.*, **41**, 45 (1973).

[31]. J. W. Nicholson, *The Chemistry of Polymers*, The Royal Society of Chemistry, Cambridge, 1997.

[32]. G. Unnikrishnan and S. Thomas, *Polymer*, **35**, 5504 (1994).

[33]. B. T. Poh, K. Adachi and T. Kotaka, *Macromol.*, **20**, 2574 (1987).

[34]. I. Arvanitoyannis, I. Kolokuris, A. Nakayama, N. Yamamoto and S. Aiba, *Carbohydr. Polym.*, **34**, 9 (1997).

[35]. R. M. Barrer, R. Mallinder and P. S-L. Wong, *Polymer*, **8**, 321 (1967).

[36]. S. G. Kazarian, B. L. West, M. F.Vincent, N. H. Brantley and C. A. Eckert, *Proceedings of the ACS Division of Polymeric, Mater. Sci. Eng.*, **76**, 364 (1997).

[37]. J. Crank and G. S. Park, *Diffusion in Polymers*, New York, Academic Press, 1968.

[38]. Z. F. Wang, B. Wang, N. Qi, H. F. Zhang and L. Q. Zhang, *Polymer*, **46**, 719 (2005).

[39]. S. C. George and S. Thomas, *Prog. Polym. Sci.*, **26**, 985 (2001).

[40]. S. N. Lawandy, and S. H. Botros, *J. Appl. Polym. Sci.*, **42**, 137 (1991).

[41]. M. Mohsen, M. H. Abd-EI Salam, A. Ashry, A. Ismail and H. Ismail, *Polym. Degr. Stab.*, **87**,381 (2005).

[42]. C. Gauthir, E. Reynaud, R. Vassoil and L. Ladouce- Stelandre, *Polymer*, **45**, 2761 (2004).

[43]. C. E. Rogers in: *Encyclopedia of Polymer Science and Technology*, F. Mark and N. Gaylord (Eds.), Interscience, New York, **12**, 692 (1970).

[44]. M. Aminabhavi, H. T. S. Phayde, J. D. Ortego and J. M. Vergnaud, *Polymer*, **37**, 1677 (1996).

[45]. H. Fujita, A. Kishimoto and K. Mutsumoto, *Trans. Faraday Soc.*, **56**, 424 (1967).

[46]. S. U. Hong, *J. Appl. Polym. Sci.*, **61**, 833 (1996).

[47]. D. Kim, J. M. Caruthers and N. A. Peppas, *Macromol.*, **26**, 1841 (1993).

[48]. N. Yi-Yan, R. M. Felder and W. J. Koros, *J. Appl. Polym. Sci.*, **25**, 1755 (1980).

[49]. A. Garcia, M. Iriarte, C. Uriarte and A. Etxeberria, *J. Membr. Sci.*, **284**, 173 (2006).

[50]. S. N. Lawandy and F. H. Helaly, *J. Appl. Polym. Sci.*, **32**, 5279 (1986).

[51]. K. Swamy, B. K. Siddaramaiah, Naidu, B. Vijaya Kumar, N. N. Mallikarjuna and T. M. Aminabahvi., *J. Appl. Polym. Sci.*, **96**, 874 (2005).

[52]. C. W. C. Hung, *Microchem. J.*, **19**, 130 (1974).

[53]. K. T. Chiang and M. V. Sefton, *J. Polym. Sci., Polym. Phys.*, Ed. **15**, 1927 (1977).

[54]. W. R. Vieth, C. S. Frangoulis and J. A. Rionda, Jr, *J. Colloid Interface Sci.*, **22**, 454 (1966).

[55]. S. Hirose, W. R. Vieth and M. Takao, *J. Molec. Catal.*, **18**, 11 (1983).

[56]. D. R. Paul and O. M. Ebra-Lima, *J. Appl. Polym. Sci.*, **19**, 2759 (1975).

[57]. J. M. Bouvier and M. Gelus, *Rubber Chem. Technol.*, **59**, 233 (1986).

[58]. S. C. George, K. N. Ninan and S. Thomas, *Polymer*, **37**, 5839 (1996).

[59]. A. E. Mathai and S. Thomas, *Micromol. Sci. Phys.*, B **35**, 229 (1996).

[60]. T. Johnson and S. Thomas, *Micromol. Sci. Phys.*, B **36**, 401(1997).

[61]. J. J. Manikath and S. Thomas, *J. Appl. Polym. Sci.*, **82**, 2404 (2001).

[62]. R. Stephen, K. Joseph, Z. Oommen, and S. Thomas, *Compos. Sci. Technol.*, **67**, 1187 (2007).

[63]. V. Stannett and H. B. Hopfenberg, *The Physics of Glassy Polymers* (Ed. R. N. Haward) Appl. Sci. Publ, London, 1973.

[64]. G. A. Orchard, I. M. Ward, *Plast. Rubber Process. Appl.*, **6**, 51 (1986).

[65]. J. S. Vrentas, C. M. Vrentas, *Macromol.*, **24**, 2404 (1991).

[66]. J. K. Battacharya, in: *Polymer Blends and Alloys-An Overview,* R.P. Singh, C. K. Das and S. K. Mustafi (Eds.), Asian Books, New Delhi, 2002.

[67]. H. Ismail, S. Tan and B.T. Poh, *J. Elast. Plast.*, **33**, 251 (2001).

[68]. M. Nasir and C. H. Choo, *Eur. Polym. J.*, **25**, 355 (1989).

[69]. A. F. Abd-El Salam, M. H. Abd-El Salam, M.T. Mostafa, M.R. Nagy and M. I. Mohamed, *J. Appl. Polym. Sci.*, **90**, 1539 (2003).

[70]. A. S. Sirqueira, B.G. Soares, *Eur. Polym. J.*, **39**, 2283 (2003).

[71]. L. A. Utracki, *Commercial Polymer Blends*, Chapman and Hall, New York, 1998.

[72]. A. K. Kulshreshta, B. P. Singh and Y. N. Sharma, *Eur. Polym. J.*, **24**, 29 (1988).

[73]. D. R. Paul, C. E.Vinson and C. E. Locke, *Polym. Eng. Sci.*, **12**, 157 (1970).

[74]. K. Min, J. L.White and J. F. Feller, *J. Appl. Polym. Sci.*, **29**, 2117 (1987).

[75]. J. C. Huarng, K. Min and J. L.White, *Polym. Eng. Sci.*, **28**, 1590 (1988).

[76]. H. R. Brown, *Macromolecules*, **22**, 2859 (1989).

[77]. S. D. Hong and C. M. Burns, *J. Appl. Polym. Sci.*, **15**, 1995 (1971).

[78]. R. Chakrabarti, M. Das and D. Chakraborty, *J. Appl. Polym. Sci.*, **93**, 2721 (2004).

[79]. G. Akovali and T. T. Torun, *Polym. Int.*, **42**, 307 (1997).

[80]. W. K. Fisher, U.S. Pat. 3835201 (1972).

[81]. W. K. Fisher, U.S. Pat. 3,758,643 (1972).

[82]. D. S. Campbell, D. J. Elliot and M. A. Wheelans, *NR Technol.*, **9**, 21 (1978).

[83]. B. Kuriakose and S. K. De, *Polym. Eng. Sci.*, **25**, 630 (1985).

[84]. S. Akhtar, P. P. De and S. K. De, *Mater. Chem. Phys.*, **12**, 235 (1985).

[85]. S. Thomas, B. Kuriakose, B. R. Gupta and S. K. De, *Plast. Rubber. Compos. Process. Appl.*, **6**, 85 (1986).

[86]. S. Thomas, B. Kuriakose, B. R. Gupta and S. K. De, *J. Mater. Sci.*, **21**, 711 (1986).

[87]. A.Y. Coran and R. Patel, *Rubber Chem. Technol.*, **53**, 141 (1980).

[88]. A.Y.Coran, R. Patel and D. Williams, *Rubber Chem. Technol.*, **55**, 116 (1982).

[89]. A.Y. Coran and R. Patel, *Rubber Chem. Technol.*, **56**, 210 (1983).

[90]. A.Y. Coran and R. Patel, *Rubber Chem. Technol.*, **56**, 1045 (1983).

[91]. C. Radhesh Kumar, K. E. George and S. Thomas, *J. Appl. Polym. Sci.*, **61**, 2383 (1996).

[92]. G. Josephine, J. Reethamma, K. T. Varughese and S. Thomas, *J. Appl. Polym. Sci.*, **57**, 449 (1995).

[93]. A. T. Koshy, B. Kuriakose, S. Thomas, and S. Varghese, *Polymer*, **34**, 3428 (1993).

[94]. M. G. Oliveira, and B. G. Soares, *Polym. Polym. Compos.*, **9**, 459 (2001).

[95]. A. K. Ghosh, S. C. Debnath, N. Naskar and D. K. Basu, *J. Appl. Polym. Sci.*, **81**, 800 (2001).

[96]. H. Ismail and H. C. Leong, *Polym. Test.*, **20**, 509 (2001).

[97]. V. Tanrattanakul and W. Udomkichdecha, *J. Appl. Polym. Sci.*, **82**, 650 (2001).

[98]. Saad, L. G. Azima and El-Sabbagh Salwa, *J. Appl. Polym. Sci.*, **79**, 60 (2001).

[99]. H. J. Kim and G. R. Hamed, *Rubber Chem. Technol.*, **73**, 743 (2000).

[100]. D. Feldman, *J. Micromol. Sci., Part: A Pure and Appl. Chem.*, **42**, 587 (2005).

[101]. N. C. Liu, and W. E. Baker, Adv. *Polym. Technol.*, **11**, 249 (1992).

[102]. R. Ashaletha, M. G. Kumaran, and S. Thomas, *Eur. Polym. J.*, **35**, 253 (1999).

[103]. D. A. Baker, P. J. Brown and M. S. Ellison, *Polym. Mater. Sci. Eng.*, **89**, 122 (2003).

[104]. N. M. Ahmed and S. H. EI-Sabbagh, *Polym. Plast. Technol. Eng.*, **45**, 275 (2005).

[105]. N. Suzuki, M. Ito and F. Yatsuyanagi, *Polymer,* **46**, 193 (2005).

[106]. A. M. Shanmugharaj and A. K. Bhowmick, *Radiation Phys. Chem.* **69**, 91 (2004).

[107]. A. Gnatowski and J. Koszkul, *J. Mater. Proces. Technol.*, **162**, 52 (2005)

[108]. V. G. Pavlii, A. Ye. Zaikin and Ye. V. Kuznetsov, *Polym. Sci. USSR*, **29** (3), 497 (1987).

[109]. D. M. Cates and H. J. White Jr., *J. Polym. Sci.*, **20**, 155 (1946).

[110] . D. M. Cates and H. J. White Jr., *J. Polym. Sci*, **20**, 181 (1956).

[111]. D. M. Cates and H. J. White Jr., *J. Polym. Sci*, **21**, 125 (1956).

[112]. R. B. Mesrobian, C. J. Ammondson, US Patent No.3, 1963, 093 235.

[113]. P. M. Subramanian, *Int. Polym. Proc.*, **III (1),** 33 (1988).

[114]. P. M. Subramanian, *Polym. Prepr.(Am. Chem. Soc., Div. Polym. Chem.*, **30,** 28 (1989).

[115]. P. M. Subramanian and V. Mehra, *Polym. Eng. Sci.*, **29**, 663 (1987).

[116]. A. Joseph, E. M. Asha and S. Thomas, *J. Memb. Sci.*, **13**, 220 (2003).

[117]. S. N. Dhoot, B. D. Freeman, and M. E. Stewart, *Polymer*, **45,** 5619 (2004).

[118]. S. Marais, E. Bureau, F. Gouanvé, E. Ben Salem, Y. Hirata, A. Andrio, C. Cabot and H. Atmani, *Polym. Test.*, **23,** 475 (2004).

[119]. N. Lutzow, A. Tihninluoglu, R. P. Danner, J. L. Duda, A. D. Haan, G. Warnier, and J. M. Zielinski, *Polymer*, **40**, 2797 (1999).

[120]. S. G. Harding and L. F. Gladden, *Magn. Reson. Imaging*, **16**, 647, 1998.

[121]. Siddaramaiah, S. Roopa and K. H. Guruprasad, *J. Appl. Polym. Sci.*, **88**, 1366 (2003).

[122]. G. Barra, D. 'Aniello, C. Guadagno and L. Vittoria, *J. Mater. Sci.*, **34,** 4601 (1999).

[123]. M. A. Markevich, V. N. Stogova and A. Ya. Gorenberg, *Polym. Sci.*, **33**,132 (1991).

[124]. C-L. Wang, Zhao-Rong Qiu and Min-lian Cheng. *J. Chem. Eng.*, **15**, 521 (2001).

[125]. G. Unnikrishnan, S. Thomas and S. Varghese, *Polymer*, **37**, 2687 (1996).

[126]. G. Unnikrishnan and S. Thomas, *J. Appl. Polym. Sci.*, **60**, 963 (1996).

[127]. G. Unnikrishnan, P.H. Gedam, V. S. Kishan Prasad and S. Thomas, *J. Appl. Polym. Sci.*, **64**, 2597 (1997).

[128]. K. Priya Dasan, A.P. Haseena, G. Unnikrishnan, R. Alex and E. Purushothaman, *Polym. Polym. Compos.*, **12**, 599 (2004).

[129]. S. V. Nair, M. S. Sreekala, G. Unnikrishnan, T. Johnson, S. Thomas and G. Groeninckx, *J. Membr. Sci.*, **177,** 1 (2000).

[130]. A. A. Basfar and J. Silverman, *Polym. Degrad. Stab.*, **46**, 1 (1994).

[131]. F. Findik, R. Yilmaz, and T. Koksal, *Mater. Des.*, **25**, 269 (2004).

[132]. R. S. Popovic, M. Plavsic, R. G. Popovic, M. Milosavljevic, *Kautsch, Gummi, Kunstst.*, **50**, 861(1997).

[133]. P. Zhou, Zaijian, Sun, *Plast. Rubber Process. Appl.*, **7**, 229 (1987).

[134]. S. C. George, K. Prasad, J. P. Misra and S. Thomas, *J. Appl. Polym. Sci.*, **74**, 3059 (1999).

[135]. S. C. George, K. N. Ninan, G. Gueskens and S. Thomas, *J. Polym. Eng.*, **23**, 423 (2003).

[136] S. C. George, K. N. Ninan, and S. Thomas, *Eur. Polym. J.*, **37**, 183 (2001).

[137]. S. C. George, K. N. Ninan, and S. Thomas, *J. Membr. Sci.*, **176**, 131 (2000).

[138]. K.A. Dubey, Y. K. Bhardwaj, C. V. Chaudhari, S. Bhattacharya, S. K. Gupta, and S. Sabharwal, *J. Polym. Sci., Part B: Polym. Phys.*, **44**, 1676 (2006).

[139]. D. E. EI-Nashar, *Polym. Plast. Technol. Eng.*, **43**, 1425 (2004).

[140]. S. C. George, M. Knorgen, S. Thomas, *J. Membr. Sci.*, **163**, 1 (1999).

[141]. H. Ismail. and S. Suzaimah., *Polym. Test.*, **19**, 879 (2000).

[142]. S. H. Botros and S.Y. Tawfik, *Polym. Plast. Technol. Eng.*, **45**, 829 (2006).

[143]. Siddaramaiah, S. Roopa and K. H. Guruprasad, *J. Polym. Eng.*, **23**, 55 (2003).

[144]. K. H. Rahiman and G. Unnikrishnan, *J. Polym. Rese.*, **13**, 297 (2006).

[145]. K. H. Rahiman, G. Unnikrishnan, C. K. Radhakrishnan, and A. Sujith, *Mater. Lett.*, **59**, 633 (2005).

[146]. M. S. Kim, C. C. Park, S. R. Chowdhury and G. H. Kim, *J. Appl. Polym. Sci.*, **94**, 2212 (2004).

[147]. E. Kovacs, and D. Kallo, *Int. Polym. Sci. Technol.*, **8**, T/23 (1981).

[148]. S. Chattopadhyay, T. K. Chaki, and A. K. Bhowmick, *J. Appl. Polym. Sci.*, **79**, 1877 (2001).

[149]. S. Xio, D. De Kee and J. Bovenkamp, *Rubber Chem. Tecnol.*, **72**, 758 (1999).

[150]. G. Markovic, B. Radovanovic, M. Marinovic Cincovic and Budinski-Simendic, *Kautsch, Gummi, Kunstst.*, **59**, 251(2006).

[151]. A. R. Bhattacharyya, A. Misra, and S. N. Maiti, *J. Appl. Polym. Sci.*, **85**, 1593 (2002).

[152]. L. W. Tang, K. C. Tam, C.Y. Yue, X. Hu, Y. C. Lam, and L. Li, *Polym. Int.*, **50**, 95 (2001).

[153]. P. P. Kundu and D. K. Tripathy, *Kautsch, Gummi, Kunstst.*, **49**, 666 (1996).

[154]. P. P. Kundu and D. K. Tripathy, *Kautsch, Gummi, Kunstst.*, **49**, 268 (1996).

[155]. H. Varghese, S. S. Bhagawan, and S. Thomas, *J. Appl. Polym. Sci.*, **71**, 2335 (1999).

[156]. H. Varghese, S. S. Bhagawan, N. Prabhakaran, and S. Thomas, *Mater. Lett.*, **24**, 333 (1995).

[157]. J. L. Graham, R. C. Striebich, K. J. Myers, D. K. Minus and W. E. Harisson, Enery Fuels., **20**, 759 (2006).

[158]. H. Varghese, J. S. Anand, K. Ramamurthy, R. Janardhanan, S. S. Bhagawan, and S. Thomas, *Polym. Plast. Technol. Eng.*, **38**, 319 (1999).

[159]. H. Varghese, S. S. Bhagawan, and S. Thomas, *J. Therm. Anal. Calorim*, **63**, 749 (2001).

[160]. H. Varghese, J. Seena, S. Thomas, T. Johnson, S. S. Bhagawan and G. Groeninckx, *J. Polym. Sci., PartB: Polym. Phys.*, **40**, 1556 (2002).

[161]. A. T. Koshy, B. Kuriakose and S. Thomas, *Polym. Degrad. Stab.*, **36**, 137 (1992).

[162]. A. T. Koshy, B. Kuriakose, S. Thomas, C. K. Premalatha, and S. Varghese, *J. Appl. Polym. Sci.*, **49**, 901 (1993).

[163]. A. T. Koshy, B. Kuriakose, S. Thomas and S. Varghese, *Polym. Plast. Technol. Eng.*, **33**, 149 (1994).

[164]. P. P. Kundu, R. N. P. Choudhury and D. K. Tripathy, *J. Appl. Polym. Sci.*, **71**, 551 (1999).

[165]. E. K. L. Lee, H. K. Lonsdale, R.W. Baker, E. Drioli and P.A. Bresnahan, *J. Membr. Sci.*, **24**, 125 (1985).

[166]. A. Joseph, M. A. Elizabeth and S. Thomas, *J. Memb. Sci.*, **220**, 13 (2003).

[167]. H. Varghese, S. S. Bhagawan and S. Thomas, *J. Polym. Sci., Part B: Polym. Phys.*, **37**, 1815 (1999).

[168]. E. Foldes, *Polym. Degrad. Stab.*, **49**, 57 (1995).

[169]. C. K. Radhakrishnan, A. Sujith, G. Unnikrishnan and S. Thomas, *J. Appl. Polym. Sci.*, **94**, 827 (2004).

[170]. C. K. Radhakrishnan, B.Ganesh, A. Sujith, G. Unnikrishnan and S. Thomas, *Polym. Polym. Compos.*, **13**, 335 (2005).

Chapter 2

Materials and Experimental Methods

Summary

This chapter discusses the characteristics of the materials used and the experimental techniques adopted for the present investigation. The formulations of the blends and the sample preparation procedures have been given. The methodology for the examination of the transport process through the blends has been described. The procedures for the blend characterization methods such as scanning electron microscopy and mechanical property measurements have been highlighted.

2.1 Materials

2.1.1 Styrene Butadiene Rubber (SBR)

Styrene butadiene rubber (SBR), formerly known as GR-S, is a general purpose synthetic rubber having wide range of commercial applications. It is a co-polymer of styrene and butadiene, manufactured by cold emulsion polymerization either by batch process or by continuous process.

SBR used in the present investigation, with the trade name syanoprene (SBR–1502), was obtained from Korea Kumho Pertro Chemicals Company Ltd., Korea. The basic characteristics of SBR are given in Table 2.1. The structure of SBR is given in Figure 2.1.

Table 2.1 Characteristics of SBR

Description	Value
Styrene content (%)	24.00
Volatile matter (%)	0.75
Organic acid (%)	4.75
Soap (%)	0.50
Ash (%)	1.50
Antioxidant (%)	0.50
Density (kg/m^3)	940.00
Mooney viscosity (ML_{1+4}; 100° C)	46.00

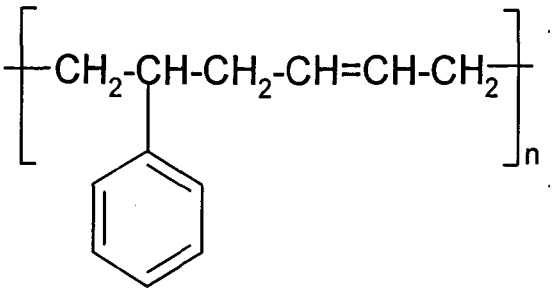

Figure 2.1 Structure of SBR

2.1.2 Poly (ethylene-*co*-vinyl acetate) (EVA)

EVA is a synthetic polymer which is produced commercially by three different basic methods. They are continuous bulk, solution and emulsion polymerization techniques. Only the first two of these are used commercially to produce copolymers having 5 to 50 % vinyl acetate content. These materials are classified as thermoplastic elastomers. Emulsion polymerization is used to produce copolymers containing 60-90 % vinyl acetate and these cannot be classified as thermoplastic elastomers [1]. The structure of EVA is given in Figure 2.2.

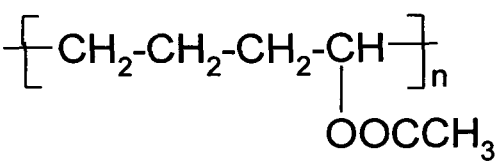

Figure 2.2 Structure of EVA

The saturated polyethylene chain and the bulky nature of the acetoxy side chain of EVA are responsible for its semi-crystalline nature.

EVA used for the present work was EVA-1802 (Pilene-1802), having 18 % vinyl acetate content, supplied by National Organic Chemical Industries Ltd., (NOCIL), Mumbai. The basic characteristics of EVA are given in Table 2.2.

Table 2.2 Characteristics of EVA

Description	Value
Vinyl acetate content (%)	18.00
Melt flow index (kg/10 min)	0.002
Vicat softening point (°C)	59.00
Density (kg/m^3)	950.00
Solubility parameter $(MPa)^{1/2}$	18.30

2.1.3 Rubber Compounding Chemicals

The vulcanizing agents used for crosslinking the matrix were elemental sulphur and dicumyl peroxide (40 % active). The accelerator used in this study was mercapto benzothiazyl disulphide (MBTS). A combination of zinc oxide and stearic acid was used as the activator. All the compounding chemicals used were of commercial grade.

2.1.4 Fillers

The fillers used were SRF (semi-reinforcing furnace), HAF (high abrasion furnace), ISAF (intermediate super abrasion furnace), and silica, supplied by Rubo-Chem Industries, Mumbai, India. The properties of the fillers used are given in Table 2.3. Chitin filler was supplied by Marine Chemicals, Ccchin, Kerala India. The characteristics of chitin are given in Table 2.4.

Table 2.3 Properties of fillers

Filler Type	Grade	Surface Area (m^2/g)	Particle Size (nm)
SRF	N 762	20	60
HAF	N 330	80	29
ISAF	N 220	120	23
Silica	Ultrasil VN3	176	18

Table 2.4 Characteristics of chitin

Description	Value
Colour	Off white
Ash content (%)	1.25
Moisture (%)	7.0
Protein (%)	1.80

2.1.5 Compatibilizer

Dichlorocarbene modified SBR (DCSBR), used as a compatibilizer for SBR/EVA systems, was prepared by the reaction of dichlorocarbene, produced by the alkaline hydrolysis of chloroform, with SBR using cetyl trimethyl ammonium bromide (CTAB) as phase transfer catalyst [2]. The level of modification was monitored by the determination of chlorine content using chemical techniques. DCSBR of 25% chlorine content was used for the compatibilization.

2.1.6 Solvents

The solvents used in this work such as aromatic hydrocarbons (benzene, toluene and xylene), aliphatic hydrocarbons (*n*-pentane, *n*-hexane, *n*-heptane and *n*-octane) and chlorinated hydrocarbons (dichloromethane, chloroform and carbon tetrachloride) were obtained from E. Merck (India) Ltd., Mumbai, India. They were of reagent grade (99 % pure) and were distilled twice before use to ensure purity.

The fuels (petrol, kerosene and diesel) used were also of commercial grade. The physical properties of the liquids used are given in Table 2.4.

Table 2.4 Physical properties of solvents

Solvent	Molecular Weight	Density (kg/m^3)	Boiling Point (°C)
Benzene	78.11	874	79
Toluene	92.14	867	109
Xylene	106.17	860	137
n-pentane	72.15	625	35
n-hexane	86.18	659	68.7
n-heptane	100.21	673	80.5
n-octane	114.23	703	125.7
Dichloromethane	84.93	1323	39.0
Chloroform	119.38	1492	59.5
Carbon tetrachloride	153.82	1594	76
Petrol	80-100	710-737	30-150
Kerosene	150-170	810-817	140-230
Diesel	170-330	820-950	240-350

2.2 Experimental Techniques

2.2.1 Blending and Compounding

Blends of SBR/EVA were prepared on a two-roll mixing mill (1.5 m × 0.3 m) with a nip gap of 1.3 mm and a friction ratio of 1:1.4, as per ASTM D-15-627 (1994). The temperature of the rollers of the mill was kept at 30 °C by the circulation of cold water. The nip gap, mill speed ratio and time of mixing of the rolls were kept

the same for all mixes. SBR was masticated for two minutes initially and then blended with EVA for an additional 2.5 minutes. The formulations of the mixes viz. SBR/EVA, SBR/EVA/compatibilizer or filler are given in Tables 2.5 and 2.6 respectively.

Table 2.5 Formulations of SBR/EVA mixes

Ingredient	Vulcanizing System (phr)		
	Sulphur	DCP	Mixed
Polymer	100.0	100.0	100.0
Zinc oxide	4.0	4.0	4.0
Stearic acid	2.0	2.0	2.0
MBTS [a]	1.5	-	1.5
Dicumyl peroxide (40% active)	-	4.0	4.0
Sulphur	2.0	-	2.0

[a] Mercaptobenzothiazyl disulphide

Table 2.6 Formulations of SBR/EVA/compatibilizer and SBR/EVA/filler mixes

Ingredient	Vulcanizing system (phr)		
	Sulphur	DCP	Mixed
Polymer	100.0	100.0	100.0
Zinc oxide	4.0	4.0	4.0
Stearic acid	2.0	2.0	2.0
MBTS[a]	1.5	-	1.5
Dicumyl peroxide (40% active)	-	4.0	4.0
Sulphur	2.0	-	2.0
DCSBR (Compatibilizer)	Varying amounts (3, 6, 9, 12 phr)		
Carbon black	Varying amounts (10, 20, 30 phr)		
Silica	Varying amounts (10, 20, 30 phr)		
Chitin	Varying amounts (10, 20, 30 phr)		

2.2.2 Time for Optimum Cure

The optimum cure time (t_{90}) at 160 °C was determined by using a Monsanto Rheometer (R-100) at a rotational frequency of 100 cycles/min (MDR 2000), according to ASTM D-5289 (2001). The optimum cure time corresponds to the time to achieve 90 % (t_{90}) of the maximum torque.

2.2.3 Moulding of Test Samples

The uncured samples were marked along the direction of the mill grain and were vulcanized at 160 °C using a hydraulic press having electrically heated platens, under a pressure of 689.4 kPa (mould dimension:150 × 150 × 2 mm^3). The different crosslinking systems used were sulphur (S), dicumyl peroxide (DCP), and mixed (S+DCP). The blend compositions have been designated as 100/0 (pure SBR), 80/20 SBR/EVA, 60/40 SBR/EVA, and so on upto 0/100 (pure EVA). Due to the processing difficulty, sulphur vulcanized 0/100 SBR/EVA and mixed 0/100 SBR/EVA samples could not be prepared.

2.2.4 Sorption Experiments

For diffusion experiments, circular samples of diameter 1.9 cm were punched out from the vulcanized sheets and were dried overnight in a vacuum desiccator. The thickness of the samples was measured using a micrometer screw gauge with an accuracy of ±0.01mm. The samples were immersed in stoppered test bottles, kept in a thermostatically controlled air oven. At regular intervals, the test samples were removed from the solvents; solvent adhered to the surface was rubbed off, and weighed on a highly sensitive electronic balance (Shimadzu AW 210, Japan) that measured reproducibly within ±0.0001g. They were then placed back into the test

bottles. The process was continued until equilibrium swelling was achieved. To minimize the error due to the evaporation of the solvent from the samples, the time for weighing was kept to a minimum of 30s in all the experiments [3]. Similar methodology has been adopted by several researchers [4-11]. The experiments were duplicated in most cases and the deviation was within ± 0.07 to 0.1 mole %. The results of sorption experiments have been expressed by plotting the mole% uptake, Q_t, of the liquid by 0.1kg of the polymer blend against square root of time. Q_t was calculated according to the equation [12]:

$$Q_t = \frac{[\text{Mass of solvent sorbed/Molar mass of solvent}]}{\text{Mass of polymer blend}} \times 100 \quad \text{.....2.1}$$

2.2.5 X-ray Studies

In order to find out the degree of crystallinity of different blends, X-ray diffraction patterns of the samples were recorded using an X-ray diffractometer with Ni-filtered CuK_α radiation from a Bruker D8 instrument. The angular range was 5 to 40° (2θ). Samples having same thickness and area were exposed to the X-ray source. The operating voltage and the current of the tube were kept at 40 kV and 20 mA respectively, throughout the experiments.

From the X-ray diffraction pattern, the areas under the crystalline (I_c) and amorphous portions (I_a) were measured in arbitrary units and the degree of crystallinity (X_C) of the samples was calculated as:

$$X_C = \frac{I_c}{I_c + I_a} \quad \text{.....2.2}$$

where I_c and I_a represent the integrated intensities corresponding to the crystalline and amorphous phases respectively, i.e., the area under the respective curves.

2.2.6 Morphological Studies

Scanning electron microscopy (SEM)

The blend samples for scanning electron microscopy (SEM) were prepared by cryogenically fracturing them in liquid nitrogen. These samples were sputter coated with gold to eliminate the problems with sample charging and SEM examinations were performed on a Cambridge Instrument (S360),

2.2.7 Mechanical Properties

The mechanical properties of the blends were examined to complement the observations from transport studies. For this, the samples were dried at 60 °C for 3 hours to remove the moisture prior to the tests.

a) Stress-strain properties

Tensile testing of the samples was done at 25 ±2 °C according to ASTM D-412 test method using dumb-bell shaped test specimens at a cross head speed of 500 mm/min using a series IX automated material testing system 1.38 by Instron Corporation Model 4411 (Canton, MA, USA). The properties were calculated using the equations:

$$\text{Tensile strength} = \frac{\text{Load at failure (N)}}{\text{Area of cross section (mm}^2\text{)}} \quad \text{.....2.3}$$

$$\text{Ultimate elongation (\%)} = \frac{\text{Displacement at failure (mm)}}{\text{Effective gauge length (mm)}} \times 100 \quad \text{.....2.4}$$

For the measurement of mechanical properties, a minimum of five specimens per sample were tested and an average of the values obtained has been reported.

b) Tear strength

The tear strength of the samples was determined by using unnicked 90° angle test pieces according to ASTM D-624 (2002) test method. The instrument and the experimental conditions were the same as in the case of tensile testing. The tear strength was calculated using the equation:

$$\text{Tear strength} = \frac{\text{Load at failure (N)}}{\text{Thickness (mm)}} \qquad \text{.....2.5}$$

References

[1]. G. W. Gllby, *Developments in Rubber Technology-3, Thermoplastic Rubbers*, Applied Science Publishers, London, 1982.

[2]. M.T. Ramesan, G. Mathew, B. Kuriakose and R. Alex, *Eur. Polym. J.*, **37**, 719 (2001).

[3]. S. C. George, K.T. Varughese and S. Thomas, *Polymer*, **41**, 579 (2000)

[4]. E. B. Mano and R. C. R. Nunes, *Eur. Polym. J.*, **19**, 919 (1983).

[5]. S. B. Harogoppad and T. M. Aminabhavi, *Macromol.*, **24**, 2598 (1991).

[6]. D. Q. Vu, W. J. Koros and S. J. Miller, *J. Membr. Sci.*,. **211**, 311 (2003).

[7]. G. Flodberg, M. S. Hedengvist and U. W. Gedde, *Polym. Eng. Sci.*, **43**, 1044 (2003).

[8]. A. Sujith, C. K. Radhakrishnan, G. Unnikrishnan and S. Thomas, *J. Appl. Polym. Sci.*, **90**, 2691 (2003).

[9]. A. P. Haseena, K. Priya Dasan, R. Namitha, G. Unnikrishnan and S. Thomas, *Compos. Interface*, **11**, 489 (2004).

[10]. C. K. Y. Yiu, N. M. King, M. R. O. Carrilho, S. Sauro, F. A. Rueggeberg, C. Prati, R. M. Carvalho, D. H. Pashley and F. R. Tay, *Biomaterials*, **27**, 1695 (2006).

[11]. R. Stephen, K. Joseph, Z. Oommen and S. Thomas, *Compos. Sci. Technol.*, **67**, 1187 (2007).

[12]. S. B. Harogoppad and T. M. Aminabhavi, *Polymer*, **37**, 870 (1991).

Chapter 3

Molecular Transport of Aliphatic Hydrocarbons through SBR/EVA Blends

Summary

The sorption and diffusion of four aliphatic hydrocarbons viz. n-pentane, n-hexane, n-hetpane and n-octane through SBR/EVA blends were investigated in the temperature interval of 26-56 ° C, with special reference to the effects of blend composition, penetrant size and temperature. It has been observed that the solvent uptake decreases with increase in EVA content of the blends. This has been attributed to the increase in crystallinity when EVA content in the sample is increased. The blends have been found to sorb more amount of octane than hexane and heptane even though the former has the highest molecular mass among the penetrants; accounted in terms of the dominance of solubility parameter over the molecular mass of the solvents in controlling the solvent transport.

The contents of this chapter have been published in *Journal of Applied Polymer Science*, **101**, 2884 (2006).

3.1 Introduction

The importance of the examination of diffusion and transport behaviour of aliphatic hydrocarbons through polymeric materials, which are used in a wide variety of engineering applications, has been widely recognized [1-6]. George et al. [7] prepared blends of styrene-butadiene rubber (SBR) and natural rubber (NR) and studied their morphology, transport behaviour, and mechanical properties. The transport characteristics of SBR/NR blends were examined in an atmosphere of *n*-alkanes in the temperature range of 25-60 °C. Transport parameters such as diffusivity, sorptivity, and permeability were also estimated. Hao [8] studied the transport properties of sulphonyl containing polyimide membranes with aromatic/aliphatic hydrocarbon mixtures. The sorbed amounts of benzene and toluene in the membranes were 11 and 15g /100g dry sample, and those of aliphatics were much lower. The diffusion coefficient of the pure liquid was in the order: n-hexane > n-octane > benzene > toluene > cyclo-hexane > iso-octane. Aminabhavi et al. [9] investigated the sorption and diffusion of *n*-alkanes through EPDM/*i*PP blends at the temperature interval of 25-70 °C. Activation parameters for different transport processes and molar mass between crosslinks were evaluated and the results were used to discuss the polymer-solvent interactions. Unnikrishnan and Thomas [10] conducted diffusion experiments, using different aliphatic hydrocarbons, through crosslinked natural rubber.

This chapter deals with investigation of the transport behaviour of *n*-pentane, *n*-hexane, *n*-heptane and *n*-octane through SBR/EVA blends in the temperature range of 26 - 56 °C, with special reference to the effects of blend composition,

penetrant size and temperature. Different kinetic and thermodynamic parameters have also been evaluated from the diffusion data.

3.2 Results and Discussion

3.2.1 Effect of Blend Ratio

Figure 3.1 shows the liquid sorption behaviour of SBR/EVA blend systems vulcanized by sulphur at 26 °C. The penetrant used was hexane. The graphs clearly show that pure SBR has the highest equilibrium uptake, and upon blending it with EVA, the Q_t values regularly decrease. Pure EVA is semi-crystalline in nature. Upon blending semi-crystalline EVA with SBR, the rigidity of the matrix increases due to the introduction of crystallites in the matrix. The crystallites so introduced put up stiffer resistance to the penetrant molecules and result in a reduction in the free volume available within the matrix for solvent transport.

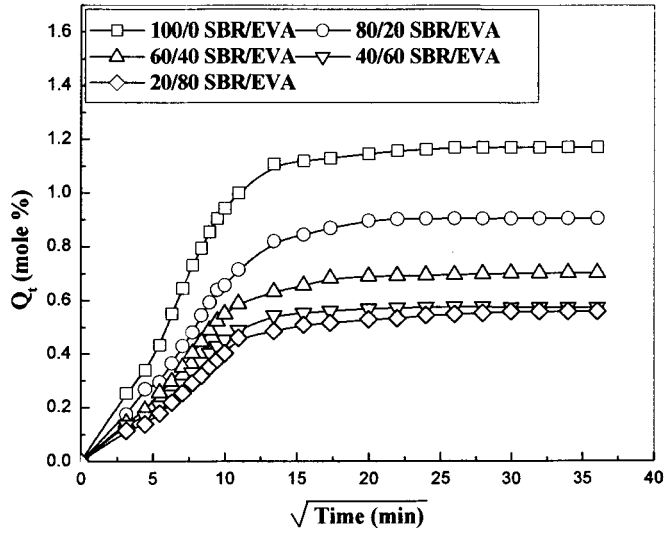

Figure 3.1 Mole % uptake of hexane by different blend compositions crosslinked by sulphur at 26 °C

The crystallinity of uncrosslinked EVA and crosslinked SBR/EVA blends, investigated by using wide angle X-ray scattering, has been given in Table 3. 1. The degree of crystallinity decreases with an increase in the SBR content. This is due to the migration of the amorphous component, SBR, to the crystalline regions of pure EVA. The introduction of crosslinks further reduces the crystallinity of the system which hinders the regular arrangement of the crystalline regions within the sample.

Table 3.1 Crystallinity of SBR/EVA blends

Sample	Degree of crystallinity (%)
0/100	34.50
20/80	26.10
40/60	19.80
60/40	12.60
80/20	6.60

Figure 3.2 (a) shows the SEM photograph of sulphur vulcanized 60/40 SBR/EVA blend. The EVA particles have been found to be dispersed as domains in the continuous SBR matrix. Figures 3.2 (b) and 3.2 (c) show the change in phase morphology of the blends upon increasing the EVA content to 60 and 80 percent respectively. The domain size of the dispersed phase has been found to decrease and the blend attains a co-continuous morphology from the samples with 60% to 80% of EVA. It is clear from the SEM photographs that the free volume of the blends decreases with increase in EVA content, which contributes to the decrease in diffusion of the solvents through the blends with higher EVA content.

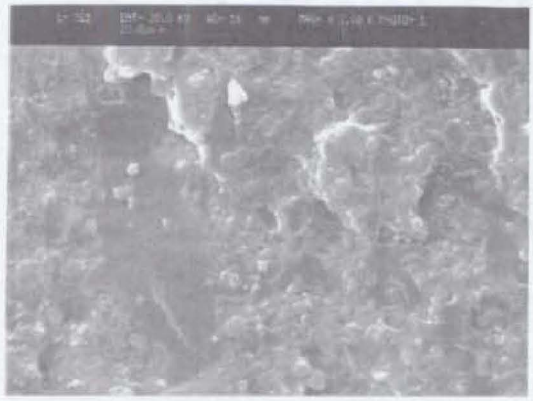

3.2 (a)

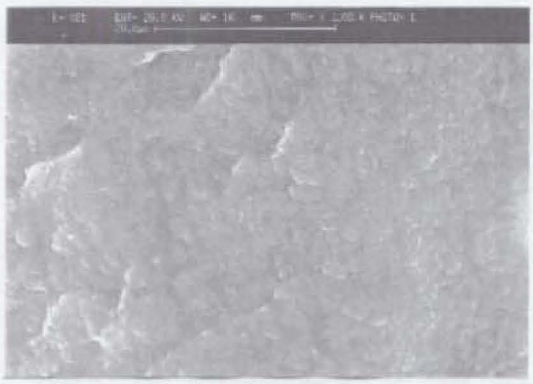

3.2 (b)

3.2 (c)

Figurer 3.2 (a) **60/40 SBR/EVA Sulphur system**
(b) **40/60 SBR/EVA Sulphur system**
(c) **20/80 SBR/EVA Sulphur system**

3.2.2 Effect of Penetrant Size

Figure 3.3 shows the effect of the penetrant size on the sorption and diffusion of four aliphatic hydrocarbons through sulphur vulcanized SBR/EVA systems. It follows from the graph that the trend is in the order: octane > hexane > pentane >

heptane for a gven blend ratio. Generally, the molecular mass and the solvent transport are inversely related [11]. However, it is interesting to note that the observation is not in full agreement with the normal effect of molecular mass on the solvent transport. Similar anomalous results were reported earlier too [12].

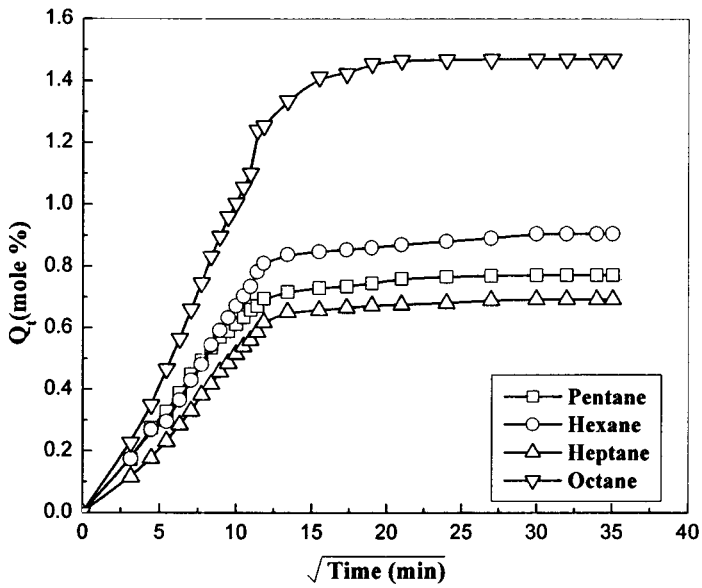

Figure 3.3 Mole % uptake of sulphur crosslinked 80/20 SBR/EVA in pentane, hexane, heptane and octane

The permeation through any matrix is a combination of sorption and diffusion processes. The diffusion kinetics depends on the molecular mass of the solvent whereas the sorption depends on the difference in the solubility parameter values. The net effect of these two parameters varies for different polymer-solvent systems. The lesser the difference in the solubility parameter values, the greater is the affinity of a polymer towards the solvent. The highest uptake exhibited by octane is due to the dominance of solubility parameter over the molecular mass factor during transport. The difference in the solubility parameters of the solvents and the polymer blend (δs - δp) has been plotted against the equilibrium sorption values in

Figure 3.4, which shows that as (δs - δp) increases, the equilibrium sorption value decreases.

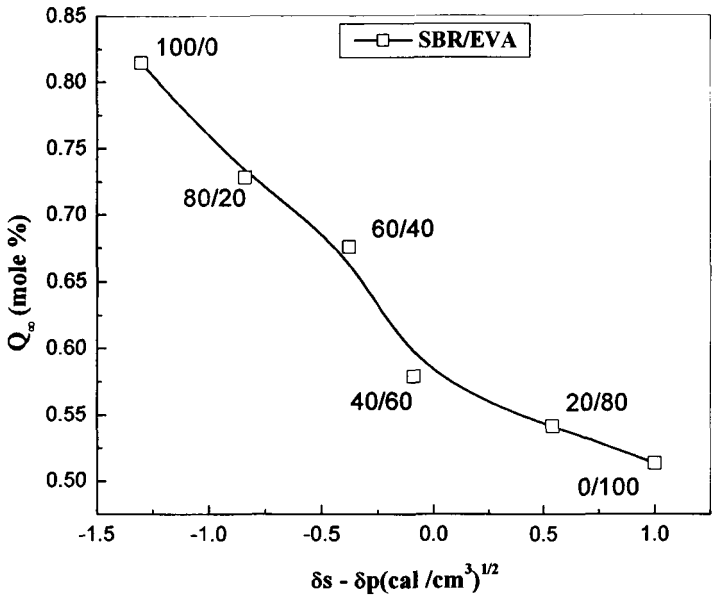

Figure 3.4 Variation of Q_∞ with δs -δp values for SBR/EVA blend in hexane

3.2.3 Intrinsic Diffusion Coefficient

The diffusion coefficient is a kinetic parameter related to polymer segmental mobility, penetrant nature, and to the type of crosslinks present in a polymer matrix. The diffusion coefficient of a polymeric material can be calculated by using the equation [13]:

$$\frac{Q_t}{Q_\infty} = 1 - 8/\pi^2 \sum_{m=0}^{m=\infty} \left[1/(2m+1)^2\right] \exp[-D(2m+1)^2 \pi^2 t/h^2] \quad \text{.....3.1}$$

where Q_t, and Q_∞, are the mol % uptake at time t and at equilibrium and m is an integer, whose values ranges from 0 to 1. D is the diffusion coefficient and h is the initial thickness of the sample. The modified equation for short time limiting is:

$$\frac{Q_t}{Q_\infty} = 4\left[\frac{Dt}{\pi h^2}\right]^{1/2} \quad \text{.....3.2}$$

By rearranging this equation, the overall diffusion coefficient can be calculated using the equation [15]:

$$D = \pi\left[\frac{h\theta}{4Q_\infty}\right]^2 \quad \text{.....3.3}$$

Where θ is the slope of the diffusion curves before attaining 50% of the equilibrium. A correction to diffusion coefficients under swollen conditions has been found to be essential because significant swelling was observed during sorption experiments in all the solvents. This was done by calculating the intrinsic diffusion coefficient D^* from the volume fraction V_r of the polymer blend samples using the expression [14]:

$$D^* = \frac{D}{V_r^{7/3}} \quad \text{.....3.4}$$

The computed D^* values are given in Tables 3.2. It has been found that D^* values decrease with EVA content in the blends, for a given solvent.

Table 3.2 Values of intrinsic diffusion and permeation coefficients

SBR/EVA	$D^* \times 10^6$ (m^2/s)			$P \times 10^6$(m^2/s)		
	Hexane	**Heptane**	**Octane**	**Hexane**	**Heptane**	**Octane**
100/0	6.65	4.78	45.62	6.69	4.45	100.72
80/20	3.39	2.78	19.26	2.64	2.64	32.28
60/40	2.77	2.04	8.45	1.67	1.09	9.81
40/60	1.53	0.91	3.50	0.81	0.54	3.14
20/80	1.23	0.76	2.60	0.63	0.31	3.05

The permeation coefficient for all the systems under investigation was also calculated by the equation [15]:

$$P = D^* S. \qquad \text{.....3.5}$$

where S is sorption coefficient, which is the ratio of the mass of the solvent absorbed to that of the initial weight of the polymer. The values of P are also given in Table 3.2, which show the same trend as that of D^* values. The variation in the values of D^* and P with blend composition for hexane is shown in Figure 3.5

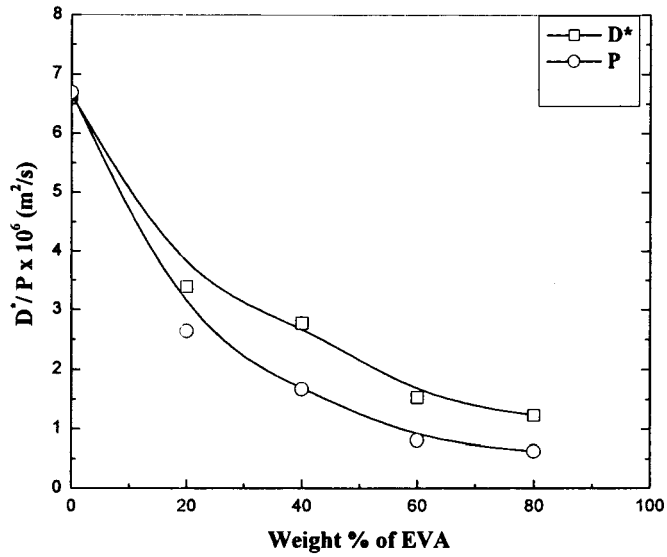

Figure 3.5 Variation of D^* and P with blend composition in hexane

3.2.4 Effect of Temperature

Figure 3.6 shows the temperature dependence of sulphur vulcanized SBR/EVA 80/20, in hexane. The rate of diffusion and the maximum uptake (Q_∞) have been found to increase with temperature. The disruption of the crystalline regions of EVA at elevated temperature and the increase in the kinetic energy of the penetrant molecules account for the observed activation of the transport process through the

blend systems. The variation of D^* values with temperature is shown in Figure 3.7. The solvents used were hexane and heptane. It was found that the D^* values increase with increase in temperature.

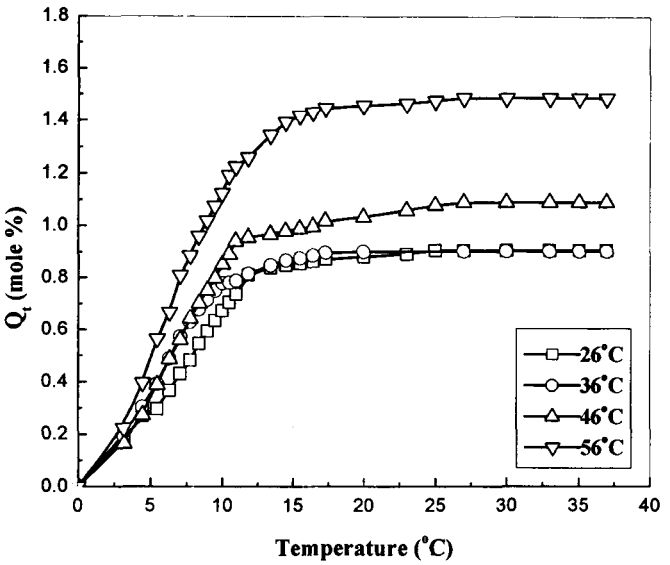

Figure 3.6 Temperature dependence of sulphur vulcanized 80/20 SBR/EVA blend in hexane

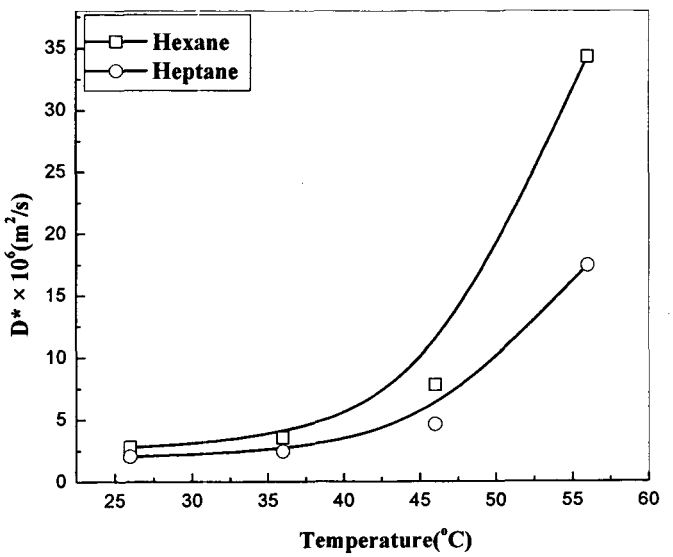

Figure 3.7 Variation of D^* values with temperature for 60/40 SBR/EVA blend in hexane and heptane

3.2.5 Interaction Parameter

Interaction parameter is a dimensionless quantity that characterizes the interaction energy per solvent molecule divided by *kT*. This indicates that interaction parameter χ is inversely related to temperature. The χ has been computed from Flory – Huggins theory of dilute polymer solutions [16] :

$$\chi = \beta + \frac{V_s}{RT}(\delta_s - \delta_p)^2 \qquad \text{.....3.6}$$

where δ_s and δ_p are the solubility parameters of the solvent and the polymer blends respectively. β is a lattice constant whose value is generally taken to be 0.34 for elastomer- solvent systems and *RT*, the usual energy term. Table 3.3 (a) gives the effect of blend ratio on interaction parameter. Similarly Table 3.3 (b), shows the effect of temperature on interaction parameter. It has been found that the χ values increase with EVA content in the blends, and decrease with the molecular mass of the penetrants. Further the χ values decrease with increase in temperature. Lower values of χ indicate higher polymer-solvent interactions [17].

Table 3.3 (a) Effect of blend ratio and penetrant size on interaction parameter χ at 26 °C

SBR/EVA	χ			
	Pentane	**Hexane**	**Heptane**	**Octane**
100/0	0.8366	0.7113	0.7001	0.6129
80/20	0.8875	0.7584	0.7497	0.6583
60/40	0.9409	0.8077	0.8026	0.7072
40/60	0.9896	0.8543	0.8514	0.7529
20/80	1.0477	0.9095	0.9102	0.8083

Table 3.3 (b) Effect of temperature on interaction parameter χ, in hexane

SBR/EVA	χ			
	26 °C	36 °C	46 °C	56 °C
100/0	0.7113	0.6992	0.6879	0.6773
80/20	0.7584	0.7448	0.7321	0.7200
60/40	0.8077	0.7931	0.7788	0.7655
40/60	0.8543	0.8376	0.8219	0.8072
20/80	0.9095	0.8909	0.8736	0.8574
0/100	0.9675	0.9471	0.9280	0.9101

3.2.6 Molecular Mass between Crosslinks

In order to find out how well the observed solvent uptake behavior correlates with the crosslink distribution in the matrix, the molecular mass between crosslinks M_c has been calculated using Flory – Rehner equation [18]:

$$M_c = \frac{-\rho_p V_s V_r^{\frac{1}{3}}}{\left[\ln(1-V_r+V_r+\chi V_r^2\right]} \qquad \text{.....3.7}$$

where ρ_p is the density of the matrix, V_s is the molar volume of the solvent and χ is the blend – solvent interaction parameter, as determined by Equation 3.6 The computed M_c values are given in Table 3.4. It has been observed that there is a regular decrease in the M_c values with increase in EVA content. These values are in good agreement with the observed effects of blend ratio and the penetrant size on solvent transport. However it is interesting to note a change in the M_c values for a given blend ratio with the change of penetrants. This can be explained by distinguishing between the apparent concentration of physical crosslinks $X_{(phy)}$ and the concentration of chemically discrete crosslinks $X_{(che)}$ that result directly from

vulcanization. The physical and chemical effects are additive, and $X_{phy} = X_{che} + X_{int}$, where X_{int} is the initial crosslink density due to entanglements, constrains or other effects due to chemical changes. Since the rubber chain entanglements can be different in different solvents, the M_c values obtained from Florry-Rehner theory, applied to a series of rubber-solvent systems, can be regarded as physical crosslinks. The changes in the rubber chain entanglement density in different solvents can probably be the reason for the variation of M_c values with change of solvent [19].

Table 3.4 Values of molecular mass between crosslinks M_c

SBR/EVA	M_c (kg/mol)			
	Pentane	**Hexane**	**Heptane**	**Octane**
100/0	4.379	8.563	1.650	36.215
80/20	2.648	3.544	1.366	27.676
60/40	0.830	1.320	0.825	4.873
40/60	0.723	0.881	0.567	4.129
20/80	0.653	0.804	0.649	3.772

3.2.7 Mechanism of Sorption

In order to find the mechanism of transport phenomenon, the dynamic swelling data have been fitted to the equation [20]

$$\log Q_t/Q_\infty = \log k + n \log t \quad \text{..... 3.8}$$

Here Q_t and Q_∞ are the mole % increase in sorption at time t and at equilibrium respectively. k is constant depending on the structural characteristics of the polymer blend in addition to its interaction with the solvent. The magnitude of n denotes the transport mode. When $n = 1$, the diffusion mechanism is said to be non-Fickian and the rate of relaxation of the polymer chain is slower than the solvent

diffusion. If the value is 0.5, then the mechanism is Fickian and the rate of polymer chain relaxation is higher compared to the diffusion rate of the penetrant and if the value lies between 1 and 0.5 the mechanism is said to follow an anomalous trend where the polymer chain relaxation rate and the solvent diffusion rate are similar. The values of n and k are given in Table.3.5. The n values indicate that the mechanism of transport slightly deviates from the normal Fickian behaviour, observed for conventional elastomers.

Table 3.5 Values of *n* and k

SBR/EVA	*n*				$k \times 10^2$ (g/g min^2)			
	Pentane	Hexane	Heptane	Octane	Pentane	Hexane	Heptane	Octane
100/0	0.54	0.58	0.62	0.63	10.13	4.99	4.84	4.40
80/20	0.55	0.59	0.63	0.64	6.54	4.78	3.55	3.34
60/40	0.58	0.62	0.64	0.65	5.44	4.51	3.79	4.13
40/60	0.58	0.63	0.65	0.66	5.44	5.78	3.65	3.36
20/80	0.59	0.63	0.64	0.67	3.35	5.28	3.25	3.13

The experimental sorption results were compared with the Fickian mode curves generated using the Equation 3.8. Figures 3.8 and 3.9 show a comparison of experimental sorption curves with Fickian mode curves for 60/40 and 40/60 SBR/EVA blends vulcanized by sulphur, in octane and hexane respectively. These curves indicate a deviation from the normal Fickian mode of diffusion. Out of this, more deviation from the Fickian trend is observed for 40/60 SBR/EVA which has higher EVA content than 60/40 system.

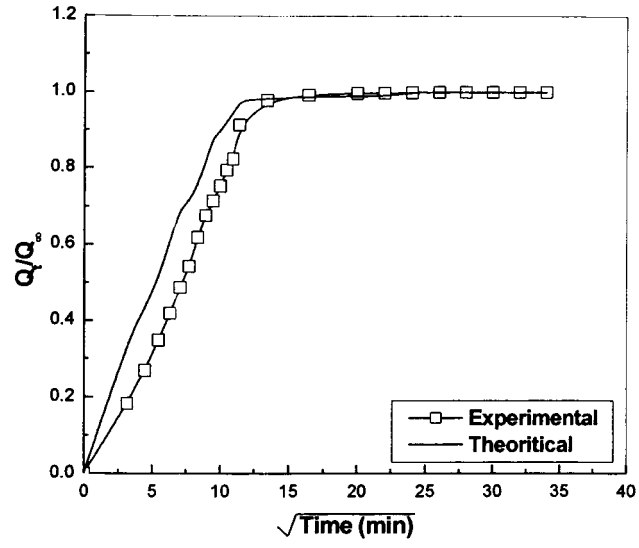

Figure 3.8 Experimental and theoretical sorption curves of 60/40 SBR/EVA, in octane

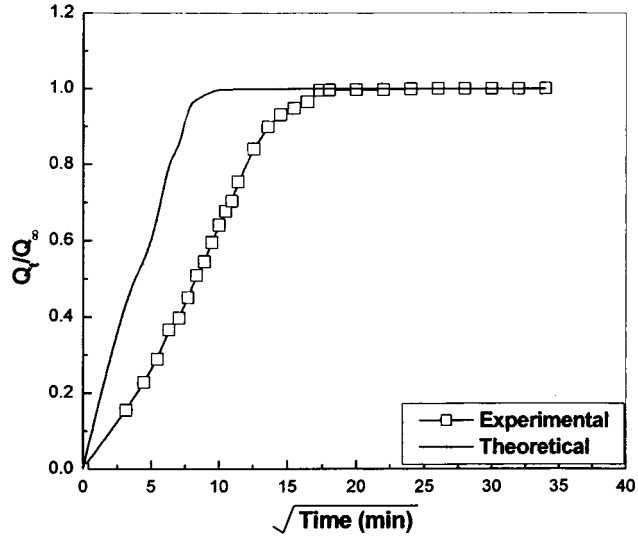

Figure 3.9 Experimental and theoretical sorption curves of 40/60 SBR/EVA, in hexane

3.3. Conclusion

The transport characteristics of sulphur crosslinked SBR/EVA blends were studied using *n*-pentane, *n*-hexane, *n*-heptane and *n*-octane as penetrants in the temperature

range of 26-56 °C, with special reference to the effects of blend ratio, penetrant size and temperature. The regular reduction in solvent uptake by the blends with increase in EVA content has been attributed to the increase in the crystalline nature of the matrix. The solvent uptake followed the order: octane > hexane > pentane > heptane for a given blend system. The mechanism of transport deviated regularly from the normal Fickian behaviour with an increase in the proportion of EVA in the blends. The diffusion and permeation coefficient values decreased with increase in EVA content in the blends. The interaction parameter values were found to be increased with increase in EVA content and decreased with temperature. The calculated M_c values were observed to complement the experimental sorption values.

References

[1]. S. V. Dixon-Garrett, K. Nagai and B. D. Freeman, *J. Polym. Sci., Part B: Polym. Phys.*, **38**, 1078 (2000).

[2]. J. M. Vergnaud, *Liquid Transport Process in Polymeric Materials – Modeling and Industrial Applications*; Englewood Cliffs, NJ: Prentice-Hall, 1991.

[3]. G. Wiberg, M. S. Hedenqvist, R. H. Boyd and U. W. Gedde, *Polym. Eng. and Sci.*, **38**, 1640 (1998).

[4]. B. D. Freeman, I. Pinnau, *Polymeric Membranes for Gas and Vapour Separations*: Chemistry and Material Science. B. D. Freeman, I. Pinnau, editors. ACS Symposium Series Number 733: American Chemical Society. Washington, DC., 1999,

[5]. S. Schlick, Z. Gao, S. Matsukawa, I. Ando, E. D. Fred and G. Rossi, *Macromol.*, **31**, 8124 (1998).

[6]. A. Y. Polishchuk, A. J. M. Valent, G. Camino, M. P. Luda, N. N. Madyuskin, V. M. M. Lobo, G. E. Zaikov, and M. Revellino, *J. Appl. Polym. Sci.*, **83**, 1157 (2002).

[7]. S. C. George, K. N. Ninan, G. Groeninckx and S. Thomas *J. Appl. Polym. Sci.*, **78**, 1280 (2000).

[8]. J. Hao, *J. Membr. Sci.*, **132**, 97 (1997).

[9]. T. M. Aminabhavi, H. T. S. Phayd, J. D. Ortego, C. Elliff and A. Rao, *J. Polym. Eng.*, **16**, 121 (1996).

[10]. G. Unnikrishnan and S. Thomas, *J. Polym. Sci; Part B: Polym. Phys.*, **35**, 725 (1997).

[11]. A. E. Mathai and S. Thomas, *J. Macromol. Sci., Phys.*, **35**, 229 (1996).

[12]. G. Unnikrishnan and S. Thomas, *Polymer*, **39**(17), 3933 (1998).

[13]. S. C. George, K. T. Varughese and S. Thomas, *Polymer*, **41**, 579 (2000)

[14]. W. R. Brown, R. B. Jenkins and G. S. Park, *The Sorption and Diffusion of Small Molecules in Amorphous and Crystalline Polybutadienes,* Charles, A. Kumins, editors, New York: Inter Science, 1973.

[15]. J. Brandrup and E. H. Immergut, *Polymer Hand Book.* New York: Wiley, 1975.

[16]. P. J. Flory. *Principles of Polymer Chemistry*; Cornell University Press: Ithaca, NY, 1953.

[17]. M. H. V. Mulder, in: *Pervaporation Membranes Separation Processes*, Huang, R. Y. M. (Ed.), Elsevier Science, Amsterdam, 1991.

[18]. T. M. Aminabhavi and H. T. S. Phayde, *J. Appl. Polym. Sci.,* **55**, 1335 (1995).

[19]. G. Unnikrishnan, S. Thomas and S. Varghese, *Polymer,* **37**, 2687 (1996).

[20]. S. B. Harogoppad and T. M. Aminabhavi, *Polymer*, **37**, 870 (1991).

Chapter 4

Interaction of SBR/EVA Blends with Chlorinated Hydrocarbons

Summary

Diffusion and transport through crosslinked SBR/EVA blends have been studied using dichloromethane, chloroform and carbon tetrachloride as penetrants in the temperature range 26-46° C. Significant differences have been observed between the blends crosslinked by three different vulcanizing modes viz. sulphur, dicumyl peroxide (DCP) and a mixed system consisting of sulphur and peroxide. This has been attributed to the different types of crosslinks formed between the macromolecular chains during vulcanization. Among the three penetrants, the blends show the highest Q_∞ values in chloroform. This has been explained in terms of the higher polar-polar interaction between the solvent and EVA phase in the blends. Sorption, desorption, resorption and redesorption processes have been carried out to examine the structural changes occurring in the blend matrix during solvent transport. Mechanical testing of the blends under unswollen, swollen and deswollen conditions has also been carried out to complement the observations from transport experiments.

Results of this chapter have been published in *Progress in Rubber, Plastic and Recycling Technology*, **22,** 89 (2006).

4.1 Introduction

The study of the interaction of polar solvents with polymeric blends is very important from a practical point of view. The use of polymeric membranes for the separation of hazardous solvents from organic liquid mixtures, as liners and for making storage tanks, is increasing. For the proper selection of polymers and the optimization of the matrix formulations for all these applications, it is essential to examine the interaction of different matrices with different polar solvents. The investigation on the change in the mechanical properties of polymeric systems upon swelling is also important to predict their reusability.

Typical studies related to the transport of polar solvents through different macromolecular systems are available in literature. For example, Nunez et al.[1] studied the barrier properties of polyamide 6/high density polyethylene blends. A gravimetric permeation cell was used for determining the permeability of different solvents (CH_2Cl_2, $CHCl_3$ and CCl_4) through these blends. The results showed that the permeability decreased with increase in the size of penetrant molecules and this decrease was more notable for a compatibilized blend. Johnson and Thomas [2] prepared transparent non-porous membranes by blending NR with ENR. These blend membranes were used to evaluate the selective separation of chlorinated hydrocarbons from acetone. The flux and selectivity of the membranes were determined both as a function of the blend ratio and feed mixture composition. Results showed that polymer blending method could be very useful to develop new membranes with improved permselectivity and the pervaporation properties could

be optimized by adjusting the blend composition. The transport characteristics of irradiated linear LDPE were studied by Naddeo et al. [3] using a non-polar molecule *n*-pentane, and a polar molecule dichloromethane.The formation of polar groups in the irradiated samples caused a higher sorption of dichloromethane whereas the sorption of *n*-pentane was found to be dependent only on the amorphous fraction. George et al. [4] investigated the permeation of chlorinated hydrocarbons through SBR/NR blends. The effect of structure of the penetrant on the permeation through the blend membranes was investigated and the results were compared with the permeation of oxygen and nitrogen gases. The diffusion of cyclohexanone through crosslinked NBR/EVA blends was studied by Soney et al. [5], with special reference to the effect of blend composition, crosslinking systems, fillers, filler loading, and temperature. The penetrants used were dichloromethane, chloroform, and carbon tetrachloride. Anil et al.[6] reported the permeation characteristics during the pervaporation process of carbon tetrachloride-acetone mixtures through poly(ethylene-*co*-vinyl acetate) membranes. They found that the membranes modified with dicumyl peroxide exhibited higher flux and selectivity than those with benzoyl peroxide. The response behaviour of a sensor for chlorinated hydrocarbons (CHCs) in water was evaluated practically and theoretically by Gobel et al. [7]. The experiments, containing attenuated total reflection (ATR) elements coated with polymers such as low-density polyethylene, polyisobutylene and ethylene/propylene copolymer, were based on the diffusion behaviour of the CHCs in different polymer layers. A classical Fickian response was found to be the dominant diffusion behaviour. Duncan et al. [8] measured

permeabilities and diffusivities of methyl chloride and benzene vapours at low activities in teflon membranes in a continuous-flow permeation cell, at temperatures ranging from 47 °C to 150 °C. In all the cases investigated, the permeabilities and diffusivities were found to be independent of the penetrant partial pressure and the process was well described by a Henry's law sorption-Fickian diffusion model. Unnikrishnan and Thomas [9] studied the interaction of crosslinked natural rubber with chlorinated hydrocarbons. It was observed that the kinetics of liquid sorption in every case deviated from the regular Fickian trend.

The objective of the present chapter is to study the diffusion and transport characteristics of SBR/EVA blends using three chlorinated hydrocarbons as probe molecules. The effects of blend composition, nature of crosslinks, penetrant size, and temperature on the diffusion and sorption behaviour have been studied. Sorption, desorption, resorption and redesorption processes were carried out to examine the structural changes occurring in the blend matrix during solvent transport. Mechanical testing of the blends under unswollen, swollen, deswollen conditions was also conducted to complement the observations from transport experiments and to check the reusability of the blends.

4.2 Results and Discussion

4.2.1 Effect of Blend Ratio

Figure 4.1 shows the effect of blend composition on the solvent uptake behaviour of SBR/EVA blends, vulcanized by mixed system at 26 °C. The penetrant used was CCl_4. It is clear from the figure that the liquid uptake tendency decreases with

increase in EVA content in the blends, similar to the observations using aliphatic hydrocarbons, as detailed in chapter.3.

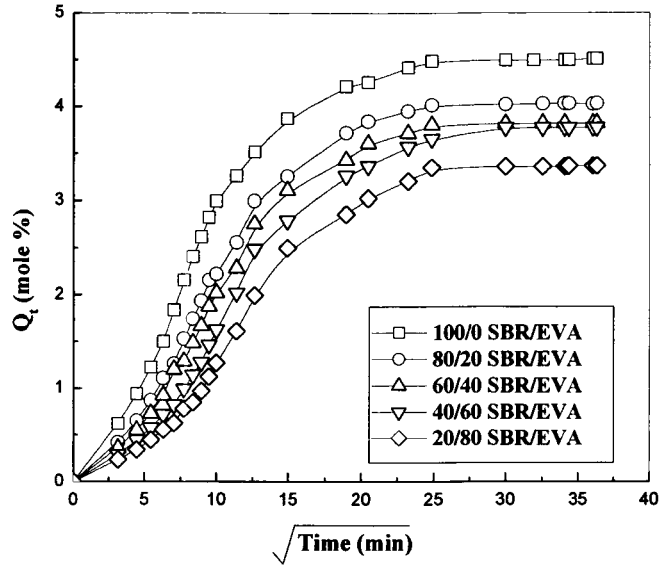

Figure 4.1 Mole % uptake of CCl_4 by different blend compositions crosslinked by mixed system, at 26 °C

4.2.2 Effect of Vulcanizing Systems

Figure 4.2 shows the sorption curves of 40/60 SBR/EVA crosslinked with three vulcanizing systems viz, sulphur, DCP and the mixed at 26 °C. The solvent used was carbon tetrachloride. It has been found that SBR/EVA blend crosslinked with sulphur system absorbs the highest amount of the penetrant, whereas that crosslinked with DCP system takes the lowest amount. The difference in the maximum uptake values of SBR/EVA blends with different crosslinking systems is defenitely due to the different types of crosslinks present in them.

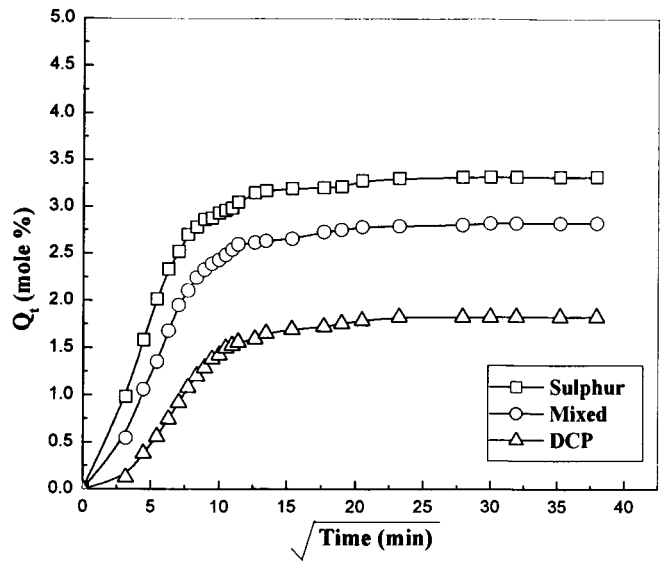

Figure 4.2 Mole % uptake of 40/60 SBR/EVA crosslinked by sulphur, mixed, and DCP, in CH_2Cl_2 at 26 °C

As shown in Figure 4.3, the sulphur vulcanization introduces flexible polysulphidic linkages between the macromolecular chains. The presence of more flexible S-S linkages permits the solvents to permeate more easily through the sulphur vulcanized samples and hence they show the highest uptake. The DCP vulcanized system has only stable C-C linkages and consequently shows the lowest Q_t values. In the mixed system, both types of crosslinks are present and hence an intermediate behaviour is observed. The values of bond length and bond energies, given in Table.4.1, also support this view.

Table 4.1 Bond length and bond energy of different types of chemical linkages

Type of bond	Bond length (nm)	Bond energy (kJ/mol)
C-C	0.154	355
C-S	0.181	267
S-S	0.188	238

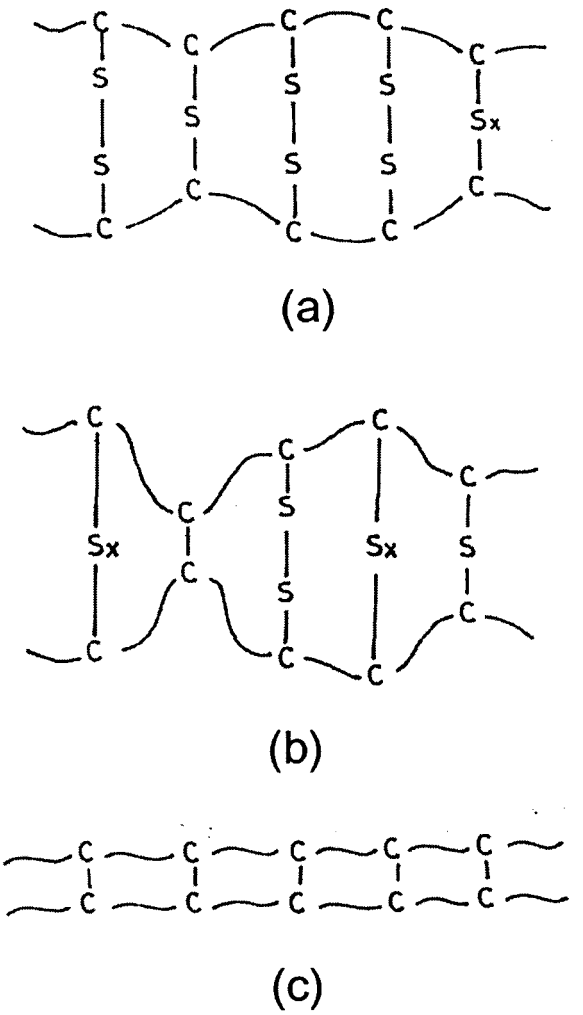

Figure 4.3 Schematic representation of different networks:

(a) Sulphur system
(b) Mixed system
(c) DCP system

Figures 4.4 (a) – (c) show the comparison between the phase morphology of 40/60 SBR/EVA blends vulcanized by sulphur, mixed and DCP system respectively. It is evident from the photographs that a fine and more uniform phase distribution is exhibited by the DCP vulcanized samples. The domain size of the dispersed phase has been found to decrease in the order sulphur > mixed > DCP. These changes in the morphology lead to a regular reduction in the free volume from sulphur to DCP

systems. Thus the observed solvent uptake behaviour of the blends with different vulcanizing systems has been found to be in good agreement with the morphology.

4.4 (a)

4.4 (b)

4.4 (c)

Figure 4.4 **SEM of (a) 40/60 SBR/EVA Sulphur system**
(b) 40/60 SBR/EVA Mixed system
(c) 40/60 SBR/EVA DCP system

4.2.3 Effect of Penetrant Size

Figure 4.5 illustrates the effect of the three penetrants on the transport through 60/40 SBR/EVA blend crosslinked with DCP. Among the three chlorinated hydrocarbons, chloroform shows the highest Q_t value. The transport behaviour through a matrix depends on many factors such as molecular size of the penetrant, polarity and its solubility in a given matrix. Generally, molecules of smaller size diffuse through a matrix faster than those with larger size and thus CCl_4, being larger in size, shows the lowest Q_t value. Further CCl_4 being non polar, its interaction with the polar polymer blend is lesser compared to the polar solvents such as CH_2Cl_2 and $CHCl_3$. The higher Q_t values for $CHCl_3$-blend system compared to the CH_2Cl_2-blend system can be explained in terms of the difference in the solubility parameter values. The solubility of a penetrant generally becomes high when the difference in the solubility parameter between the polymer and the penetrant is small [9]. In the present investigation, the difference in the solubility parameters of the polar solvents and the polymer blend, (δs - δp), is found to be in the order; $CH_2Cl_2 > CHCl_3$. [(δ_{SBR} = 17.26 (MPa)$^{1/2}$, δ_{CHCl_3} = 19 (MPa)$^{1/2}$, $\delta_{CH_2Cl_2}$ = 20.2 (MPa)$^{1/2}$ and δ_{EVA} = 18.35 (MPa)$^{1/}$2].

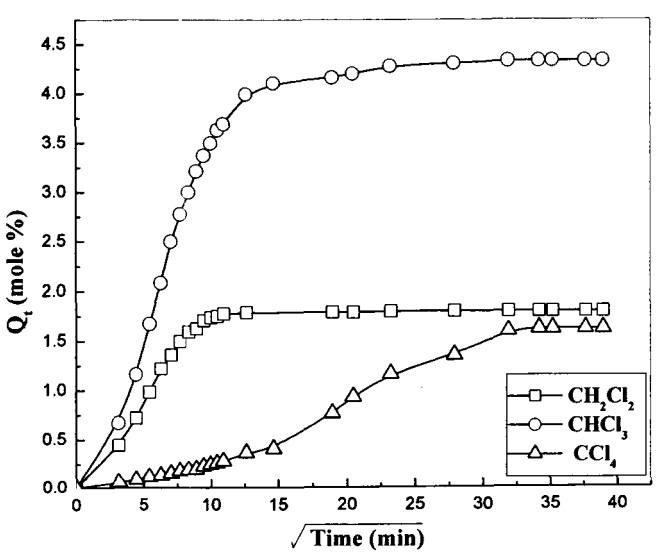

Figure 4. 5 Mole % uptake of 60/40 SBR/EVA crosslinked by DCP, in CH_2Cl_2, $CHCl_3$ and CCl_4

The highest Q_t value for the $CHCl_3$ - blend system is due to the strong dipole-dipole interaction. To evaluate the extent of interaction between the SBR/EVA matrix and the chlorinated hydrocarbons, the blend - solvent interaction parameter χ has been computed using Equation 3.6. The χ values for different blend systems vulcanized by DCP in different solvents at ambient temperature are shown in Table 4.2. It is interesting to note that the χ values increase regularly with increase in EVA content in the blends. The higher values of χ indicate lower blend - solvent interactions. Among the polar solvents used for the investigation, CH_2Cl_2 has higher χ value than $CHCl_3$ for all the blend ratios. This is in accordance with the observed solvent uptake values.

Table 4.2 Values of interaction parameter at 26 °C

SBR/EVA	χ	
	CH_2Cl_2	$CHCl_3$
100/0	0.5284	0.4043
80/20	0.5518	0.4201
60/40	0.5767	0.4376
40/60	0.6031	0.4568
20/80	0.6307	0.4778
0/100	0.6598	0.5005

4.2.4 Diffusion Coefficient and Permeation Coefficient

The diffusivity, D, of the blend - solvent systems has been calculated using the equation [10]:

$$\frac{Q_\infty - Q_t}{Q_\infty} = \sum_{n-1}^{\infty} \frac{2G^2}{\beta_n^2\left(\beta_n^2 + G^2 + G\right)} \exp\left[\frac{-\beta_n^2 Dt}{L^2}\right] \qquad \text{.....4.1}$$

where β_n are the positive roots of :

$$\beta . \tan \beta = G \quad \text{.....4.2}$$

and the dimensionless term G is given by:

$$G = \mathrm{h}.L/D \quad \text{.....4.3}$$

where 'L' is half the length of thickness of the sheet in contact with the liquid on both surfaces, and 'h' is the finite coefficient of convection at the interface. The values of intrinsic diffusion coefficient $D,^{*}$ calculated from D and the volume fraction V_r of the polymer blend samples using the expression 3.4, are given in Table 4.3. It is found that D^* values are the highest for the sulphur system and the lowest for the DCP system in a given penetrant. These observations are in good agreement with the decrease in the values of sorption equilibrium in the order: sulphur > mixed >DCP. The permeation coefficient for all the systems is also given in Table 4.3. It has been found that the trend is the same as that of D^* values.

Table 4.3 Values of diffusion coefficient and permeation coefficient

SBR/EVA	Vulcanizing system	$D^*\times10^5$ (m^2/s)	$P\times10^5$ (m^2/s)
100/0	Sulphur	12.51	108.07
	Mixed	9.11	63.17
	DCP	3.38	12.72
80/20	Sulphur	11.39	97.52
	Mixed	4.32	26.76
	DCP	0.56	1.58
60/40	Sulphur	9.66	75.29
	Mixed	4.03	23.30
	DCP	0.24	0.59
40/60	Sulphur	5.78	37.69
	Mixed	2.52	14.61
	DCP	0.15	0.41
20/80	Sulphur	2.24	15.80
	Mixed	1.76	9.13
	DCP	0.10	0.37

4.2.5 Activation Energy

The values of D^* at different temperatures have been used to estimate the activation energy for transport from the Arrhenius type relation [11]:

$$\log D^* = \log D_0^* - \frac{E_D}{2.303RT} \quad \text{.....4.4}$$

where D_0^* is the pre-exponential factor, R, the universal gas constant, T the temperature on the absolute scale and E_D the activation energy respectively. The calculated values of E_D are given in Table 4.4. The activation energy values are found to be the highest for sulphur system, and the lowest for DCP system. The highest E_D value of sulphur system clearly indicates its higher temperature sensitivity [12].

Table 4.4 Values of activation energy

SBR/EVA	Vulcanizing system	E_D (kJ/mol)	
		$CHCl_3$	CCl_4
100/0	Sulphur	34.48	13.57
	Mixed	11.54	6.04
	DCP	11.20	4.02
80/20	Sulphur	35.15	20.29
	Mixed	28.04	9.07
	DCP	21.82	8.32
60/40	Sulphur	43.48	35.38
	Mixed	35.84	15.91
	DCP	32.70	12.37
40/60	Sulphur	58.33	42.16
	Mixed	43.00	26.88
	DCP	40.17	35.42
20/80	Sulphur	65.13	49.52
	Mixed	58.22	32.53
	DCP	49.34	38.60

Figure 4.6 shows the Arrhenius plots of log D^* versus $1/T$. It is interesting to note that at 36 °C and 46 °C the D^* values show a reverse trend for blends with EVA content beyond 60 %. It can be explained on the basis of the effect of temperature on the crystallinity of EVA. At higher temperatures, higher EVA content samples lose their crystallinity and become more susceptible to temperature variations. This results in the non - torturous movement of the solvents through the matrix. Because of this, the higher EVA content samples show highest solvent uptake at higher temperature.

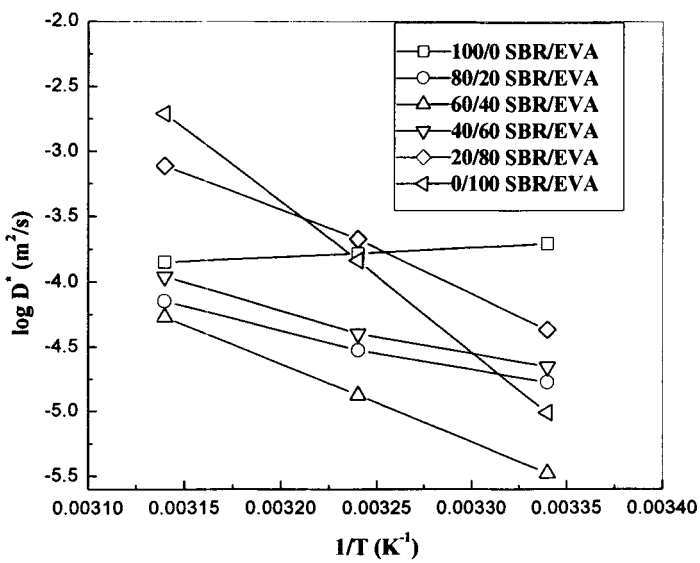

Figure 4.6 Arrhenius plots of different blend systems, vulcanized by DCP

4.2.6 Sorption (S), Desorption (D), Resorption (RS), and Redesorption (RD)

The S-D-RS-RD testing of a polymer in presence of hazardous liquids is important to judge its suitability in many field applications [13]. Figure 4.7 shows the behaviour of 80/20 SBR/EVA, vulcanized by mixed system, in CCl_4 for a cyclic process consisting of sorption, desorption, resorption, and redesorption. The initial region of the sorption and resorption curves is identical in nature. Hence it is clear

that the mechanism of transport is similar in sorption and resorption processes. However the resorption curves show that the equilibrium uptake values are higher compared to the first sorption process. In a sorption – desorption cycle the available free volume might increase due to the rearrangement of polymer chains and the subsequent sorption process is different from that of the former. Ferry [14] explained these network relaxation effects in terms of the times required for the molecular rearrangements of the chains and that of the solvent diffusion into the polymer.

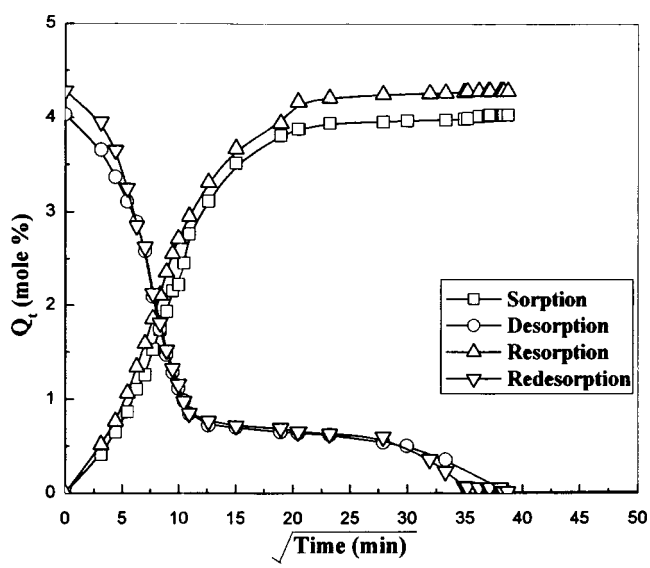

Figure 4.7 S-D-RS-RD curves for 80/20 SBR/EVA vulcanized by mixed system

4.2.7 Mechanical Properties

4.2.7.1 Effect of blend ratio

Figure 4.8 illustrates the stress-strain curves of dry samples. The samples used were 80/20, 60/40 and 40/60 SBR/EVA vulcanized by sulphur. The nature of deformation of the blends under an applied load can be understood from the stress-

strain curves. At a low strain level, 40/60 SBR/EVA sample has the maximum stress and 80/20 SBR/EVA sample has the minimum. 60/40 blend composition occupies an intermediate position. The stress required to break the samples has been found to be increased with increase in EVA content. This is due to the semi-crystalline nature of EVA. The elongation and modulus of the samples are given in Table 4.6. The sample having higher EVA content shows higher modulus and elongation.

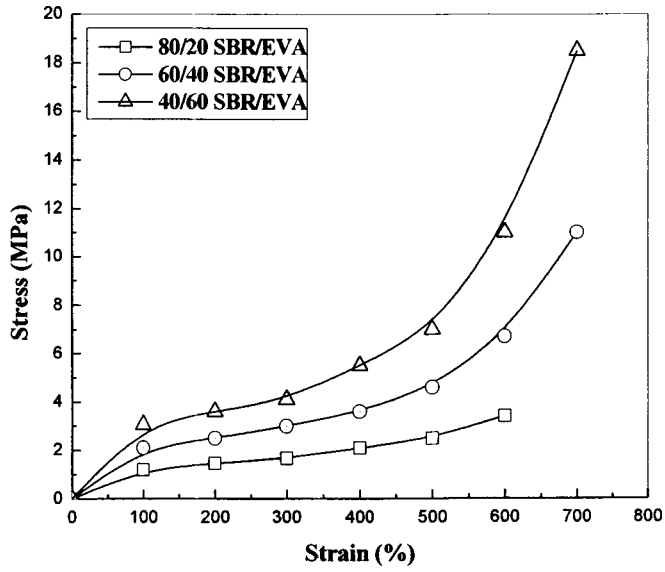

Figure 4.8 Stress-strain curves of 80/20, 60/40 and 40/60 SBR/EVA vulcanized by sulphur before swelling

Table 4.6 Effect of blend ratio on mechanical properties

Dry SBR/EVA	Elongation at break (%)	Modulus (MPa)		
		100%	200%	300%
80/20 Sulphur	581.9	1.324	1.602	1.896
60/40 Sulphur	695.6	2.060	2.533	3.026
40/60 Sulphur	704.7	3.103	3.599	4.151

Figure 4.9 shows the stress-strain curves of the samples after reaching equilibrium saturation in CCl_4. The modulus and elongation of the samples have been considerably reduced, after solvent sorption. It is due to the strong interaction between the blends and the solvents. In the equilibrium swollen state, the blend-solvent interaction is the maximum and the polymer-polymer interaction is minimum. This gives rise to an abrupt decrease in the tensile properties of the swollen samples.

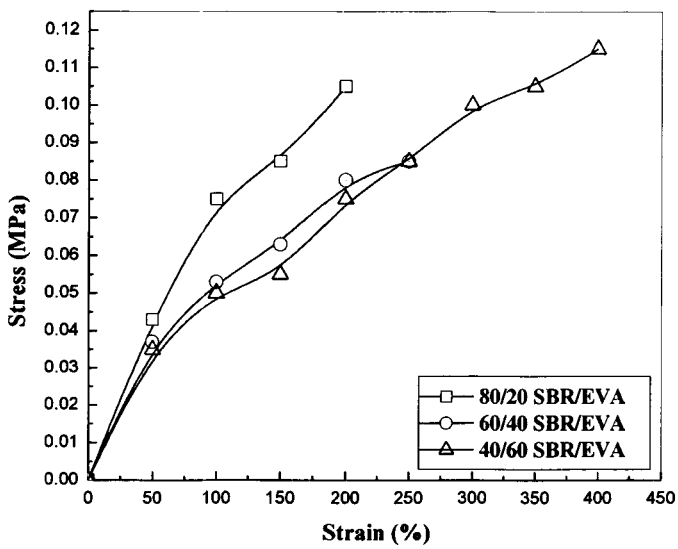

Figure 4.9 Stress- strain curves of 80/20, 60/40 and 40/60 SBR/EVA vulcanized by sulphur after reaching equilibrium in CCl_4

Figure 4.10 shows the stress-strain behaviour of the deswollen 80/20, 60/40 and 40/60 SBR/EVA samples. The plots are similar to those of the dry samples. However, there is an overall decrease in stress, strain, and elongation values, as given in Table 4.7. This decrease is attributed mainly to the disruption of EVA crystallites after a sorption-desorption cycle. The disrupted structures do not regain the original pattern, fully.

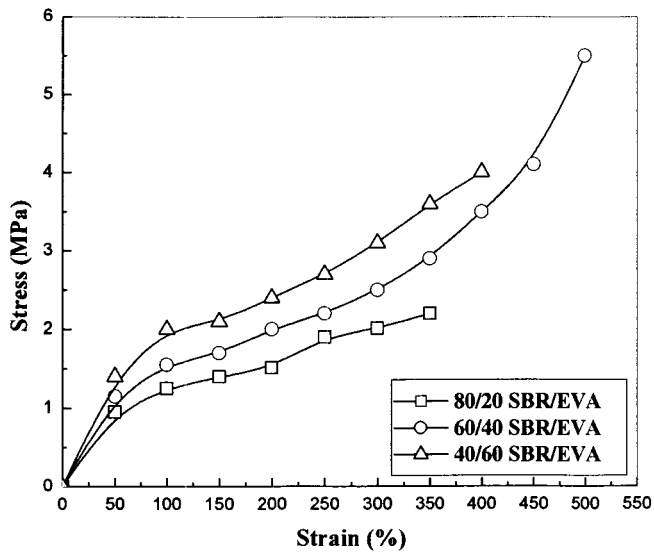

Figure 4.10 Stress-strain curves of 80/20, 60/40 and 40/60 SBR/EVA vulcanized by sulphur after a sorption-desorption cycle

Table 4.7 Effect of blend ratio on mechanical properties

Deswollen SBR/EVA	Elongation at break (%)	Modulus (MPa)		
		100%	200%	300%
80/20 Sulphur	379.9	1.340	1.739	2.176
60/40 Sulphur	416.9	1.635	2.026	2.596
40/60 Sulphur	446.1	2.051	2.518	3.398

Figure 4.11 shows the typical variation of tensile strength of 40/60 SBR/EVA samples vulcanized by DCP as a function of the exposure time in the solvent CCl_4, for the first 24 hours. It has been found that the tensile strength values of the samples decrease regularly as the time of exposure to the liquid medium increases. This is in agreement with the expectation that increase in liquid inhibition weakens the attractive forces between the macromolecular chains of the polymer blend. The rate of reduction in tensile strength is faster for the first four hours which then slowely declines with increase in exposure time.

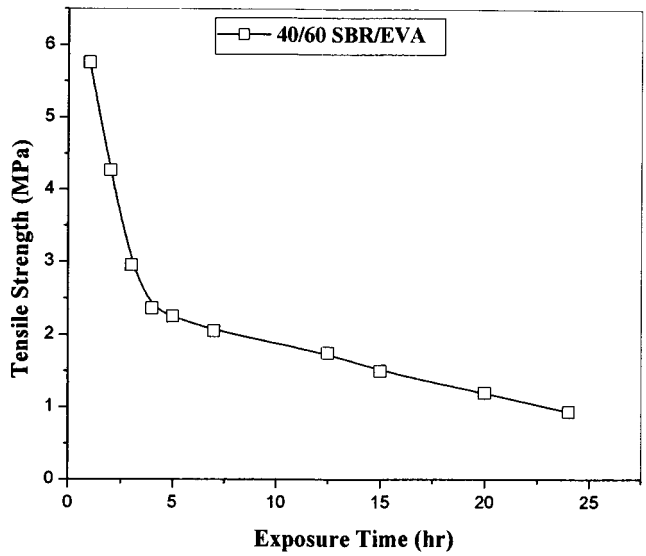

Figure 4.11 Variation of tensile strength of 4060 SBR/EVA vulcanized by DCP with exposure time in CCl_4

4. 2.7.2. Effect of crosslinking systems

Figure 4.12 shows a comparison between the tensile strength of 60/40 SBR/EVA blends crosslinked with sulphur, mixed and DCP at dry, swollen (in CCl_4) and deswollen conditions. Among all the systems, the tensile strength shows the order: DCP > mixed. > sulphur.

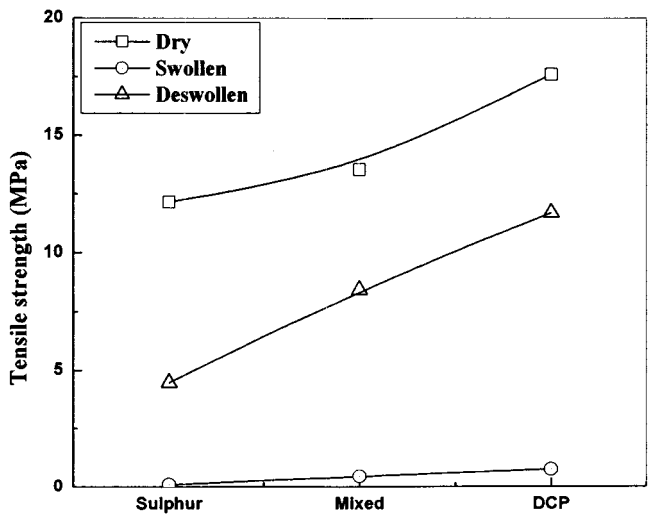

Figure 4.12 Variation of tensile strength of 60/40 SBE/EVA vulcanized by different systems under different conditions

4.3 Conclusion

Diffusion and transport through crosslinked SBR/EVA blends were studied using dichloromethane, chloroform, and carbon tetachloride as the penetrants in the temperature range of 26-46 °C. The effects of blend composition, crosslinking systems, and penetrant size on transport were analysed. The solvent uptake followed the trend: sulphur > mixed > DCP, for a given blend ratio. The examination of the tensile behaviour of the samples revealed that the stress required to break the blends increased with increase in EVA content. In the case of deswollen samples, there was a decrease in the magnitude of the maximum stress after a sorption-desorption cycle. This has been attributed to the rearrangement of polymer chains during a sorption-desorption process. The tensile properties of swollen samples were found to be significantly reduced which has been attributed to higher blend-solvent interaction than polymer-polymer interaction.

References

[1]. R. G. Nunez, H. Padilla, D. DeKee, and B. D. Favis, , *Polym. Bull.*, **46,** 323 (2001).

[2]. T. Johnson and S. Thomas, *J. Appl. Polym. Sci.*, **71**, 2365 (1999).

[3]. C. Naddeo, L. Guadagno, S. De Luca, V. Vittoria and G. Camino, *Polym. Degrad. Stab.*, **72**, 239 (2001).

[4]. S. C. George, K. N. Ninan, G. Gueskens and S. Thomas, *J. Polym. Eng.*, **23**, 423 (2003).

[5]. S. C. George, G. Groeninckx, K. N. Ninan and S. Thomas, *J. Polym. Sci., Polym. Phy.*, **37**, 1815 (1999).

[6]. S. Anil kumar, P. H. Gedam, V. S. Kishan Prasad, M. G. Kumaran, and S. Thomas, *J. Appl. Polym.* Sci., **60**, 735 (1996).

[7]. R. Gobel, R. W. Seitz, S. A. Tomellini, R. Krska, R. Kellner, *Vib. Spectrosc.*, **8**, 141 (1995).

[8]. T. Duncan, W. J. Koros, R. M. Felder, *J. Appl. Polym. Sci.*, **28**, 209 (1983).

[9]. G. Unnikrishnan and S. Thomas, *Polymer*, **39**, 3933 (1998).

[10]. T. M. Aminabhavi, H. T. S. Phayde, J. Dale Ortego, and J. M. Vergnaud, *Polymer*, **37,** 1677 (1973).

[11]. S. B. Harogoppad and T. M. Aminabhavi, *J. Appl. Polym. Sci.*, **42,** 2329 (1991).

[12]. K. J. Saunders, *Organic Polymer Chemistry*, 2nd ed., Chapman and Hall, London, 1988.

[13]. T. M. Aminabhavi, H. T. S. Phayde, J. D. Ortego and W. A. Rudzniski *J. Hazard. Mater.*, **49**, 125 (1996).

[14]. J. D. Ferry, *Viscoelastic Properties of Polymers*, John Wiley and Sons, New York, 1970.

Chapter 5

Effect of Compatibilizer on the Transport Properties of SBR/EVA Blends

Summary

The effect of a compatibilizer viz. dichlorocarbene modified SBR (DCSBR) on the sorption and diffusion characteristics of SBR/EVA blends vulcanized by DCP has been studied. Three aromatic hydrocarbons viz. benzene, toluene and xylene have been used as penetrants. A significant reduction in the sorption behaviour has been noticed after the compatibilization of the blends, which is attributed to the modification of the interface by the compatibilizer. The experimental observations on the transport behaviour of the blends have been correlated with their morphology, examined by SEM, and mechanical properties. The results of the transport experiments have been compared with different theoretical models.

Results of this chapter have been communicated to *Polymer Engineering and Science*, for publication.

5.1 Introduction

Many of the commercially available polymer blends are incompatible or immiscible and are characterized by a narrow interface and weak interfacial interaction. Such polymer blends often exhibit poor mechanical properties [1]. A variety of additives can be used to promote the miscibility by reducing the interfacial tension. Reactive compatibilizers chemically react with the blend components and are, therefore, effective for many systems. Non-reactive compatibilizers are typically block and graft copolymers of the partners and are more specific in their action. They can be useful in improving interfacial coupling [2]. The effect of compatibilizers on the properties of polymer blend matrices has extensively been studied [3-4].

Nikos et al. [5] studied the efficiency of four different compatibilizers for a poly(ethylene terephthalate)/high density polyethylene (PET/HDPE) blend. The compatibilizers used were ethylene-glycidyl methacrylate copolymer (E-GMA), ethylene ethylacrylate glycidyl methacrylate terpolymer (E-EA-GMA), hydrogenated styrene-butadiene-styrene copolymer grafted with maleic anhydride (SEBS-g-MA) and MA-modified ethylene-methyl acrylate copolymer (E-MeA-g-MA). The compatibilizing efficiency was found to be in the order: E-GMA > E-EA-GMA > SEBS-g-MA > E-MeA-g-MA. The influence of maleic anhydride grafting on the rheological properties of polyethylene terephthalate/styrene butadiene blends was studied by Sánchez-Solís et al. [6]. They measured the shear viscosity in a special capillary device mounted on an injection-moulding machine, which provided data on pressure and flow rate. They also compared the viscosity of the PET–SBR physical blend with that of a blend of PET with maleic anhydride-functionalized SBR (SBRg). Their work provided information on the effect of grafted maleic anhydride chains, at the rubber-thermoplastic interface, on the

rheological properties of the blend. Ismail et al.[7] reported the effect of a compatibilizer, styrene(epoxidised butadiene)-styrene triblock copolymer (ESBS), on the dynamic properties, curing characteristics and swelling behaviour of SBR and epoxidised natural rubber (ENR 50) blends. They found that the presence of ESBS improved the processability, increased the scorch time and reduced the cure time of the blends. Zhu and Chan [8] prepared blends of 50 wt% of poly(vinyl chloride) (PVC) and 40 wt% of styrene butadiene rubber (SBR) with 10 wt% of acrylonitrile butadiene rubber (NBR) as the compatibilizer in a Haake mixer, and reported an inversion of phase continuity when the concentration of sulphur, the curing agent, was changed from 0.0 to 2.0 parts per hundred parts of resin (phr) in the blends. The SBR phase, which was continuous in the unvulcanized blend, changed progressively into the dispersed phase as sulphur concentration was increased.

The objective of the present chapter is to study the effect of a compatibilizer viz. dichlorocarbene modified SBR on the transport behaviour of SBR/EVA blends. The influence of compatibilizer loading, blend composition and penetrant size on the sorption and diffusion characteristics of the blends has been investigated. The mechanical properties of the blends and the transport coefficients have also been evaluated.

5.2 Results and Discussion

5.2.1 Effect of Compatibilizer

Figure 5.1 shows the rheographs of compatibilized and uncompatibilized SBR/EVA blends vulcanized by DCP. The initial decrease in torque is due to the softening of the matrix. Torque then increases due to the formation of C-C crosslinks between

the macromolecular chains. The presence of DCSBR brings about sufficient interfacial adhesion between the phases. As a result of this, there is a reduction of surface energy mismatch between the constituents. The addition of 3 phr DCSBR in the DCP vulcanized SBR/EVA blends results in a substantial increase in the number of interfacial crosslinks, as evidenced by the increase in the maximum torque.

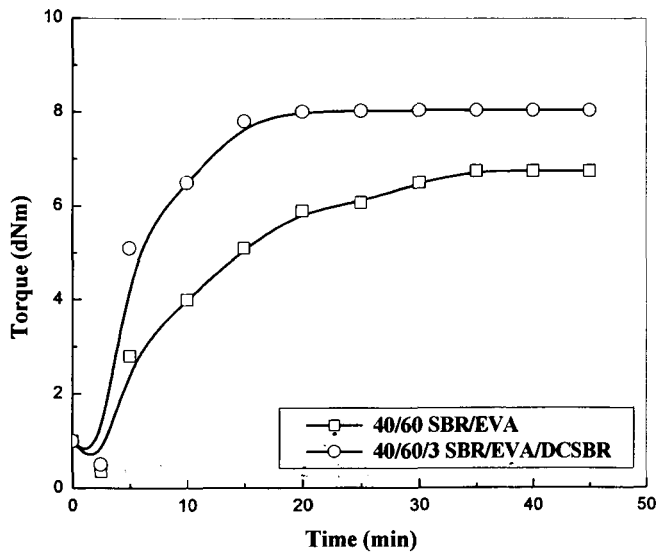

Figure 5.1 Rheographs of compatibilized and uncompatibilized SBR/EVA blends

The cure characteristics of the compatibilized and uncompatibilized samples are given in Table 5.1. The cure rate, R_H, defined as the ratio between torque and time has been determined from the following relationship:

$$R_H = \frac{M_{90} - M_2}{t_{90} - t_2} \qquad \text{.....5.1}$$

where M_{90} corresponds to 90% of the maximum torque, M_2 is the minimum torque, t_{90} is the time required to achieve 90% of the maximum torque (optimum cure time), and t_2 is the scorch time. The values of R_H are also given in Table 5.1.

Table 5.1 Effect of compatibilizer on the cure characteristics of SBR/EVA blends compatibilized by DCSBR

SBR/EVA/ DCSBR	t_2 (min)	t_{90} (min)	M_2 (dNm)	M_{90} (dNm)	M_H (dNm)	R_H (dNm/min)
40/60/0	2.2	19.0	0.31	6.07	6.74	0.3428
40/60/3	2.04	21.21	0.34	7.24	8.04	0.3597
40/60/6	2.06	19.41	0.39	8.01	8.9	0.4392
40/60/9	2.08	19.11	0.32	7.21	8.01	0.4045
40/60/12	2.11	19.02	0.31	7.11	7.95	0.4024

Figure 5.2 shows the sorption curves of compatibilized and uncompatibilized 40/60 SBR/EVA. The penetrant used was benzene. A significant reduction in diffusion rate and solvent uptake has been observed for the compatibilized sample compared to the uncompatibilized sample. This has been explained in terms of the increased interfacial adhesion between SBR and EVA components of the blends in presence of the compatibilizer. Conversely, the lower solvent uptake confirms the better interaction between the blend components in presence of the compatibilizer.

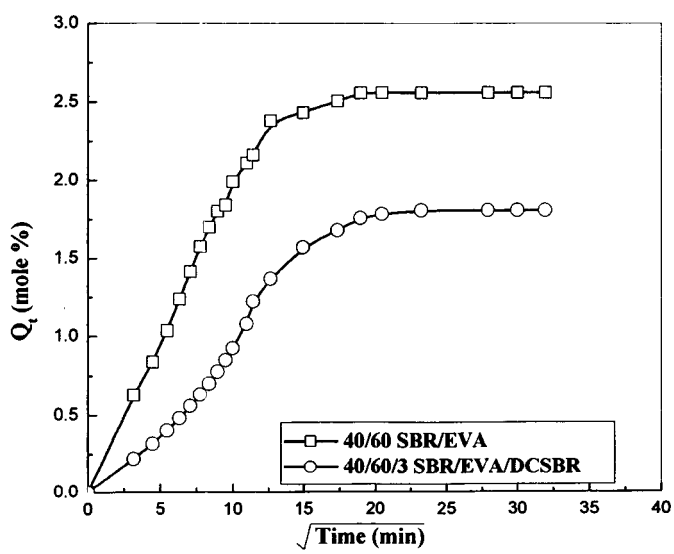

Figure 5.2 Sorption curves of compatibilized and uncompatibilized 40/60 SBR/EVA, with 3 phr of DCSBR

The mechanism of compatibilisation is schematically represented in Figure 5.3. The polar end of DCSBR interacts with the polar EVA phase and its non-polar part interacts with the non-polar SBR phase. These polar-polar and nonpolar-nonpolar interactions reduce the interfacial tension between SBR and EVA, and thus lead to a lower solvent uptake.

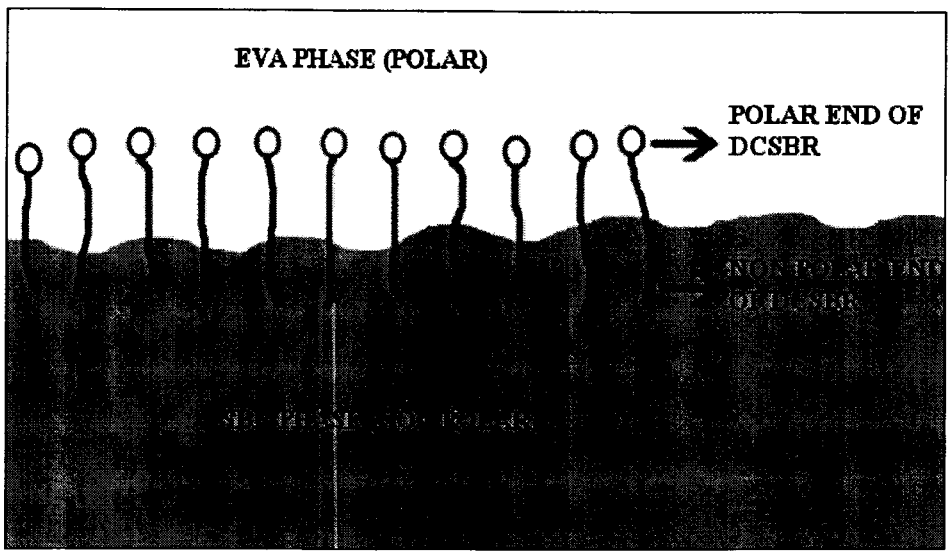

Figure 5.3 Schematic representation of mechanism of compatibilization

5.2.2 Effect of Compatibilizer Loading

Figure 5. 4 shows the rheographs of 40/60 SBR/EVA blends with different loadings of DCSBR. It has been found that SBR/EVA with 6 phr DCSBR has the highest rheometric torque. However, the torque decreases when the compatibilizer loading is increased further to 12 phr. The rheometric torque (M_H) is in the order: 3< 6> 9>12.It means that 6 phr is the optimum loading for the compatibilizer for the effective improvement in rheometric torque. The reduction in torque after 6 phr of compatibilizer has been attributed to the interfacial saturation. After the optimum

loading, the excess compatibilizer gets dispersed in the region outside the interface. Several researchers have reported the interfacial saturation of binary polymer blends by the addition of compatibilizers [9-10].

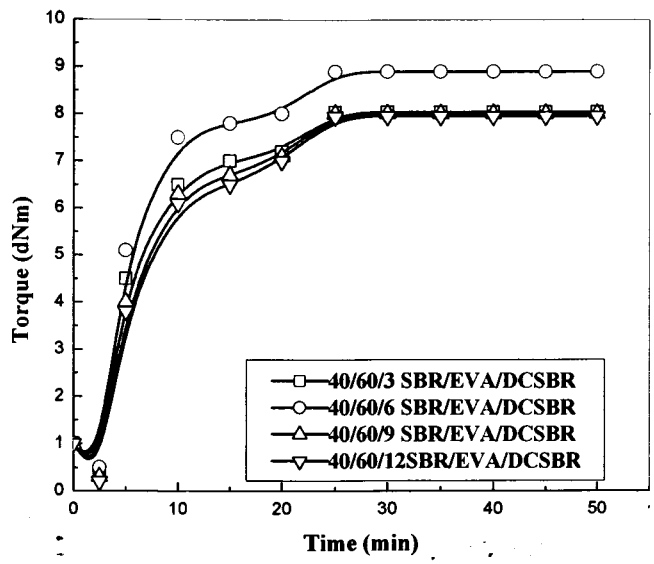

Figure 5.4 Rheographs of 40/60 SBR/EVA blends with different loadings of DCSBR

Figure 5.5 shows the effect of compatibilizer loading on the solvent uptake of 40/60 SBR/EVA blends. The penetrant used was benzene. The solvent uptake tendency decreases with increase in compatibilizer content up to a threshold level. The maximum reduction has been observed at 6 phr loading of the compatibilizer. This is definitely associated with the effective interfacial bonding at this loading. The solvent uptake has been found to be increased after further addition of the compatibilizer i.e., at 9 and 12 phr loadings. These are due to the saturation at the interface by the compatibilizer.

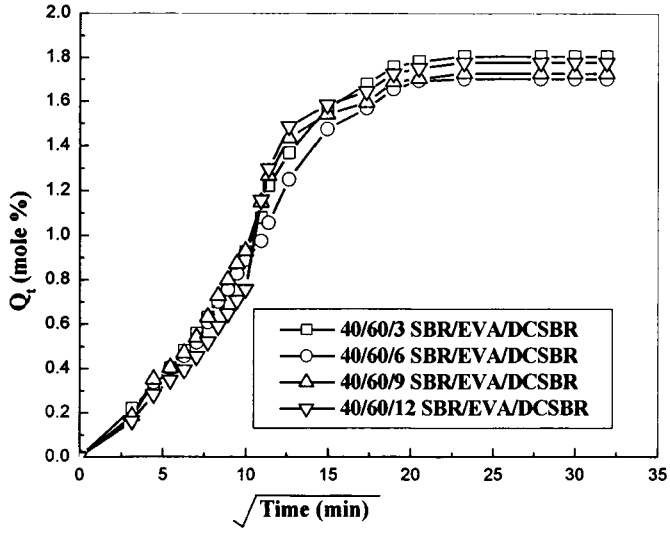

Figure 5.5 Effect of compatibilizer loading on the solvent uptake of 40/60 SBR/EVA blends

The excess DCSBR compatibilizer can be distributed within the matrix during processing which can lead to the unfolding of the crystallites of EVA. The defolding of the crystalline chains of EVA further enhances the solvent uptake tendency. This is evident from the scanning electron micrographs of 40/60 SBR/EVA and 40/60 SBR/EVA loaded with 3, 6, and 9 phr DCSBR respectively, shown in Figures 5.6 (a) - (d). At 6 phr, an interfacial saturation occurs and hence a more uniform morphology is obtained. At 9 phr loading the excess DCSBR after saturation, diffuses into the folded chains of EVA resulting in the defolding of the crystallites, and generates a more non-uniform morphology. This accounts for the enhancement in the solvent uptake tendency after the threshold value of 6 phr for compatibilizer loading.

5.6 (a)

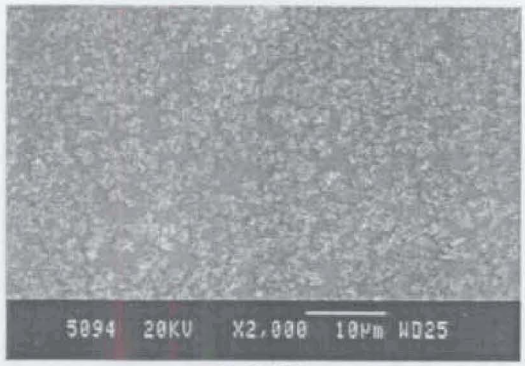

5.6 (b)

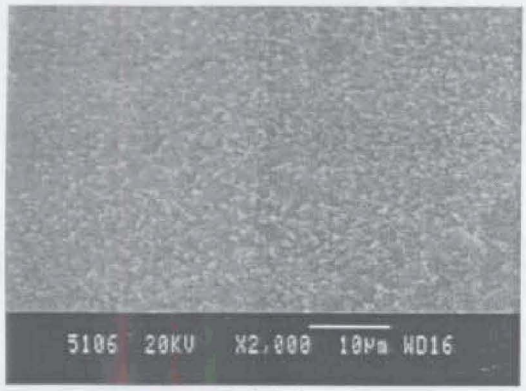

5.6 (c)

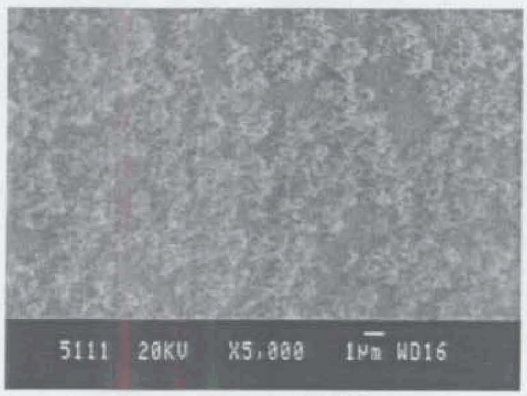

5.6 (d)

Figure 5.6 SEM of (a) 40/60 SBR/EVA
(b) 40/60/3 SBR/EVA/DCSBR
(c) 40/60/6 SBR/EVA/DCSBR
(d) 40/60/9 SBR/EVA/DCSBR

5.2.3 Effect of Blend Ratio

Figure 5.7 shows the effect of blend composition on the solvent uptake behaviour of compatibilized SBR/EVA vulcanized by DCP. These studies show that the compatibilizing action of DCSBR becomes more prominent as the proportion of EVA in the blend increases to 60%. The blends having EVA content above 60 %, however, show a slightly increased solvent uptake tendency.

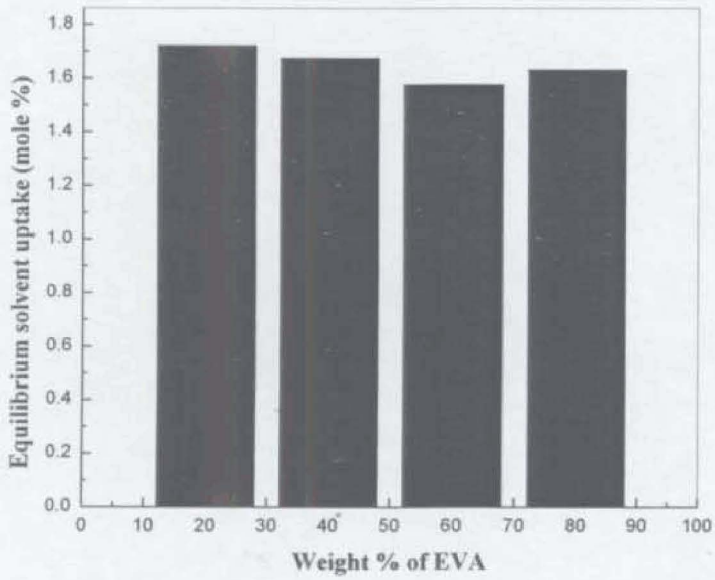

Figure 5.7 Effect of blend composition on the solvent uptake behavior of 40/60/6 SBR/EVA/DCSBR

5.2.4 Effect of Penetrant Size

Figure 5.8 shows the influence of penetrant size on the sorption of the three aromatic solvents viz, benzene, toluene, and xylene, through 40/60/6 SBR/EVA/DCSBR. As the size of the solvent molecules increases from benzene to xylene, the Q_∞ values have been found to be decreased. Benzene shows the highest Q_∞ value, while xylene the minimum. Toluene occupies an intermediate position. This trend is in agreement with the size and structure of the probe molecules.

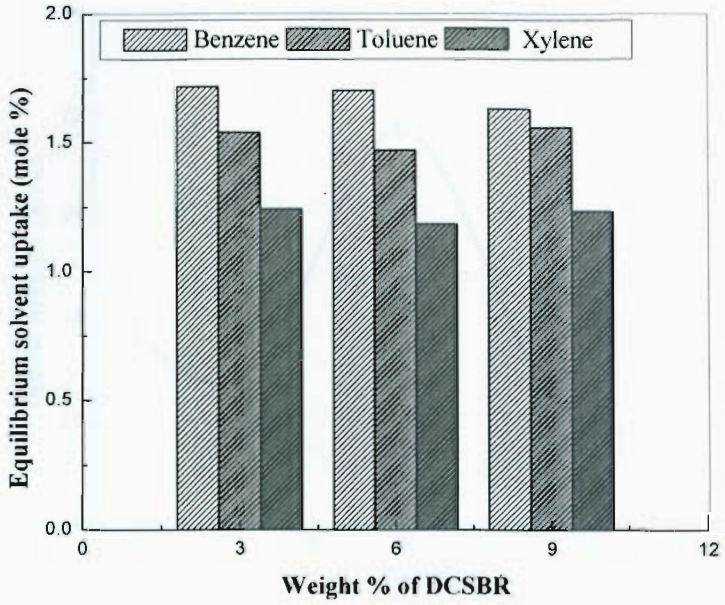

Figure 5.8 Equilibrium uptake of benzene, toluene, and xylene through 40/60/6 SBR/EVA/DCSBR

5.2.5 Effect of Compatibilizer on Mechanical Properties

Figures 5.9 (a) and (b) show the effect of amount of compatibilizer on the tensile and tear properties of 40/60 SBR/EVA, blends. It is clear from the figures that the maximum tensile and tear strengths have been obtained for 6 phr compatibilizer loaded samples. This indicates the increased interfacial crosslinking due to the better adhesion between the SBR and EVA phases, at this loading. After 6 phr compatibilizer loading, a reduction in tensile and tear strengths has been observed. These results are in accordance with the observed solvent uptake behaviour of the blends.

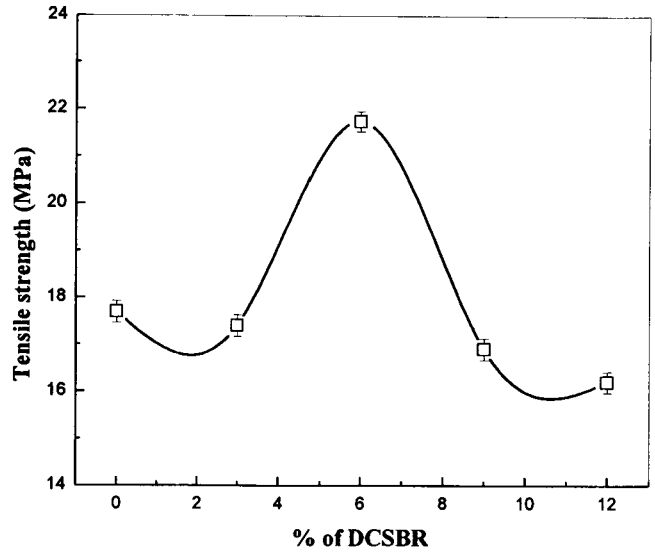

Figure 5.9 (a) Effect of amount of compatibilizer on tensile strength of 40/60 SBR/EVA

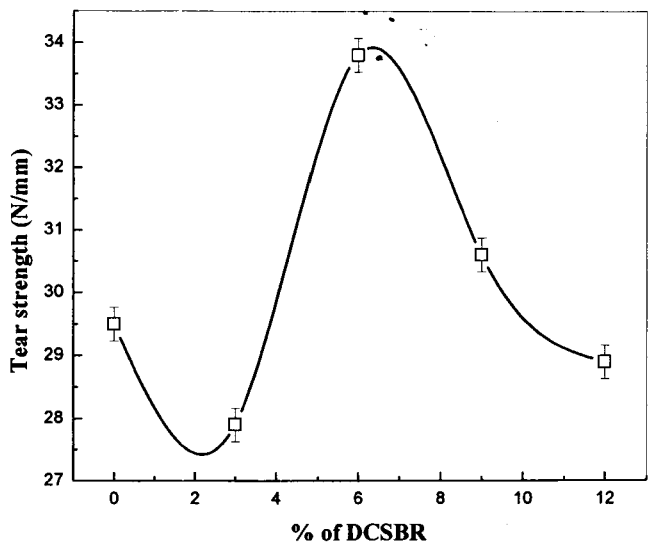

Figure 5.9 (b) Effect of amount of compatibilizer on tear strength of 40/60 SBR/EVA

Figures 5.10 (a) and (b) show the effect of blend ratio on the tensile strength and tear strength of compatibilized and uncompatibilized SBR/EVA blends. The tensile and tear strength have been found to be increased with an increase in EVA content.This improvement is definitely due to the semi-crystalline nature of EVA. The enhancement in tensile strength is predominant in 40/60 system.

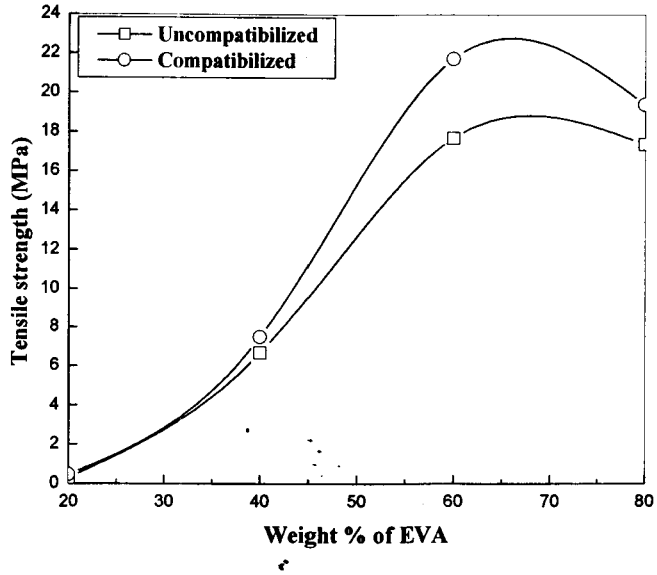

Figure 5.10 (a) Effect of blend ratio on tensile strength of compatibilized and uncompatibilized blends

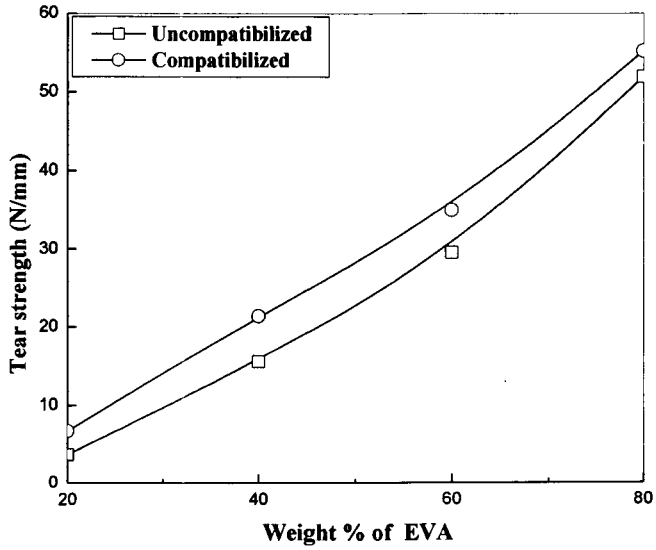

Figure 5.10 (b) Effect of blend ratio on tear strength of compatibilized and uncompatibilized blends

5.2.6 Degree of Crosslinking

In a crosslinked polymer system, different kinds of networks are formed. They include chemical and physical crosslinks. Physical crosslinks consist of chain entanglements which vary according to the stress developed in the system. However, the chemical crosslinks arise from the chemical bonds connecting the polymer segments. Network macrostructure consists of the chain ends, entanglements and crosslink clustering. A schematic model of the macro-structural network is shown in Figure 5.11.

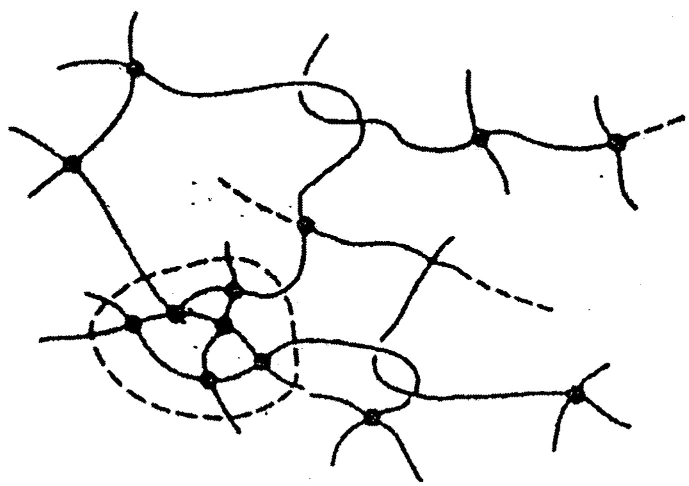

Figure 5.11 Schematic representation of macro–structural network features (-✗-) crosslinks (--) chain ends (✗) entanglements, and (⊛) crosslink cluster

The degree of crosslinking for the different blend systems has been calculated from the modified Flory–Rehner equation [11]:

$$\nu = \frac{1}{2M_C} \qquad \text{.................5.2}$$

where M_c, is the molecular mass between crosslinks computed from Equation 3.7. The blend-solvent interaction parameter χ for computing M_c was determined using the equation [12]:

$$\chi = \frac{(d\phi/dt)\{[\phi/1-\phi]+N\ln(1-\phi)+N\phi\}}{2\phi\,(d\phi/dT)-\phi^2 N\,(d\phi/dT)-\phi^2/T} \qquad \text{.....5.3}$$

where ϕ, is the volume fraction of the polymer calculated as :

$$\phi = \frac{(d-fw)\rho_P^{-1}}{(d-fw)\rho_P^{-1}+A_0\rho_s^{-1}} \qquad \text{.....5.4}$$

where 'd' is the deswollen weight of the sample, 'w' the initial weight of the sample, 'A_0', the weight of the solvent in the swollen sample, 'f' the fraction of insoluble components, and 'ρ_p' and 'ρ_s', the densities of the blend and solvent, respectively. 'N' for Equation 5.3, was computed as:

$$N = \frac{(\phi^{2/3}/3-2/3)}{(\phi^{1/3}-2\phi/3)} \qquad \text{.....5.5}$$

The crosslink density values are shown in Table 5.3. It is found that the crosslink density is the maximum for 6 phr loading, which exhibits the lowest solvent uptake value. This observation is complemented by the highest mechanical properties exhibited by the blend sample compatibilized with 6 phr of DCSBR.

Crosslink density of compatibilized blends was also calculated from the tensile values using the kinetic theory of elasticity [13]:

$$\nu = \frac{\sigma}{(\lambda-1/\lambda^2)RT} \qquad \text{.....5.6}$$

where ν is the crosslink density, σ is the modulus (100%), λ is the extension ratio, R is the gas constant and T is the temperature in absolute scale. These values are

also shown in Table 5.3. The trend has been found to be the same as observed from swelling experiments. However there exist differences in the values of crosslink density determined by swelling and those by mechanical property evaluation. This can be accounted in terms of the existence of physical entanglements (physical crosslinks) in the polymer network, in addition to the chemical crosslinks introduced by vulcanization. The loosening of the physical entanglements of the macromolecular network, and the destruction of the crystallites of EVA in the matrix due to solvent ingression can contribute to lower crosslink density values. Similar observations have been reported earlier [14].

Table 5. 3 Comparision of crosslink density of 40/60 SBR/EVA blends compatibilised with DCSBR

SBR/EVA/ DCSBR	Crosslink density (from mechanical property) $n_1 \times 10^6$ (kg mol/m^3)	Crosslink density $v_1 \times 10^7$ (kg mol/m^3)
40/60/3	10.26	6.68
40/60/6	11.98	11.29
40/60/9	10.83	6.60
40/60/12	10.45	6.33

5.2.7 Comparison with Theory

The chemical crosslink density calculated from swelling data has been correlated with those of affine and phantom network models [15]. In the affine network model, it is assumed that the junction points are embedded in the network without fluctuations. According to the affine network model, the molecular weight between crosslinks is given by:

$$M_{c(aff)} = \frac{\rho_p V_s \phi^{\frac{2}{3}} V^{\frac{1}{3}}_r \left(1 - \frac{\mu}{\gamma} V_r^{\frac{1}{3}}\right)}{-[\ln(1-V_r) + V_r + V_r^2 \chi]} \quad \text{.....5.7}$$

where μ and γ are the number of junctions and effective chains respectively. ϕ is the dry blend volume fraction and V_r the volume fraction of the belnd at swelling equilibrium. ρ_p and V_s are the density of polymer blend matrix and molar volume of the solvent respectively.

In the case of phantom network model, the chains can move freely through one another, i.e, the junction points fluctuate over time around their mean position without any hindrance from the neighboring molecules. According to this theory, a small number of junctions are assumed to be fixed at the surface of the network, and the remaining ones are free to fluctuate over time .The molar mass between crosslinks for the phantom limit model ($M_{c\ (ph)}$) has been calculated using the equation [16]:

$$M_{c(ph)} = \frac{\rho_p V_s \phi^{\frac{2}{3}} V_r^{\frac{1}{3}} \left(1 - \frac{2}{f}\right)}{-[\ln(1-V_r) + V_r + V_r^2 \chi]} \quad \text{.....5.8}$$

The results obtained from these calculations are shown in Table 5.4. It has been observed that the experimental values are closer to the affine network model. Therefore in SBR/EVA/DCSBR blends, the crosslinked junctions can be considered as embedded in the network, so that they cannot fluctuate freely and the chain vector transforms linearly with macroscopic deformation. The difference between

the theoretical and experimental values can be associated with the presence of crystalline regions of EVA in the matrix.

Table 5.4 Theoretical and experimental M_c values for SBR/EVA/DCSBR blends

SBR/EVA/DCSBR	Experimental (kg/mol)	Affine (kg/mol)	Phantom (kg/mol)
40/60/3	0.749	0.099	0.035
40/60/6	0.442	0.096	0.032
40/60/9	0.757	0.098	0.033
40/60/12	0.790	0.099	0.034

5.2.8 Kinetics of Sorption

As the swelling goes on, the surface area of the blends increases and the compressive stress developed by the underlying unswollen material decreases and finally reaches the state of equilibrium swelling. In order to study the sorption kinetics, the first order kinetic equation has been used [17].

$$k_1 t = 2.303 \log \left[\frac{Q_\infty}{Q_\infty - Q_t} \right] \qquad \text{.....5.9}$$

Figure 5.12 shows a typical plot of log (Q_∞ - Q_t) versus time of 40/60/6 SBR/EVA/DCSBR, in three aromatic solvents. The observed linearity suggests a sorption process following first order kinetics.

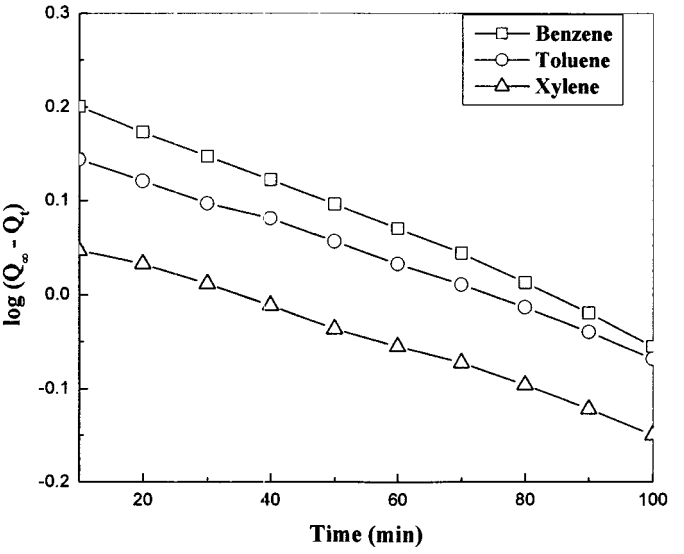

Figure 5.12 Plots of log (Q_∞ - Q_t) versus time in benzene, toluene and xylene

5.3 Conclusion

Dichlorocarbene modified SBR acts as an effective compatibilizer, for SBR/EVA blends, as evident from the increase in the maximum torque exhibited by the compatibilized blends. A significant decrease in the solvent uptake was observed for all the compatibilized blends, especially for those with 6 phr of compatibilizer loading. The solvent uptake followed the trend: benzene > toluene > xylene for a given blend system as expected from their molecular weights. The compatibilization has been found to be accompanied by an improvement in the mechanical properties. A comparison of the computed M_c values with phantom and affine network models indicat that, in SBR/EVA/DCSBR blends, the network structure could be modeled by affine theory. The diffusion process has been found to fit well with the first order kinetic equation.

References

[1]. D. R. Paul, *Polymer Blends*, Academic Press, New York, 1976.

[2]. D. Feldman, *J. Macromol. Sci.*, **42**, 587 (2005).

[3]. J. C. Cabanelas, B. Serrano, M.G. Gonzalez and J. Baselga, *Polymer*, **8**, 6633 (2005).

[4]. S. H. Ismail and A. A. Baker, *Polym. Plast. Technol. Eng.*, **44**, 863 (2005).

[5]. K. Nikos, Kalfoglou, S. Dimitrios, Skafidas, K. Joannis, KallitsisJean-Claude Lambert and Luc Van der Stappen, *Polymer*, **36,** 4453 (1995).

[6]. A. Sánchez-Solís, F. Calderas and O. Manero, *Polymer*, **42**, 7335 (2001).

[7]. H. Ismail, H. P. S Khalel, and Y. Tsukahare, *Inter. J. Polym. Mat.*, **51**, 1031 (2002).

[8]. S. H. Zhu and C. M. Chan, *Polymer*, **39**, 7023 (1998).

[9]. H. A. Spiros, G. Irena and J. T. Koberstein, *Macromol.*, **22**, 1449 (1989).

[10]. R. Fayt, R. Jerome and P. Teyssie, *Macromol. Chem.*, **187**, 837 (1986).

[11]. P. J. Flory and J. Rehner. Jr, *J. Chem. Phys.*, **11**, 313 (1943).

[12]. R. S. Khinnavar and T. M Aminabhavi,. *J. Appl. Polym. Sci.*, **42**, 2321 (1991).

[13]. C. M. Blow and C. Hepburn, *Rubber Technology and Manufacture*, Second Edition, Butterworth, London, 1981.

[14]. N. S. Schneider, J. L. Illinger, and M. A. Cleaves, *J. Polym. Eng. Sci.*, **26**, 1547 (1986).

[15] L. R. G. Treloar, *The Physics of Rubber Elasticity*, Clarendon Press, Oxford, 1975.

[16] J. E. Mark and B. Erman, *Rubber Like Elasticity, a Molecular Primer*, Wiley, New York, 1988.

[17] T. M. Aminabhavi and S. B. Harogoppad, *J. Chem. Educ.*, **68,** 343 (1991).

Chapter 6

Transport of Fuels through Carbon Black Filled SBR/EVA Blends

Summary

This chapter discusses the improvement in the barrier properties of SBR/EVA blends by the reinforcement with different carbon black fillers viz. SRF (semi-reinforcing furnace), HAF (high abrasion furnace) and ISAF (intermediate super abrasion furnace). Three industrial liquids have been used to examine the barrier properties. It has been found that the blends loaded with ISAF take the lowest amount of liquids among all the samples. This has been attributed to the differences in the degree of reinforcement due to the particle size of fillers, and the crosslink density of the matrices. From the temperature dependence of diffusivity, the activation energy for the diffusion process has been computed.

Results of this chapter have been communicated for publication in *Polymer*.

6.1 Introduction

The transport process through filled polymers depends upon the characteristics of the matrix and the fillers, their degree of adhesion, polymer crosslink density, penetrant size, temperature etc. Inert and compatible fillers will take up the free volume within the polymer matrix and create a tortuous path for the penetrating molecule [1]. The degree of tortuosity is dependent on the volume fraction of the filler and the shape and orientation of the filler particles. Lowering of equilibrium swelling in filled samples generally indicates an excellent filler-matrix adhesion. A large number of fillers including silica, carbon black, mica, TiO_2 and $CaCO_3$ are extensively used in rubber industry. Carbon blacks are lesser expensive and form an integral part of many rubber products. Many rubbers would be of little value in modern industry without the reinforcing effect of carbon black. Reinforcement usually improves the modulus, tensile strength, swelling resistance and abrasion resistance of elastomers.

Outstanding studies regarding the influence of fillers on the swelling of elastomers exist [2-5]. Typically, Stickney and Mueller [6] studied the kinetics of swelling of carbon black filled styrene butadiene vulcanizates in the presence of octane. It was found that, for rubber vulcanizates, the diffusivity increased with the concentration of the penetrants. Segal et al. [7] examined the diffusion of liquids through electrically conductive immiscible PP/thermoplastic polyurethane (TPU) blends containing carbon black. They found that the interphase region, its quantity, and

continuity played a significant role in the liquid transport process. Thomas and co-workers [8, 9] investigated the transport of solvents through black filled elastomers. The solvent resistance of the elastomers was found to be increased with filler loading.

The aim of the present chapter is to study the influence of three different black fillers viz. semi-reinforcing furnace (SRF), high abrasion furnace (HAF) and intermediate super abrasion furnace (ISAF) on the transport properties of SBR/EVA blends. The penetrants used are petrol, kerosene and diesel. Special attention has been given to examine the effects of filler loadings, particle size of fillers, and temperature on the transport properties.

6.2 Result and Discussion

6.2.1 Processing Characteristics

Figure 6.1 shows the rheographs of 20/80 SBR/EVA blend filled with 10 phr of different carbon blacks. It has been found that the filler reinforcement enhances the torque for all the systems. Among the different black fillers used, ISAF system shows the highest M_H value reflecting the increased crosslink density, which can be attributed to the better reinforcement. The lowest M_H value has been observed for the SRF black filled sample due to the lowest reinforcement, which in turn is due to highest size of the filler particles. The HAF black filled sample shows an intermediate M_H value.

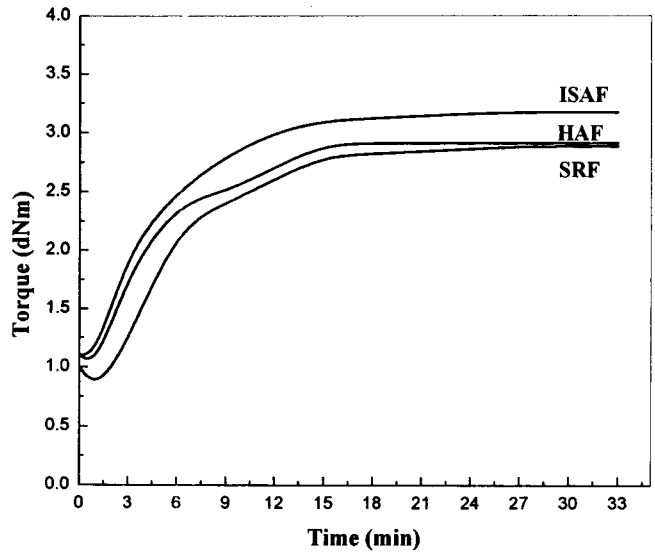

Figure 6.1 Rheographs of 20/80 SBR/EVA blends with 10 phr loading of ISAF, HAF and SRF black

Figure 6. 2 shows the rheographs of 40/60 SBR/EVA blends with different loadings of ISAF black, with DCP as the vulcanizing agent. The M_H value increases with filler content in all the samples. This is due to the increase in rigidity of the blend samples with increase in filler loading, which reduces the mobility of the chains. Figure 6.3 shows the rheographs of 20/80 SBR/EVA/ISAF composites vulcanized with two different crosslinking systems viz. sulphur and DCP. The DCP vulcanized system has been found to exhibit the highest M_H value. This is due to the reason that, unlike sulphur system, DCP can cure both SBR and EVA phases uniformly and can induce C-C bonds between the macromolecular chains, which make the matrix more rigid. The sulphur vulcanization introduces flexible polysulphidic linkages, which makes the matrix relatively flexible, as discussed in chapter, 4.

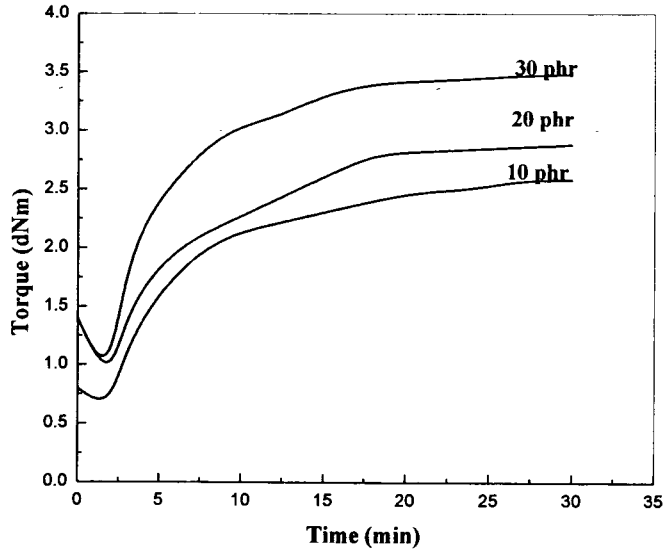

Figure 6.2 Rheographs of 40/60 SBR/EVA blends with different loadings of ISAF black

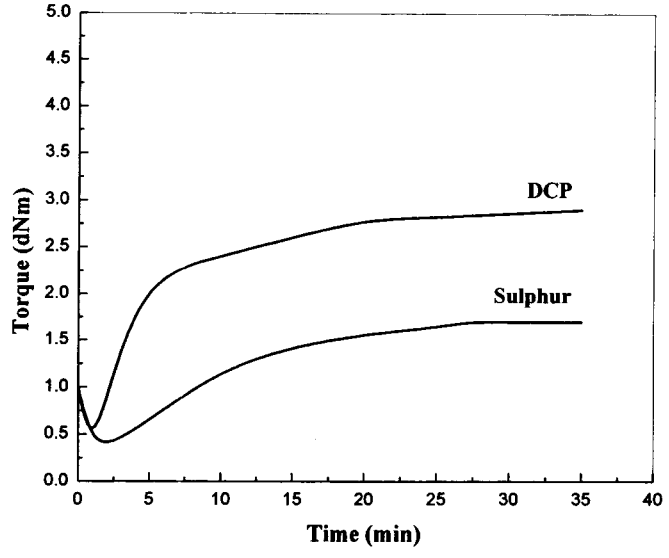

Figure 6.3 Rheographs of 20/80/10 SBR/EVA/ISAF composites vulcanized by sulphur and DCP

6.2.2 Comparison of Transport Properties

Figure 6.4 represents the comparison of solvent interaction behaviour of unfilled and 30 phr SRF, HAF and ISRF loaded 40/60 SBR/EVA blends. The penetrant

used was petrol. It is evident from the figure that the solvent uptake is higher for the unfilled sample, which has been considerably reduced upon loading with black fillers. Among the three fillers used, the blends with 30 phr of ISAF exhibit the lowest solvent interaction than the other two filler loaded systems. This trend can be explained on the basis of the difference in the particle size of the fillers. For maximum reinforcement, the filler particles must be of the same size or smaller than the chain end-to-end distance [10]. The degree of filler reinforcement increases with decrease in particle size or increase in surface area. Thus, the degree of reinforcement of ISAF with the lowest particle size is the highest and therefore it prevents the diffusion of penetrants more effectively compared to other two carbon black fillers.

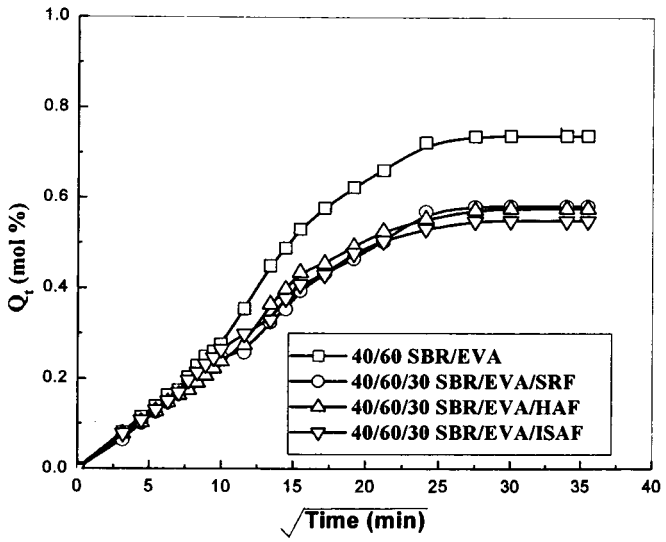

Figure 6.4 Sorption curves of unfilled and 30 phr SRF, HAF, ISAF loaded 40/60 SBR/EVA blends

Figures 6.5 (a) - (d) show the scanning electron micrographs of unfilled and filled SBR/EVA blends. A better dispersion of filler particles has been observed for the ISAF loaded blends.

6.5 (a)

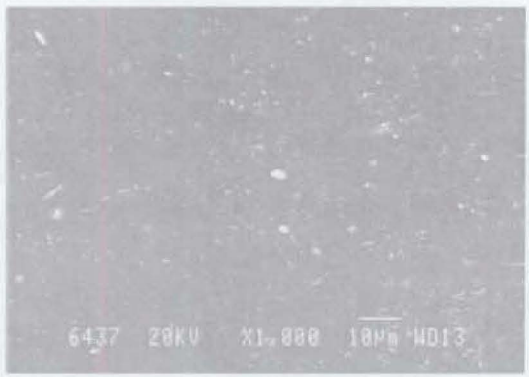

6.5 (b)

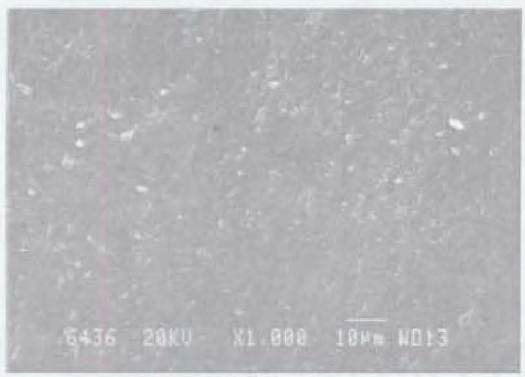

6.5 (c)

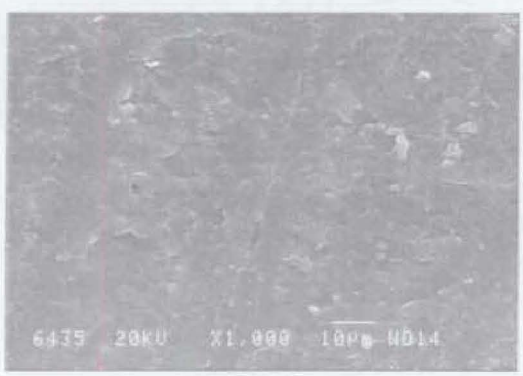

6.5 (d)

Figure 6.5 **SEM of (a) 40/60 SBR/EVA**
(b) 40/60/30 SBR/EVA/ISAF
(c) 40/60/30 SBR/EVA/HAF
(d) 40/60/30 SBR/EVA/SRF

6.2.3 Effect of Amount of Filler

Figure 6.6 shows the sorption curves of 40/60/ SBR/EVA with different loadings of ISAF, vulcanized with DCP, in petrol, at 26 °C. The solvent uptake decreases in the order: 10 > 20 > 30 phr ISAF loaded blends. The increase in the filler content restricts the macromolecular chain mobility resulting in lower solvent uptake.

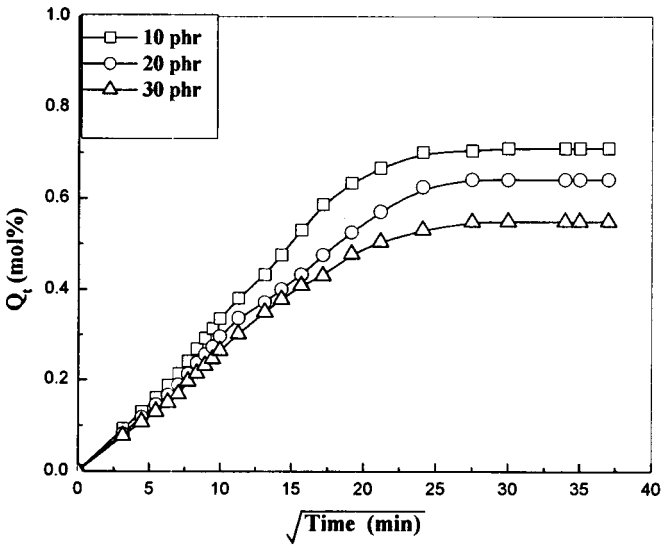

Figure 6.6 Sorption curves of 40/60/ SBR/EVA with different loadings of ISAF, at 26 °C in petrol

6.2.4 Effect of Crosslinking Systems

Figure 6.7 shows the sorption curves of 40/60 SBR/EVA blends, loaded with 30 phr ISAF, crosslinked by sulphur and DCP, with petrol as the penetrant molecule. It has been found that the equilibrium sorption uptake is in the order: sulphur > DCP. The difference in the transport behaviour through the matrices with different vulcanizing agents arises due to the different types of crosslinks formed during vulcanization, as already explained in the chapter 4. The sulphur system with flexible polysulphidic linkages yields under solvent stress and accommodates more penetrant molecules.

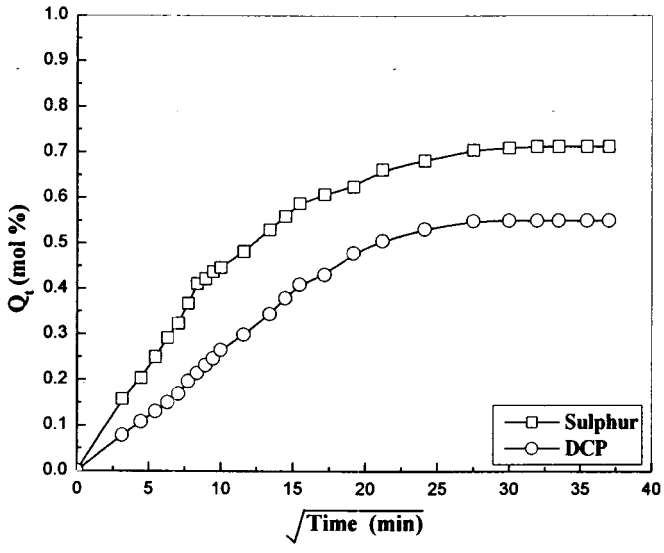

Figure 6.7 Sorption curves of 40/60/30 SBR/EVA/ ISAF, crosslinked by sulphur and DCP, in petrol

6.2.5 Kraus Equation

The extent of filler reinforcement has been assessed by using the Kraus Equation [11] , according to which :

$$\frac{V_r}{V_{rF}} = 1 - m\left[\frac{F}{1-F}\right] \qquad \text{.....6.1}$$

where V_r and V_{rF} are the volume fractions of the polymer blend in the fully swollen unfilled sample and in the fully swollen filled sample respectively. F is the volume fraction of filler and m is a measure of the extent of reinforcement. Figure 6.8 shows the plot of V_r/V_{rF} versus F / 1- F. According to Kraus theory, the curve with higher negative slope represents a better reinforcing effect. From the figure it is clear that the negative slope is in the order: ISAF > HAF > SRF, highlighting the degree of reinforcement in the same order. The order of reinforcement is

complementary to the observed solvent uptake trend for the different filler loaded matrices used.

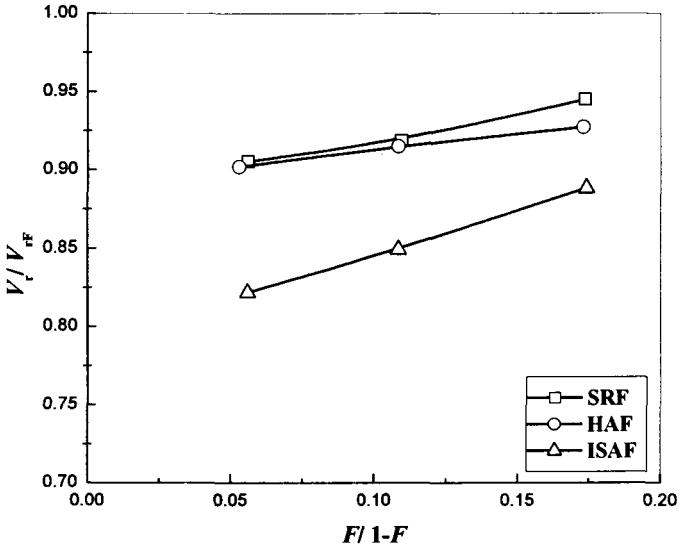

Figure 6.8 Plots of V_r/V_{rF} versus F / 1- F for 40/60 SBR/EVA filled with 30 phr of SRF, HAF and ISAF

6.2.6 Effect of Temperature

Figure 6.9 shows the diffusion curves of 40/60/30 SBR/EVA/ISAF in petrol at different temperatures. The rate of diffusion and the maximum solvent uptake values have been found to increase with temperature because of the increase in the free volume and the favourable chain conformation during the rise in temperature. It has been found that the increase in the equilibrium uptake is more dominant at 46 °C. This is due to the disruption of the crystalline regions of EVA in the matrix and the increased mobility of the polymer chains at higher temperatures.

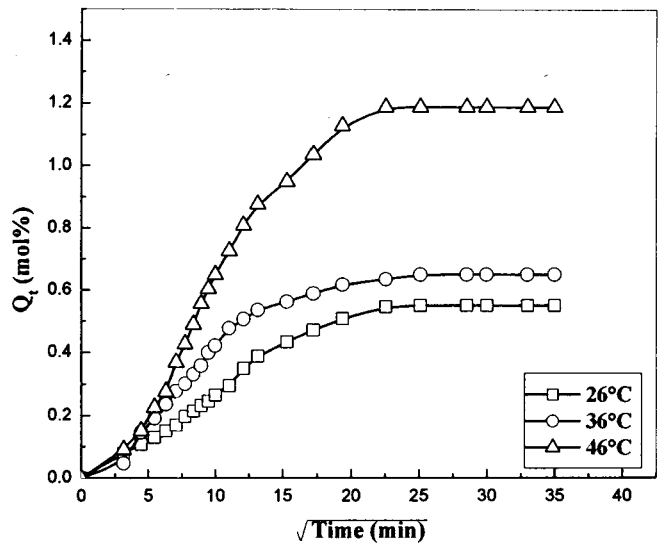

Figure 6. 9 Sorption curves of 40/60/30 SBR/EVA/ISAF composite in petrol at different temperatures

6.2.7 Activation Energy

Figure 6.10 shows the typical Arrhenius plots of log D^* versus $1/T$ for 40/60/30/ ISAF in three different solvents. Figure 6.11 shows the plots of log P versus $1/T$ for 40/60 SBR/EVA blends loaded with different carbon blacks, in petrol. From the Arrhenius plots, the values of activation energy for diffusion and permeation were calculated and are shown in Tables 6.1 and 6.2 respectively. The values of activation energy for diffusion (E_D) increase regularly from ISAF filled samples to SRF loaded ones for a given solvent. This readily suggests the higher temperature susceptibility of the samples loaded with bigger particles. An increase in the value of E_D has been observed with an increase in size of the penetrants. This suggests that the larger molecules require more energy to create what are known as "Eyring holes" with in the polymer matrix [12]. The same trend has been observed for the activation energy for permeation (E_P) values also.

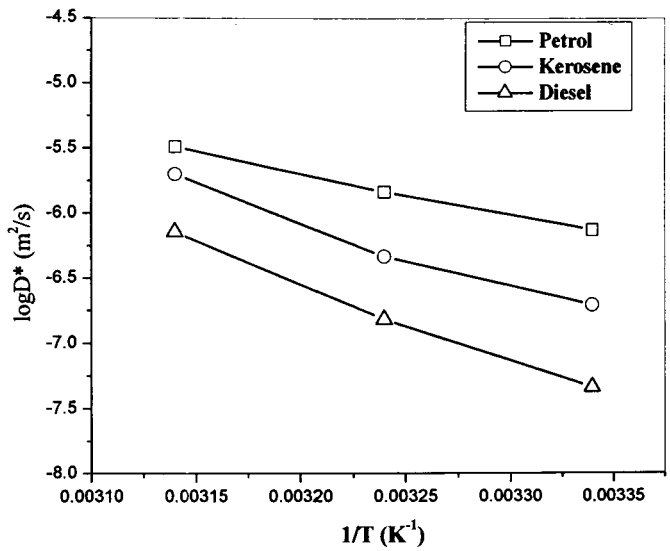

Figure 6.10 Plots of log D^* versus $1/T$ for 40/60/30/ ISAF in three different solvents

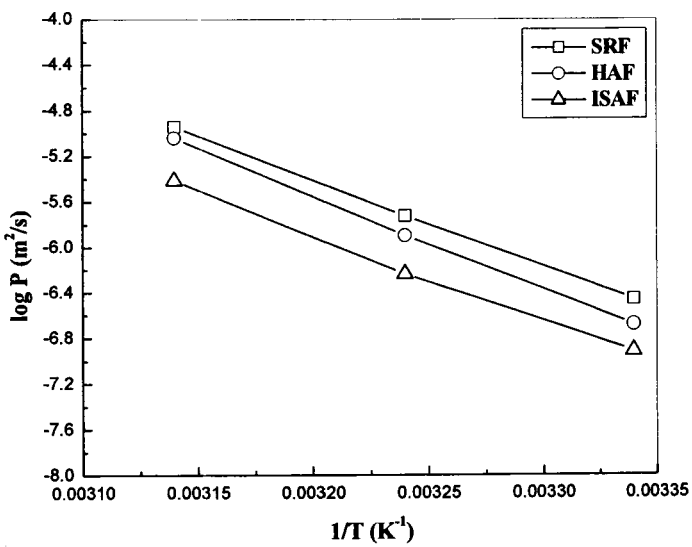

Figure 6.11 Plots of log P versus $1/T$ for 40/60/30/ SRF, HAF and ISAF in petrol

Table 6.1 E_D values

SBR/EVA	E_D (kJ/mol)		
	Petrol	Kerosene	Diesel
40/60/30 ISAF	61.07	96.44	122.4
40/60/30 HAF	87.33	104.26	115.3
40/60/30 SRF	96.99	119.19	114.3

Table 6.2 E_P values

SBR/EVA	E_p (kJ/mol)		
	Petrol	Kerosene	Diesel
40/60/30 ISAF	143.85	158.03	160.66
40/60/30 HAF	145.69	162.33	181.25
40/60/30 SRF	157.41	184.78	192.51

6.3 Conclusion

The transport properties of SBR/EVA blends reinforced with three carbon blacks have been studied with petrol, kerosene and diesel as penetrants, with special reference to the effects of the amount of fillers, their particle size and temperature. The ISAF filled blends showed the lowest equilibrium uptake and SRF system, the highest for a given penetrant at a particular temperature. The reason for this trend has been attributed to the differences in the particle size of the fillers reinforced into the polymer matrix. The calculated values of molecular mass between crosslinks have been found to be in the order: ISAF < HAF < SRF systems, for a given blend ratio which is in agreement with the observed Q_∞ values. The activation energy values for diffusion and permeation were found to be decreased with the decrease in the particle size of the fillers.

References

[1]. S. C. George and S. Thomas, *Prog. Polym. Sci.*, **26**, 985 (2001).

[2]. C. Gauthier, L. Chazeau, T. Prasse and J. Y. Cavaille, *Comp. Sci. and Tech.*, **65**, 335 (2005).

[3]. Faud El Tantawy, *Polym. Degrad. Stab.*, **73,** 289 (2001).

[4]. A. Gnatowski and J. Koszkul, *J. Mater. Proces. Technol.*, **162,** 52 (2005).

[5]. A. Sujith and G. Unnikrishnan, *J. Mater. Sci.*, **40**, 4625 (2005).

[6]. P. B. Stickney and W. J. Mueller, *Rubber Chem. Technol.*, **42**, 604 (1969).

[7]. E. Segal, R. Tchoudakov, M. Narkis and A. Siegmann, *J. Polym. Sci., Part B: Polym. Phys.*, **41**, 1428 (2003).

[8]. T. Johnson and S. Thomas, *J. Polym. Sci., Part B: Polym. Phys.*, **37**, 415 (1999).

[9]. S. C. George and S. Thomas, *J. Macromol. Sci. Phys.*, **39**,175 (2000).

[10]. J. A. Manson and L. H. Sperling, *Polymer Blends and Composites*, Plenum Press, New York, 1976.

[11]. G. Kraus, *J. Appl. Polym. Sci.*, **7**, 861 (1963).

[12]. S. C. George, M. Knorgen and S. Thomas, *J. Mater. Sci.*, **163,** 11 (1999).

Chapter 7

Effects of Carbon black and Silica Fillers on Liquid Transport through SBR/EVA Blends

Summary

The transport characteristics of SBR/EVA blends loaded with black filler (ISAF) have been compared with those of a white filler (silica, Ultrasil VN3) loaded blends. The penetrants used are petrol, kerosene and diesel. The blends have been vulcanized by DCP. The silica incorporated blends have been found to sorb higher amount of the fuels compared to the ISAF filled systems. However, the difference between the equilibrium sorption values of carbon black and silica loaded blends have been found to be decreased with increase in EVA content of the matrix. For pure EVA, silica loading gives better solvent resistance than carbon black filling. The cure characteristics, swelling coefficient, diffusion coefficient and crosslink density have been computed to complement the experimental results.

7.1 Introduction

Reinforcing fillers such as silica and carbon black have a significant influence upon the properties of an elastomer, often increasing its mechanical durability and elastic properties, and modifying the sorption and permeability of diffusants through it. [1]. Excellent reports on the interaction of carbon black and silica filler reinforced polymer blends with solvents exist in literature. For example, Ismail et al.[2] studied the effect of filler loading on the cure time (t_{90}) and swelling behaviour of standard Malaysian rubber/ epoxide natural rubber (SMR L/ENR 25) and standard Malaysian rubber/styrene butadiene rubber (SMR L/SBR) blends, using carbon black (N 330), silica (Vulcasil C) and calcium carbonate. They found that for SMR L/ENR 25 blends, the t_{90} decreased with increase in carbon black loading, whereas the silica loaded systems showed an increasing trend. The calcium carbonate filled blends also exhibited a decreasing trend for the t_{90} with increase in filler loading. The percentage swelling in toluene and ASTM oil No. 3 decreased for both the blends (SMR L/ENR 25 and SMR L/SBR) with increase in filler loading; calcium carbonate system giving the highest swelling value, followed by silica and carbon black filled blends. Sirisinha et al.[3] investigated the phase morphology and oil resistance of 20/80 NR/NBR blends filled with different black fillers viz. N220, N330 and N660 and with non-black reinforcing fillers viz. precipitated and silane treated silica. The results revealed that the addition of filler, either carbon black or silica, to the blends caused a decrease in the dispersed phase (NR) size. It was also

found that silica filled blends showed lower resistance to oil than the carbon black loaded ones. The effect of silica filler on a foam of EPDM/water-swellable rubber (WSR) has been investigated by Sun et al. [4]. The silica filler has been found to accelerate the rate of swelling of the foam in water. The reinforcing ability and the increased solvent resistance by different fillers, for various polymeric systems, have been studied by several other researchers also [5-8].

The present work compares the effects of two fillers viz. intermediate super abrasion furnace (ISAF) and silica (SiO_2), of same loading, on the sorption and diffusion properties of SBR/EVA blends, vulcanized by DCP. The swelling coefficient, diffusion coefficient and crosslink density have been calculated to support the experimental observations.

7.2 Results and Discussion

7.2.1 Effect of ISAF Black on the Transport Behaviour of Pure SBR and EVA

Figure 7.1 shows the sorption behaviour of pure SBR, pure EVA, 30 phr ISAF loaded SBR and 30 phr of ISAF loaded EVA. The penetrant used was petrol. It has been found that the EVA matrix exhibits higher equilibrium sorption compared to the SBR matrix, unlike the behaviour in the other organic solvents such as aliphatic, chlorinated and aromatic hydrocarbons, as discussed in the previous chapters. 3, 4 and 5. Petrol, with a higher *iso*-octane content, unlike the individual straight chain hydrocarbons, can cause a plasticization effect on EVA. Due to plasticization the crystallites can undergo defolding to generate more free volume. This accounts for

the higher penetrant transport through EVA matrix. A similar trend has been shown by diesel and kerosene. On loading with ISAF black filler, Q_∞ values of SBR and EVA matrices have been reduced significantly. This can be accounted in terms of the reinforcement of the filler particles within SBR and EVA matrices. However, the percentage reduction has been found to be higher for SBR/ISAF systems.

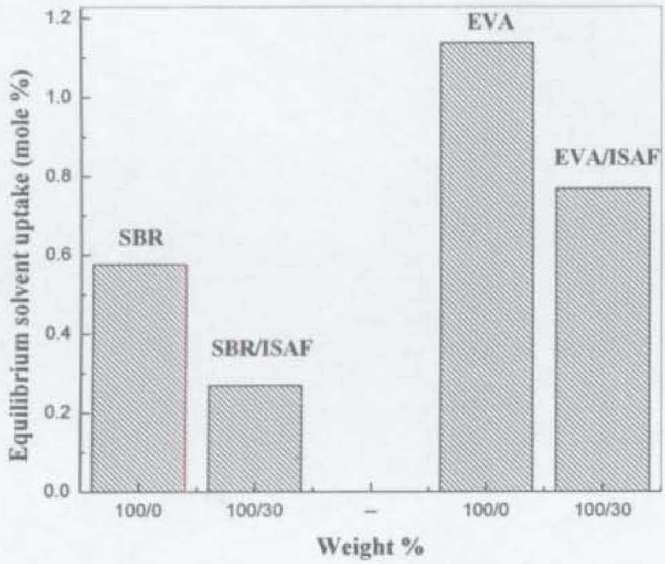

Figure 7.1 Effect of ISAF black on pure SBR and EVA

7.2.2 Effect of of Silica on the Transport Behaviour of Pure SBR and EVA

Figure 7.2 shows the effect of silica on the sorption behaviour of pure SBR and EVA matrices. A sharp increase in the equilibrium sorption uptake has been observed when the SBR matrix was loaded with silica. However, the filled EVA matrix shows a reduction in the solvent uptake. The polar nature of the silica particles accounts for the difference in the sorption behaviour exhibited by the silica filled matrices. The surface of silica is polar due to siloxane and silanol groups as

shown in Figure 7.3. Since the reinforcement of the polar silica with the non-polar SBR matrix is poor, a higher Q_∞ value has been observed compared to the unfilled sample. The polar silica particles can form aggregates of different sizes (filler-filler interaction) which may get distributed in a non-polar matrix non-uniformly. The filled EVA samples, however, has been found to exhibit a lower Q_∞ value due to the better reinforcement of polar silica particles into the polar matrix.

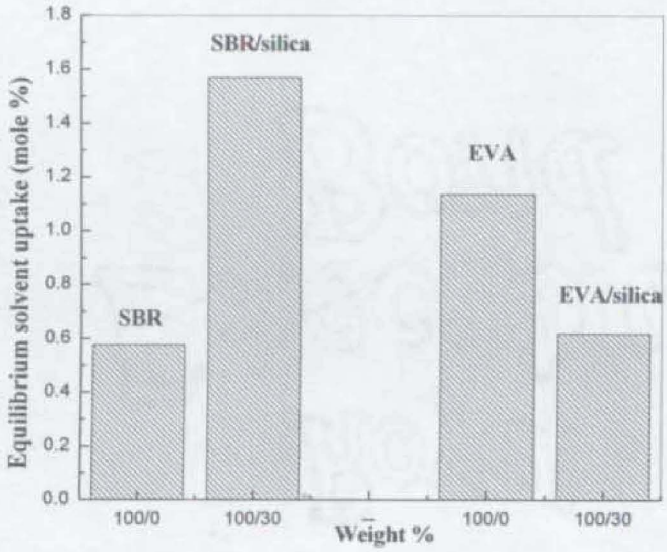

Figure 7.2 Effect of silica on the sorption behaviour of pure SBR and EVA

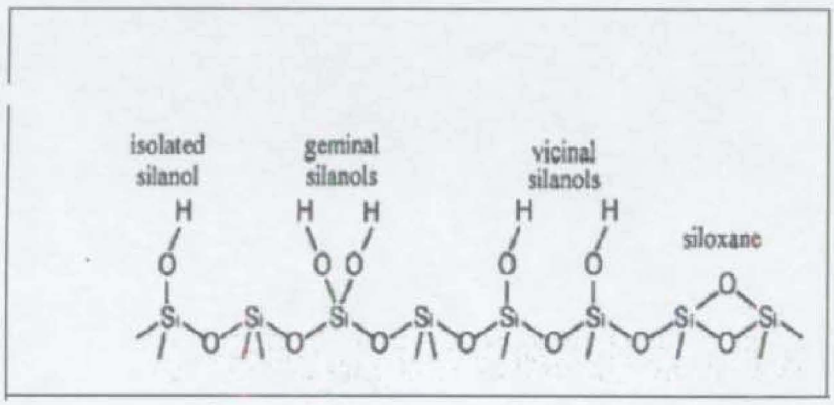

Figure 7.3 Surface chemistry of silica

7.2.3 Effect of Fillers on Cure Properties of SBR/EVA Blends

SBR/EVA blends were incorporated with varying amounts of silica and ISAF black to study the cure characteristics. Figure 7.4 shows the optimum cure time (t_{90}) of 40/60/ SBR/EVA blends containing 10, 20 and 30 phr of silica and ISAF black. The t_{90} value of the blend decreases upon filler incorporation, for both the silica and ISAF black filled systems. The t_{90} has been found to be higher for ISAF filled matrix than the silica filled one.

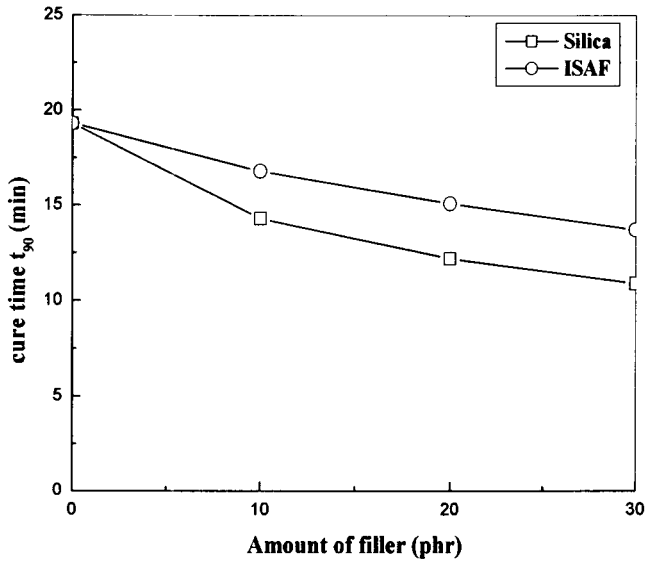

Figure 7.4 Optimum cure time (t_{90}) of 40/60 SBR/EVA with 10, 20 and 30 phr of silica and ISAF black

7.2.4 Effect of Fillers on the Transport Properties of SBR/EVA Blends

Figure 7.5 shows the sorption curves of unfilled 40/60 SBR/EVA blend and blends reinforced with 30 phr of ISAF and silica. It has been found that the loading of the matrices with carbon black and silica reduces the Q_t values. The carbon black

samples take lesser amount of solvent compared to the silica filled samples. The lower Q_t value exhibited by the black incorporated blend, compared to the white filler system, can be attributed to the heterogenity of the blends.

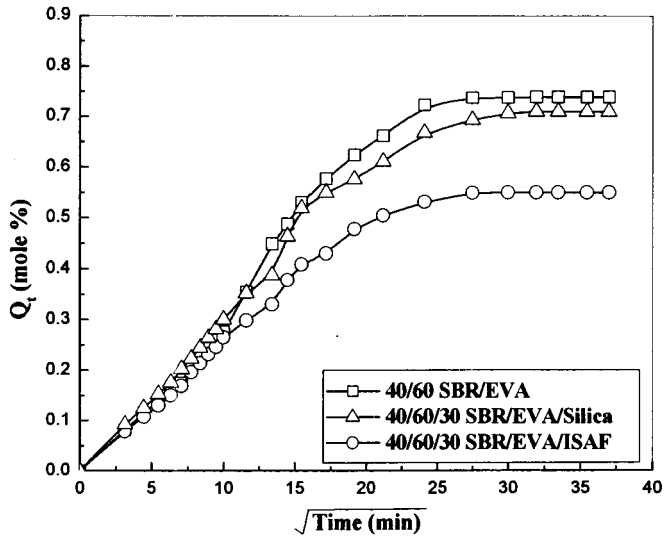

Figure 7.5 Sorption curves of 40/60/SBR/EVA and 40/60/30 SBR/EVA loaded with 30 phr of silica and ISAF black, in petrol

The difference in the equilibrium solvent uptake exhibited by ISAF black and silica filled blends can be justified from the surface morphology as shown in Figures 7.6 (a) and (b). It has been found that ISAF filled blend is more uniform than the silica filled one. This accounts for the observed solvent uptake behaviour of the blends reinforced with the two fillers.

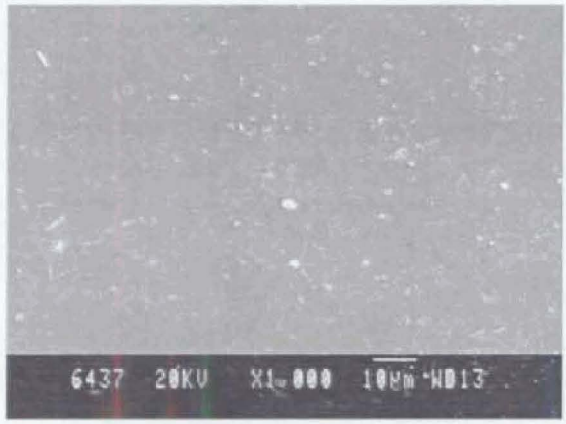

7.6 (a)

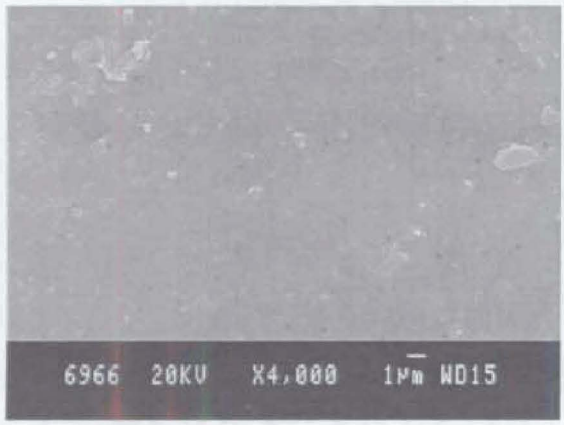

7.6 (b)

Figure 7.6 SEM of (a) 40/60/30 SBR/EVA/ISAF black
(b) 40/60/30 SBR/EVA/silica

7.2.5 Effect of Blend Ratio

Figure 7.7 shows the mole percent uptake of kerosene by the different SBR/EVA blends, reinforced with 30 phr of ISAF and silica. It has been found that the silica filled blends sorb higher amount of solvent than black loaded systems for all blend ratios. However, the difference between the Q_∞ values of carbon black loaded system and those of silica filled blends, decrease with increase in EVA content in the blends. This can be attributed to the high interaction between silica particles and EVA. The polar groups of silica can interact with the polar groups of EVA to reduce the free volume.

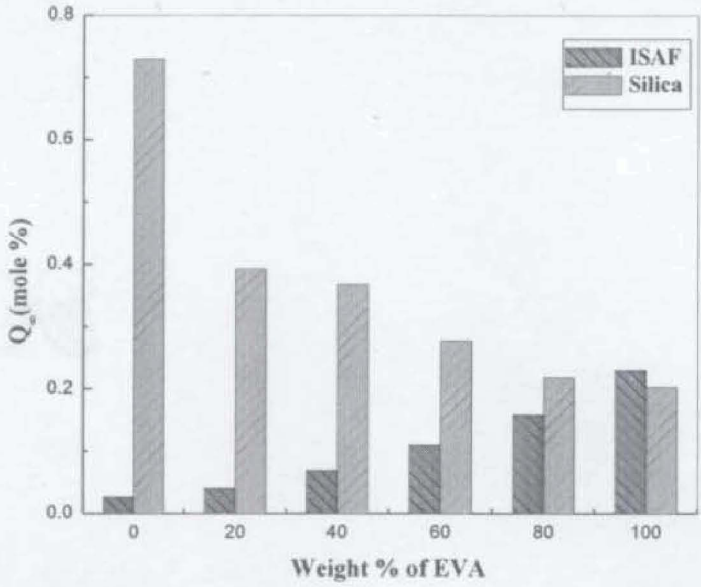

Figure 7.7 Mole % uptake of kerosene by SBR/EVA blends reinforced with ISAF and silica

7.2.6 Swelling Coefficient

In order to assess the extent of the swelling behaviour of the blends reinforced with ISAF and silica, the swelling coefficients were calculated by the following equation [10] :

$$\alpha = \frac{w_2 - w_1}{w_1} \times \rho_s^{-1} \qquad \text{.....7.1}$$

where w_1 and w_2 are the weights of the samples before swelling and at equilibrium swelling and ρ_s is the density of the solvent. Table 7.1 shows the swelling coefficient values of different filled blends in petrol and kerosene. The ISAF filled blends show lower swelling coefficient values, particularly when the SBR content in the blends is higher. However, the values gradually increase with increase in EVA content. The silica filled samples exhibit a reverse trend for the swelling coefficient values.

Table 7.1 Values of swelling coefficient

SBR/EVA	ISAF (30 phr)		Silica (30 phr)	
	Petrol	Kerosene	Petrol	Kerosene
100/0	0.3805	0.0555	2.1997	1.5309
80/20	0.5651	0.0845	1.4371	0.8247
60/40	0.6845	0.1453	1.1230	0.7719
40/60	0.7746	0.2308	0.9991	0.5805
20/80	0.9212	0.3327	0.8882	0.4590
0/100	1.0832	0.4829	0.8697	0.4431

7.2.7 Effect of Penetrants

Figure 7.9 shows the sorption curves of 80/20/30 SBR/EVA/silica blends in different solvents viz. petrol, kerosene and diesel. It is clear from the figure that petrol has higher interaction with the matrix compared to the other two penetrants used. The equilibrium solvent uptake is in the order: petrol > kerosene > diesel.

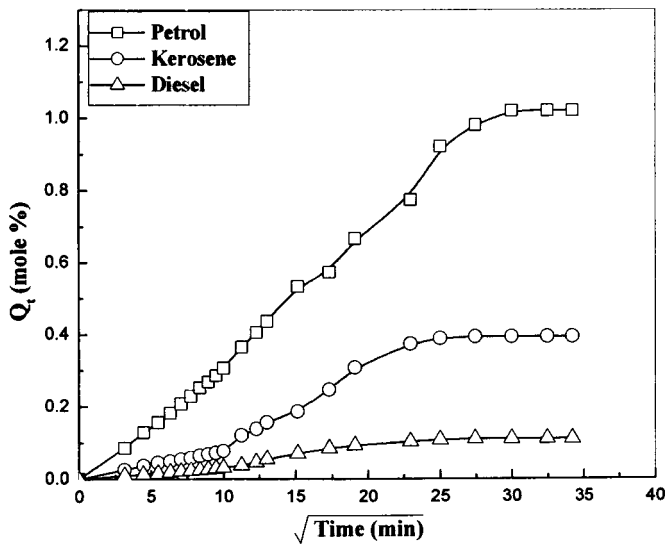

Figure 7.9 Sorption curves of 80/20/30 SBR/EVA/silica blends in petrol, kerosene and diesel at 26 °C

Figure 7.10 presents a comparison of the equilibrium solvent uptake of 80/20 SBR/EVA blends loaded with the same amounts of ISAF black and silica. It follows from the figure that the Q_∞ values decrease with increase in molecular weight of the solvents used.

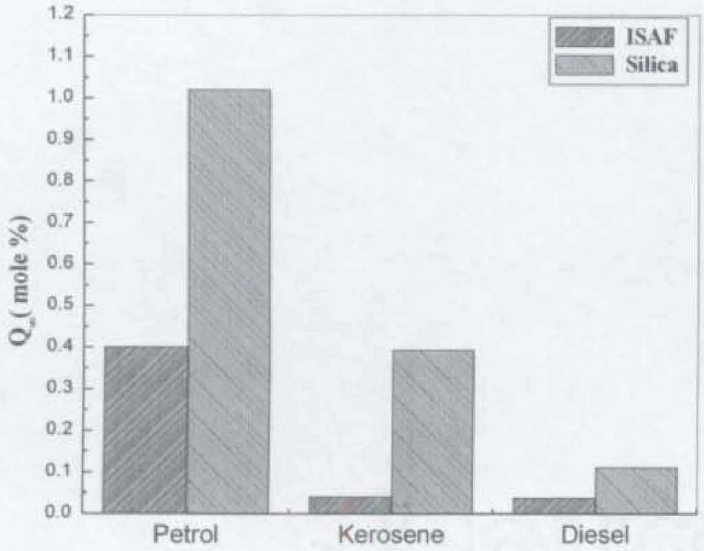

Figure 7.10 Comparison of equilibrium solvent uptake of 80/20 SBR/EVA blends loaded with 30 phr of ISAF black and silica

7.2.8 Comparison of Crosslink Density

Figure 7.11 shows the comparison of crosslink density of SBR/EVA blends filled with silica and ISAF black fillers, computed as per Equation 5.2. It has been found that the crosslink density is inversely proportional to the solvent uptake value, which is in agreement with the Q_∞ values.

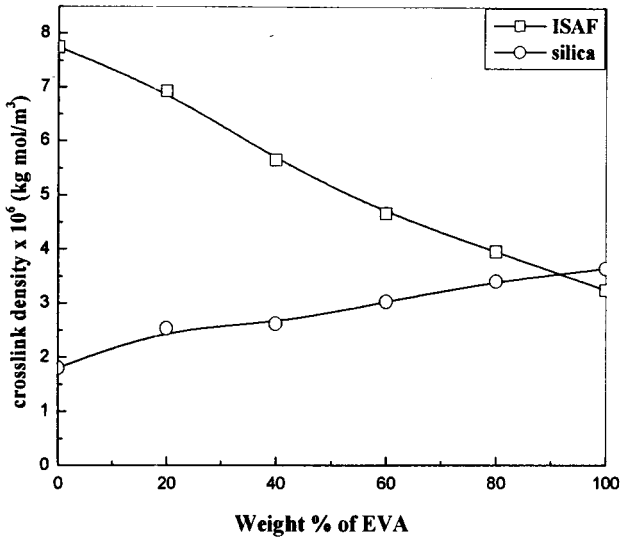

Figure 7.11 Comparison of crosslink density of blends filled with ISAF black and silica, in kerosene

7.2.9 Diffusivity and Permeability

Diffusion of a solvent through a polymer matrix expands the system and thus weakens the molecular interaction between the neighbouring polymer chains. Hence the polymer chains between the crosslinks move freely and the molecular mobility of the network is enhanced by the diffusion of the molecules. The movement of the penetrants through the matrix is significantly controlled by the presence of fillers. The intrinsic diffusion coefficient values for the different blend composition filled with 30 phr of silica, calculated by Equation 3.3, are compiled in Table.7.2. It has been found that D^* values regularly decrease with increase in EVA content in the blends for a given solvent. These values also decrease with increase in the molecular weight of the probe molecules.

Table 7.2 Diffusion coefficient values at 26 °C

Sample/silica	$D^* \times 10^6$ (m^2/s)		
	Petrol	**Kerosene**	**Diesel**
100/0/30	3.50	0.559	0.016
80/20/30	1.75	0.274	0.013
60/40/30	1.04	0.161	0.011
40/60/30	0.92	0.114	0.009
20/80/30	0.62	0.099	0.006
0/100/30	0.59	0.075	0.003

Figure 7.12 shows the variation of D^* and P values of SBR/EVA loaded with 30 phr of silica, with the weight % of EVA in the blends. It has been found that the diffusion coefficient values show a gradual decrease with increase in the EVA content in the blends. This is due to the high tortuosity exhibited by the crystallites of EVA to the penetration of solvent molecules, and also due to the better reinforcement of silica in the blends with higher EVA content. The difference in D^* and P values exhibited by SBR rich blends has been found to be higher than those in the EVA rich blends. This trend can be due to the inversion of EVA from the dispersed to the continuous phase, which leads to a slower diffusion process.

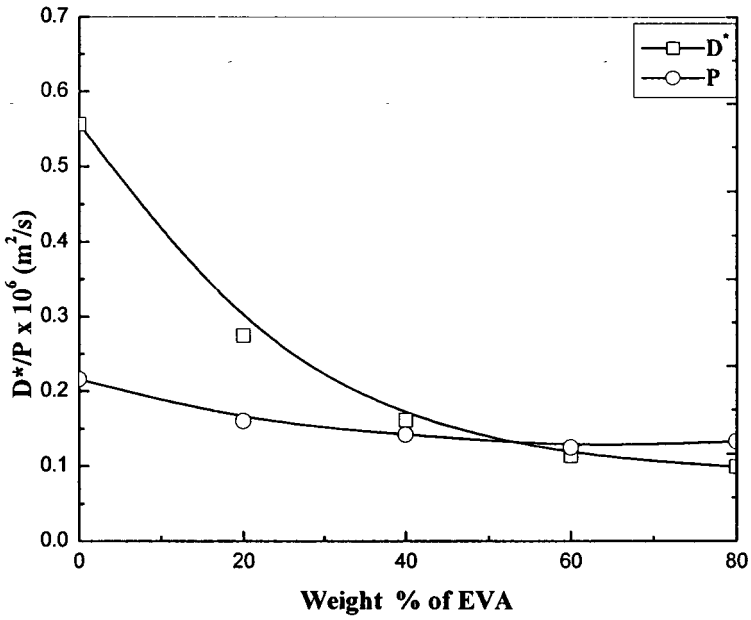

Figure 7. 12 Variation of *D and *P* values with weight % of EVA in kerosene at 26 °C**

7.3 Conclusion

SBR/EVA blends with intermediate superabrasion furnace (ISAF) and those with the same loading of silica (SiO_2) have been prepared and their transport characteristics have been compared. It was found that the ISAF filled samples sorbed lower amount of solvents compared to the silica filled ones except for pure EVA which showed better solvent resistance when loaded with silica. This trend has been attributed to the uniform distribution of the polar silica filler within the polar EVA phase. The difference between the equilibrium sorption values of black and white filler loaded blends decreased with increase in EVA content in the matrix. The swelling coefficient, diffusion coefficient, permeation coefficient, and crosslink density were calculated to support the experimental observations.

References

[1]. J. Crank and G. S. Park, *Diffusion in Polymers*, Academic Press, New York, 1968.

[2]. H. I. Ismail, B.T. I. Poh, K. S. I. Tan and M. I. Moorthy, *Polym. Inl.*, **52**, 685 (2003).

[3]. C. Sirisinha, S. Limcharoen and J. Thunyarittikorn, *J. Appl. Polym. Sci.*, **89**, 1156 (2003).

[4]. X. Sun, G. Zhang, Q. Shi, B. Tang and Z. Wu, *J. Appl. Polym. Sci.*, **86**, 3712 (2002).

[5]. K. K. Hwang, S. H. Ryu and S. Hong, *J. Polym. Sci.*, **86**, 2701 (2002).

[6]. J. A. Manson and L. H. Sperling, *Polymer Blends and Composites*, Plenum Press, New York, 1976.

[7]. I. Pinnau and Z. He, US Pat. 6, 316, 684 (2001).

[8]. T. C. Merkel, B. D. Freeman, R. J. Spontak, Z. He, I. Pinnau, P. Meakin and A. Hill, *J. Mater. Sci.*, **296**, 519 (2002).

[9]. J. L Leblanc, *Prog. Polym. Sci.*, **27**, 627 (2002).

[10]. G. Unnikrishnan and S. Thomas, *Polymer*, **35**, 5504 (1994).

Chapter 8

Transport features of Chitin filled SBR/EVA Blends

Summary

This chapter presents the results of a systematic study on the transport behaviour of SBR/EVA blends filled with a biodegradable filler viz. chitin. Primarily, water absorption of the blends has been analyzed using de-ionized water, as chitin has been reported to be water sensitive. The chitin filled SBR/EVA samples have been found to sorb water, which are otherwise water resistant. The water sorption has been found to be strongly dependent on the EVA content of the samples. A comparison has also been done between the transport features of the penetrants viz. water, pentane, hexane and kerosene through chitin filled SBR/EVA blends.

8.1 Introduction

Chitin is one of the most abundant organic materials in nature. It is generally isolated from crab and shrimp waste. Because of the availability, and many useful properties like biodegradability as well as biocompatibility chitin and its derivatives have been used for a variety of applications [1-10]. The structure of chitin is given in Figure 8.1.

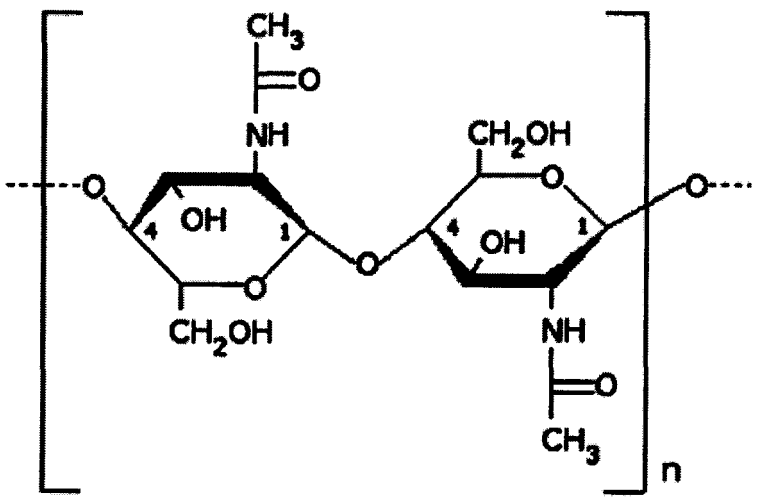

Figure 8.1 Structure of chitin

The reinforcement of polymer matrices with chitin has attracted the attention of researchers over the years. Yang et al. [11] prepared and characterized biocompatible and biodegradable chitin fibre reinforced polycaprolactone (PCL) composite, and studied the rheological and dynamic mechanical characteristics. The results indicated the differences in the rheological behaviour of the composites from that of the polymer matrix alone, attributed to the formation of a particle network. The addition of chitin powder not only increased the storage modulus and dynamic

viscosity, but also shifted the loss peak to a higher frequency. The storage modulus obtained from dynamic mechanic thermal analysis (DMTA) was found to be slightly increased with the filling of the matrix with chitin powder. Li and Feng [12] reinforced porous poly-L-lactic acid (PLLA) scaffold by chitin fibres (CF). To enhance the strength of the scaffold further, they launched a treatment with dicyclohexyl carbodimide (DCC). The results suggested that through the chemical treatment, the CR could reinforce the scaffold much more effectively. Chen et al. [13] prepared poly(ε-caprolactone)/chitin fibre (PCL-CF) composites as potential bone substitutes using a simple melt-processing method. The results from DSC and DMTA proved the strong interaction between PCL and CF. The measurements from DMTA and an advanced rheometric expansion system indicated that both the storage modulus and loss modulus were enhanced by CF. The PCL-CF composite with CF of 45% by mass had the best properties among all the tested composites.

Some interesting studies on the transport behaviour of chitin and its derivative systems can be seen in literature. Typically, the swelling behaviour of chitin reinforced natural rubber nanocomposites was investigated by Kalaprasad and Alain [14]. The composites were processed by different methods and the values of diffusion coefficient, and bound rubber content were evaluated. They proposed the presence of three dimensional chitin networks within the evaporated samples. α-chitin whisker-reinforced poly(vinyl alcohol) (PVA) nanocomposite films were prepared by solution-casting technique by Sriupayo et al. [15]. They found that both the addition of α-chitin whiskers and a heat treatment helped to improve water resistance leading to decreased percentage degree of swelling of the nanocomposite

films. Gravimetric and spetrophotometric studies on the kinetics of water sorption, from air of various water activities, by chitosan of different deacetylation degrees (and molecular weights) and by chitosan/poly(vinyl alcohol) blends were conducted by Mucha et al.[16]. Related analysis showed a clear effect of the degree of deacetylation of chitosan on the water sorption rate. The character of sorption curves, calculated values of diffusion coefficients and micropore volumes had shown that the higher the chitosan deacetylation, the lower the sorption of water vapours. The observed effect was explained in terms of the ordering of molecular chains leading to an increased structural packing in chitosan. They also explained the compatibility of the components in terms of the presence of hydrogen bonds between specific groups (hydroxyl, amide) of chitosan and poly(vinyl alcohol) chains, which caused an increase in molecular packing and thus a decrease of pore volume and a rate of water diffusion. Mucha and Ludwiczak [17] also conducted gravimetric studies on the kinetics of water sorption by chitosan of different deacetylation degrees and chitosan/hydroxypropyl cellulose (HPC) blends. The modification of the chitosan structure was reflected in the sorptive properties of the blends. Assuming a capillary structure for the free volume space of nano size, the total volume of the pores was calculated by them as a function of deacetylation degree of chitosan and weight fraction of HPC in the blends.

The goal of this chapter is to examine the sorption and diffusion characteristics of SBR/EVA/chitin systems. Water has been used as the probe, since chitin is reported to be sensitive to it. The results have been compared with the behaviour of the filled blends with other penetrants such as pentane, hexane and kerosene.

8.2 Results and Discussion

8.2.1 Effect of Chitin on Pure SBR and EVA

Figure 8.1 shows the rheographs of pure SBR and SBR filled with 30 phr of chitin. It has been found that SBR filled with chitin exhibits a higher torque compared to pure SBR. The increase in torque observed in the case of the filled sample is definitely due to the reinforcement of the matrix chitin.

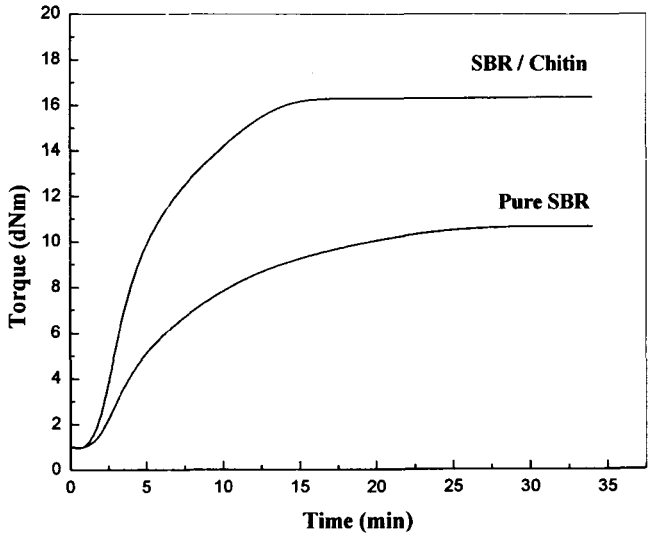

Figure 8.1 Rheographs of SBR and SBR filled with chitin

Similarly Figure 8.2 shows the rheographs of pure EVA and EVA filled with same amount of chitin. The increase in torque observed is a clear evidence for the effective reinforcement of EVA with chitin. It is interesting to note that the change in torque occurred for EVA/chitin system is much higher than that for SBR/chitin system. This shows that chitin gets reinforced into EVA better than SBR.

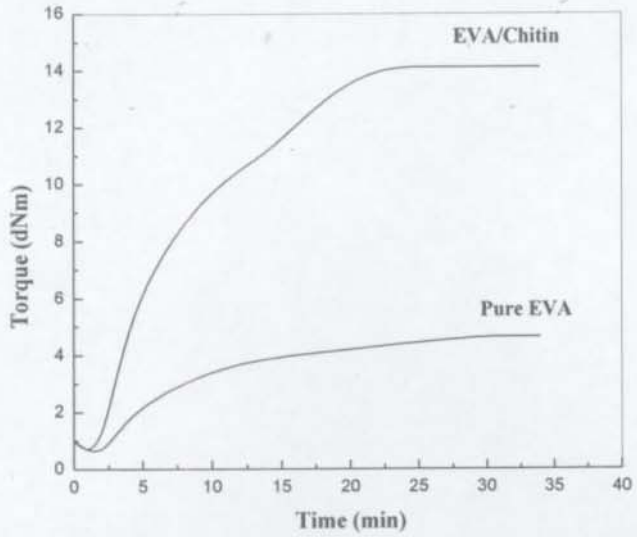

Figure 8.2 Rheographs of EVA and EVA filled with chitin

Figure 8.3 shows the effect of 30 phr of chitin on the water absorption behaviour of pure SBR and EVA. The equilibrium sorption values have been found to be significantly higher for both SBR/chitin and EVA/chitin systems compared to the pure matrices. This is definitely due to the water absorption characteristics of chitin. EVA/chitin system has been found to sorb water more than SBR/chitin system. This is due to the enhanced polar-polar interaction between water and the the matrix loaded with chitin.

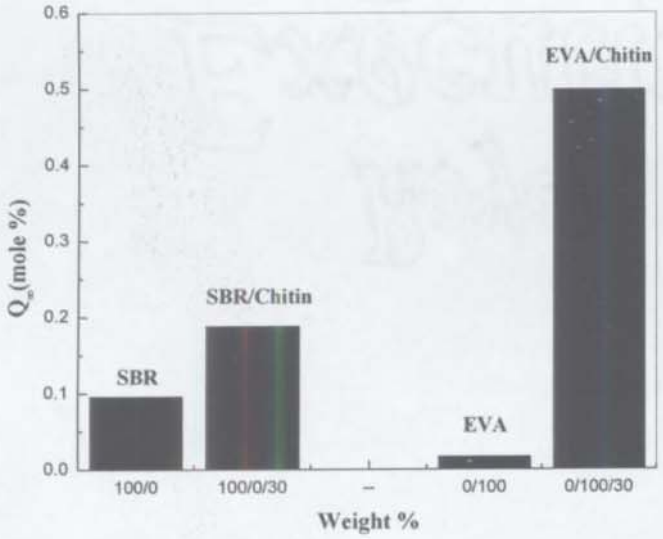

Figure 8.3 Effect of chitin loading on the water sorption of SBR and EVA

Figure 8.4 presents the effect of chitin on the swelling behaviour of pure SBR and EVA when hexane was used as the penetrant. It has been found that the equilibrium uptake of hexane is lower in both the cases, when loaded with chitin. The reduction is more prominent in the SBR/chitin system than in the EVA/chitin system. This is due to the strong nonpolar-nonpolar interaction between the matrix and the penetrant. The same trend has been observed for pentane and kerosene.

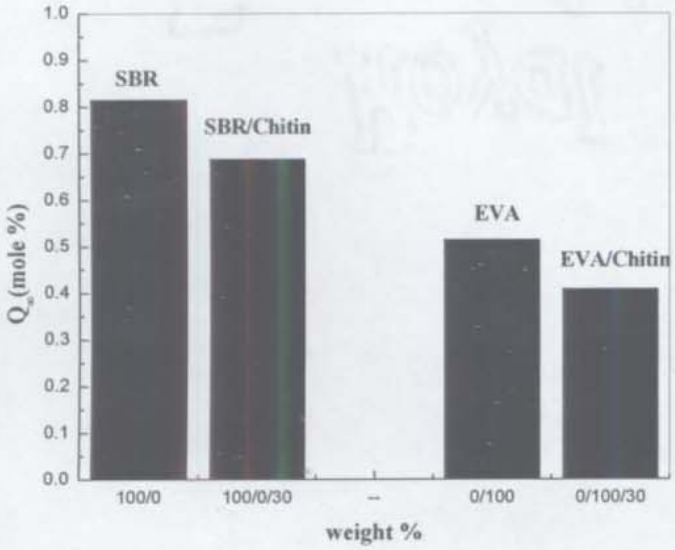

Figure 8.4 Effect of chitin on pure SBR and EVA , in hexane

8.2.2 Effect of Chitin on the Sorption Characteristics of Blends

Figure 8.5 shows the rheographs of un-filled and filled 80/20 SBR/EVA blends vulcanized by DCP. It has been found that the blends loaded with chitin shows a higher M_H value compared to the pure matrix. The increase in the torque observed in the case of filled samples is definitely due to the increased crosslink density which has been attributed to the better reinforcement of the matrix by chitin.

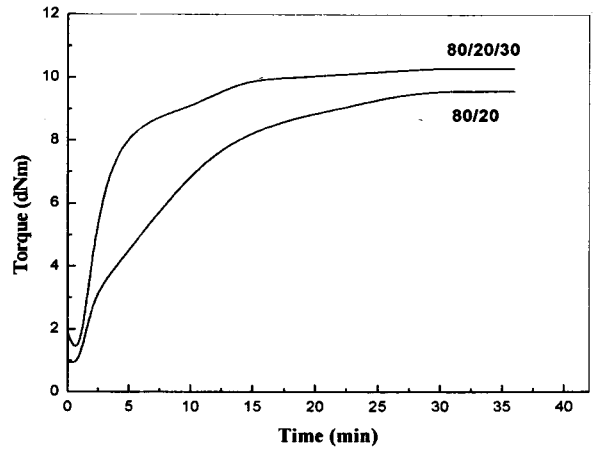

Figure 8.5 Rheographs of 80/20 SBR/EVA blends with and without chitin

Figure 8.6 shows the water sorption characteristics of 80/20 SBR/EVA blend with and without chitin. It is clear that chitin filled blends sorb more water than the unfilled systems. This has been attributed to the strong interaction of SBR/EVA/chitin system with a polar penetrant like water. Figure 8.7 shows the sorption curves of the 80/20 blend with and without chitin, in hexane. It is seen that the equilibrium solvent uptake is decreased for a non-polar solvent like hexane. Similar trend has been observed when pentane and diesel were used as penetrants.

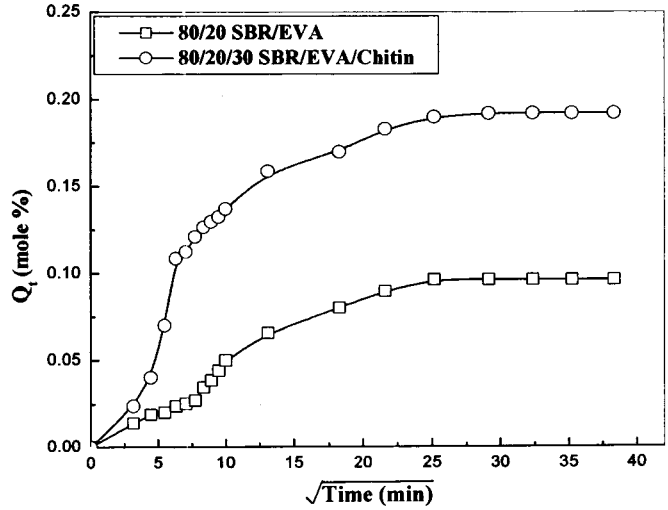

Figure 8.6 Water sorption curves of filled and unfilled 80/20 SBR/EVA blends

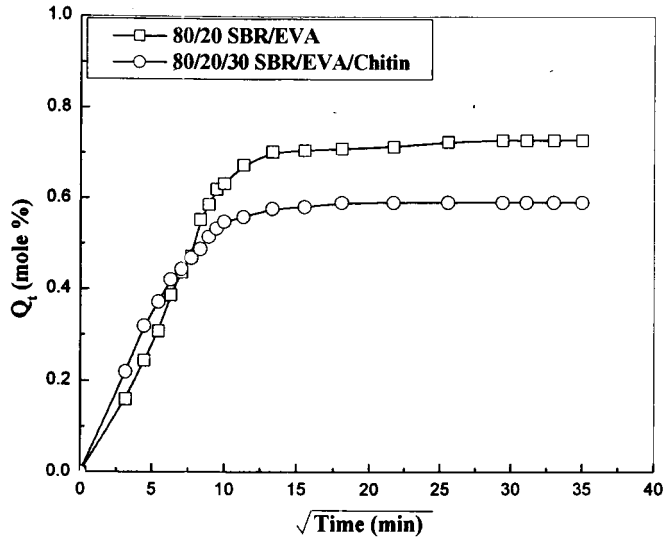

Figure 8.7 Sorption curves of filled and unfilled 80/20 SBR/EVA blends, in hexane

8.2.3 Surface Morphology of Chitin filled SBR/EVA Blends

The morphology of the blend samples loaded with chitin and without chitin was examined by using scanning electron microscopy. Figures 8.8 (a) and (b) show the SEM of 40/60 SBR/EVA and 40/60/30 SBR/EVA/chitin system respectively. The surface of the loaded sample appeares to be rougher due to the irregular distribution of the chitin wisker in the matrix. The random distribution of the chitin whisker makes the matrix harder and this change in the morphology has been highly reflected in the sorption curve of filled 100/0/30 SBR/EVA system (Figure 8.10).

8.8 (a)

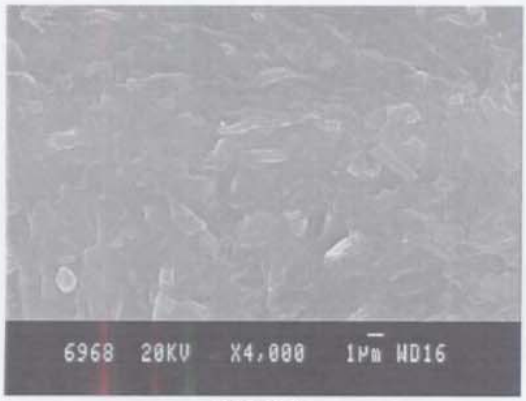

8.8 (b)

Figure 8.8 SEM of (a) 40/60 SBR/EVA
(b) 40/60/30 SBR/EVA/chitin

8.2.4 Effect of EVA on the Sorption Feature of SBR/EVA/chitin Blends

Figure 8.9 shows the sorption features of SBR/EVA/chitin systems, as a function of EVA content, with water as the penetrant. It has been found that water uptake increases as EVA content in the matrix increases. On the other hand, the hexane uptake decreases with increase in EVA content, as shown in Figure 8.10. The observed difference in the sorption behaviour can be explained in terms of the polarity of the penetrants used. Since water is polar, its interaction with the matrix increases with increase in EVA, which is also polar. Consequently water sorption is increased with EVA content in the blends. Hexane, being non-polar, the penetrant-

matrix interaction decreases with increase in EVA content. The same trend has been observed when pentane was used as penetrant.

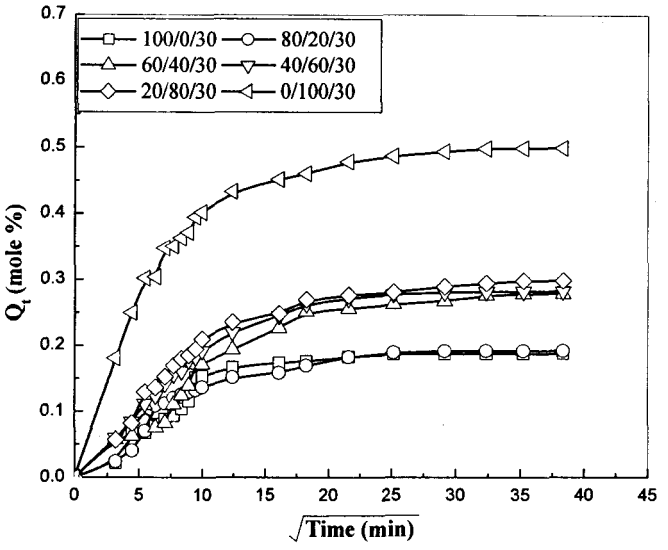

Figure 8.9 Water sorption curves of chitin filled SBR/EVA blends

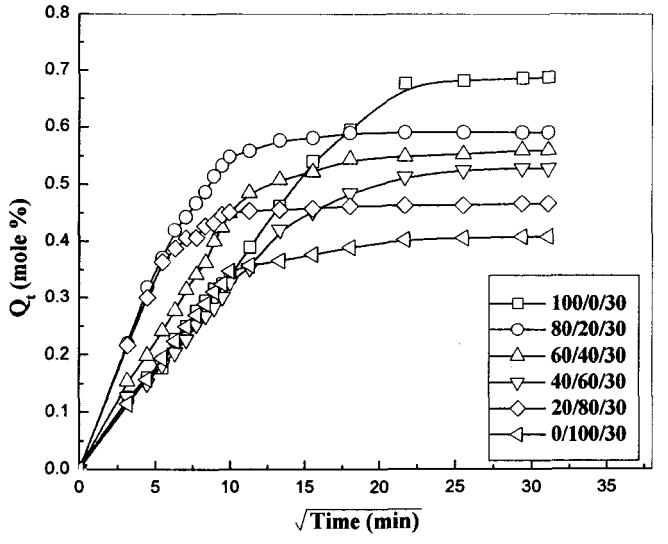

Figure 8.10 Hexane sorption curves of chitin filled SBR/EVA blends

8.2.5 Effect of Chitin Loading

To evaluate the effect of chitin loading on the solvent uptake behaviour, the SBR/EVA blends have been loaded with different amounts viz. 10, 20 and 30 phr of chitin. Figure 8.11 shows the equilibrium uptake of 20/80 SBR/EVA loaded with

different amounts of chitin for de-ionized water and hexane. The water uptake has been found to be increased, while the hexane uptake to be decreased with chitin loading.

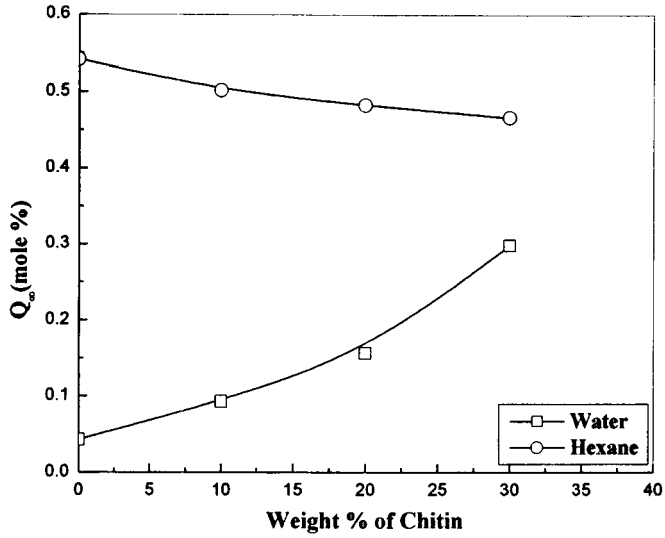

Figure 8.11 Equilibrium uptake of 20/80 SBR/EVA loaded with 10, 20 and 30 phr of chitin for de-ionized water and hexane

8.2.6 Comparison between Chitin and Carbon Black Loading

Figure 8.12 gives a comparison between the effect of chitin and one of the carbon blacks, viz. semi reinforcing furnace (SRF) black on the sorption behaviour of SBR/EVA blends, with kerosene as the penetrant. Both the fillers restrict the solvent inhibition. However, it has been found that kerosene uptake is comparatively higher when the blend is loaded with chitin, than with SRF. This trend is attributed to the difference in the sizes of the fillers used. Figure 8.13 shows a comparison of the water sorption behaviour of 40/60 SBR/EVA blends filled with chitin and SRF black. In this case also, it has been found that the equilibrium uptake is higher for the blend filled with chitin than with SRF. The huge difference in the sorption uptake, nearly about ten times, accounts for the formation of the hydrogen bonds between chtin and water [18].

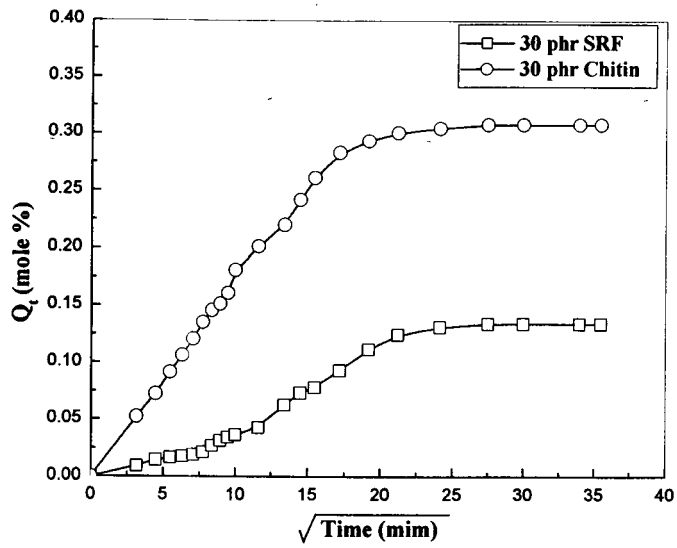

Figure 8.12 Sorption curves of 40/60 SBR/EVA loaded with 30 phr of chitin and SRF in kerosene

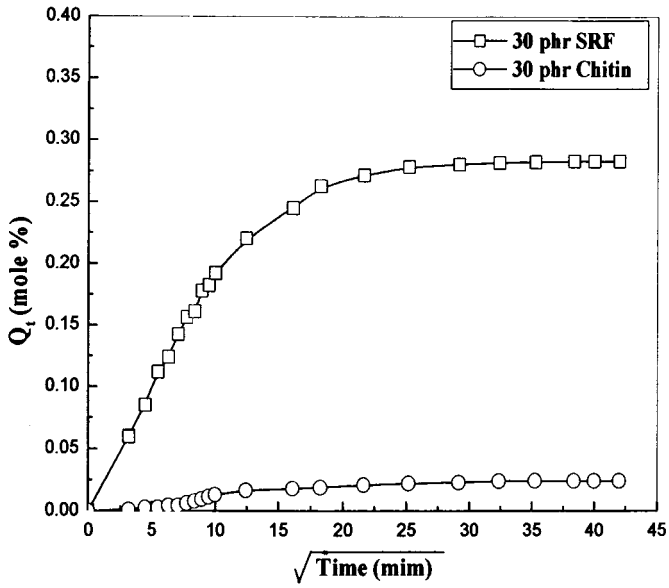

Figure 8.13 Mole % uptake of 40/60 SBR/EVA loaded with 30 phr of chitin and SRF in water

8.2.7 Modelling

The effect of filler loading has a crucial effect on the diffusion coefficient. This can be analyzed theoretically by assuming that each filler particle behaves as an

obstacle to the diffusing molecule. By analogy to electrical conductivity using the Maxwell model, the effective diffusion coefficient can be estimated as [19]:

$$D_{im} = D_{ip} \frac{2-2F+(1+2F)\frac{D_{if}/D_{ip}}{}}{2+F+(1-F)\frac{D_{if}/D_{ip}}{}} \quad \text{.....8.1}$$

where F is volume fraction of the filler, and D_{if} and D_{ip} are the diffusion coefficients of the particle and the filler respectively. For very small values of F, as in the present situation and with the limit that D_{if}/D_{ip} is very small, the equation 8.1 can be approximated as [20]:

$$D_{im} = D_{ip} \frac{2-2F}{2+F} \quad \text{.....8.2}$$

where $D_{i,m}$ is diffusivity of a substance i in a filled polymer membrane and $D_{i,p}$ is the diffusivity of a molecule i in the unfilled polymer.

La Pack et al. [21] proposed the following equation to study the effect of fillers on the permeability of different membranes, which relates the diffusivity of a filled membrane to an unfilled one as:

$$D_{im} = \frac{D_{ip}}{(1+F/2)} \quad \text{.....8.3}$$

Figure 8.14 shows a comparison between the experimental values and Maxwell and La Pack models for chitin filled SBR/EVA blends. It has been found that the experimental values are very close to those predicted by La Pack model. This shows that La Pack model is reliable to describe SBR/EVA/chitin and similar filler loaded systems.

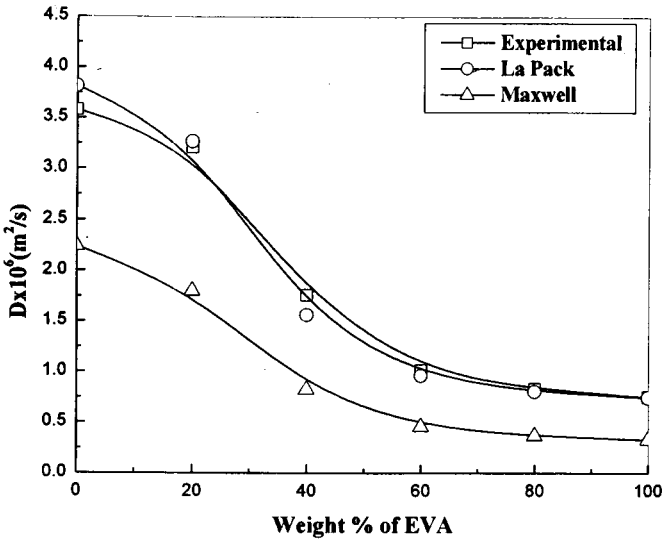

Figure 8.13 Comparison between experimental values and Maxwell and La Pack models for chitin filled SBR/EVA blends.

8.3 Conclusion

The effect of a biodegradable filler viz. chitin on the sorption characteristics of SBR/EVA blends was examined. De-ionized water was used as the probe. It has been found that with chitin loading water sorption was increased in all the blend samples and increased with EVA content in the blends. A reverse trend has been observed when the results were compared with those using non-polar solvents like *n*-pentane, *n*-hexane and kerosene. The sorption behaviour of chitin loaded blends was also compared with that with SRF black using de-ionized water and non-polar solvents. It has been found that chitin loaded samples sorbed higher amount of the penetrants. This trend has been attributed to the size and nature of the fillers used. The computed diffusion coefficient values were compared to theoretical models. It has been found that the experimental values are very close to the La Pack model.

References

[1]. R. A. A. Muzzarelli, *Ploymeric Biomaterials*, S. Dumitriu, Ed: Marcel Dekkar, New York, 1994.

[2]. J. Xu, S. P. McCarthy and R. A. Gross, *Macromol.*, **29**, 3436 (1996).

[3]. K. Kurita, T. Sannan and Y. Iwakura, *J. Appl. Polym. Sci.*, **23**,511 (1979).

[4] A. C. A. Wan, E. Khor and G.W. Hastings, *J. Biomed. Mater. Res.*, **41**, 541 (1998).

[5]. T. Mori, Y. Irie, S. I. Nishimura, S. Tokura, M. Matsuura, M. Okumura, T. Kadosawa and T. Fujinaga, *J. Biomed. Mater. Res.*, **43**, 469 (1998).

[6]. S. Minami, Y. Okamoto and K. Miyatake, *Carbohydr. Polym.*, **29**, 295 (1996).

[7]. L. Y. Chung, R. J. Schmidt, P. F. Hamlyn, B. F. Sagar, A. M. Andrews, and T. D. Turner, *J. Biomed. Mater. Res.*, **28**, 463 (1994).

[8]. H. Yano, K. Iriyama, H. Nishiwaki and K. Kifune, *Mie. Med. J.*, **35**, 53 (1985).

[9]. Y. Okamoto, K. Shibazaki, S. Minami, S. Matsuhashi, S. I. Tanioka and Y. Shigemasa, *J. Vet. Med. Sci.*, **57**, 851 (1995).

[10]. Y. W. Cho, Y. N. Cho, S. H. Chung, G. Yoo, S.W. Ko, *Biomaterials*, **20**, 2139 (1999).

[11]. A. Yang, K. Sun and R. Wu, *International SAMPE Symposium and Exhibition (Proceedings)*, **45**, 427 (2000).

[12]. X. Li and Q. Feng, *Polym. Bull.*, **54**, 47 (2005).

[13]. B. Chen, K. Sun and T. Ren, *Eur. Polym. J.*, **41**, 453 (2005).

[14]. G. N. Kalaprasad and D. Alain, *Biomacromolecules*, **4**, 657 (2003).

[15] J. Sriupayo, P. Supaphol, J. Blackwell and R. Rujiravanit, *Polymer*, **46**, 5637 (2005).

[16]. M. Mucha, S.Ludwiczak and M. Kawinska, *Carbohydr. Polym.*, **62**, 42 (2005).

[17]. M. Mucha, and S. Ludwiczak, *Mol. Cryst. Liq. Cryst.*, **448**, 133 (2006).

[18]. Y. W. Cho, J. Jang, C. R. Park and S. W. Ko, *Biomacromolecules*, **1**, 609 (2000).

[19]. G. J. Van Amerongen, *Rubber Chem. Technol.*, **37**, 1065 (1965).

[20]. M. Ouddane, and R. Boukhili, *Polym. Compos.*, **19**, 680 (1998).

[21]. M. A. La Pack, J. C. Tou, L. Mc Guffin and C. G. Enke, *J. Membr. Sci.*, **86**, 263 (1964).

Chapter 9

Conclusion and Future Outlook

Summary

The major findings of the present investigation and the scope of the future work based on SBR/EVA blends have been presented in this chapter.

9.1 Conclusion

The transport characteristics of macromolecular networks have been the object of active research for the past several years. This thesis presents the results of a systematic investigation on the transport characteristics of styrene butadiene rubber/ poly(ethylene-*co*-vinyl acetate (SBR/EVA) blends. Three sets of penetrants viz. aliphatic, chlorinated and aromatic hydrocarbons were mainly used as the probes for the sorption and diffusion studies. The blends were cured with three different vulcanizing systems viz. sulphur, dicumyl peroxide (DCP), and a mixed system consisting of sulphur and DCP. The results have been explained in terms of different kinetic and sorption parameters.

The transport behaviour of aliphatic hydrocarbons viz. *n*-pentane, *n*-hexane, *n*-heptane and *n*-octane through SBR/EVA blends in the temperature range of 26-56 °C has been studied. It was found that the EVA content in the blends effectively reduced the solvent uptake. This has been attributed to the semi-crystalline nature of EVA. The blends exhibited higher sorption values with octane compared to the other penetrants; attributed to the closer solubility parameter values. The transport process was also evaluated in terms of the blend-solvent interaction parameter. The mechanism of transport has been found to deviate from the normal Fickian behaviour observed for conventional elastomers. The diffusion coefficient values decreased with increase in EVA content in the blends. The molecular mass between crosslinks has been found to decrease with increase in EVA content in the samples, complementing the solvent uptake behaviour.

The examination of the interaction of crosslinked SBR/EVA blends with chlorinated hydrocarbons has been done in the next step of the investigation. The effects of blend composition, crosslink systems, penetrant size and temperature on the solvent transport were analysed. Among the samples crosslinked by different modes, the DCP systems showed the lowest equilibrium uptake in all penetrants compared to the other samples. This has been explained in terms of the differences in the nature and distribution of crosslinks in the network. Among the three penetrants viz. dichloromethane, chloroform and carbon tetrachloride, chloroform showed the highest Q_∞ values with the blends. This has been explained in terms of the differences in the solubility parameter values and the polarity of the solvents. A sorption (S) - desorption (DS) - resorption (RS) - redesorption (RD) technique was also carried out to check the changes in the mechanism of transport after a sorption-desorption cycle. The tensile behaviour of the samples revealed that the stress required to break the samples increased with increase in EVA content. In the case of the swollen samples, the modulus, strength and elongation were considerably lower due to the solvent molecules distributed within the matrix. There was an overall decrease in the stress, strain and elongation at break values for the blends after a sorption-desorption cycle.

SBR/EVA samples were compatibilized with a physical compatibilizer dichlorocarbene modified SBR (DCSBR). The effect of the compatibilizer on the sorption behaviour was studied using aromatic hydrocarbons. The addition of 6 phr DCSBR in the blend resulted in a significant increase in the interfacial crosslinks as evident by the values of maximum torque and crosslink densities. A decrease in solvent uptake was observed for compatibilized blends and this reduction was more

prominent in 6 phr compatibilizer loaded samples. The compatibilization has been found to be accompanied by an improvement in the mechanical properties which depended upon blend ratio and compatibilizer loading. The diffusion process was found to follow the first order kinetic equation.

Since carbon black is extensively used for rubber reinforcement in industry, the influence of carbon black particles of different sizes on the transport characteristics of SBR/EVA has been systematically analysed using petrol, kerosene and diesel. Among the carbon black filler loaded systems used, the solvent uptake tendency followed the order: SRF> HAF> ISAF. The reason for this trend has been attributed to the increased restriction to the overall chain mobility and the flexibility of the polymeric chains with the decrease in the size of carbon black particles. Among the penetrants, the solvent uptake trend followed the order: petrol> kerosene > diesel, for a given blend ratio according to the reverse trend of their molecular weight.

The liquid sorption behaviour of SBR/EVA blends loaded with carbon black (ISAF) and those with silica (Ultrasil VN3) of same loading has been compared. The black incorporated blends sorbed lesser amount of solvents compared to those with silica, particularly when SBR was the continuous phase. This has been explained in terms of the better reinforcement of carbon black in the continuous SBR phase. However, the difference between the equilibrium sorption values exhibited by black filled and silica filled samples decreased with increase in EVA content in the blends. This trend has been explained on the basis of the better filler-matrix interaction due to the different polar groups such as siloxane and silanol on the surface of silica particles.

The sorption and diffusion of SBR/EVA blends loaded with a biodegradable filler viz. chitin whisker has also been examined. Primarily de-ionized water was used as the probe, since chitin has been reported to be water sensitive. The results have been compared with the swelling behaviour of the filled blends with non-polar penetrants such as *n*-pentane, *n*-hexane and kerosene. An increase in the equilibrium water absorption was observed in the case of filled blends compared to the unfilled ones which increased regularly with the EVA content in the matrices. This trend has been explained on the basis of the higher polar-polar interaction between the solvent and the matrices. However, the filled samples sorbed lesser amount of non-polar solvents compared to the unfilled ones. The computed diffusion coefficient values have been found to be closer to the values predicted by La Pack model.

9.2 Future Outlook

The work so far completed based on SBR/EVA blends offers many interesting extensions.

9.2.1 Effect of New Compatibilizers

Dichlorocarbene modified styrene butadiene rubber (DCSBR) has been used as a compatibilizer in this work. The effects of new physical and chemical compatibilizers on the transport behaviour of SBR/EVA blends can be investigated in future.

9.2.2 New Fillers

Fillers generally reduce the equilibrium solvent uptake, increase the mechanical properties and minimize the cost of production of composite system. It will be exciting to examine the effect of various fibrous and nano fillers on the physical properties of SBR/EVA blends. Hybrid filler incorporation is another interesting possibility.

9.2.3 Development of Membranes

The development of membranes from elastomeric systems for the separation of different liquids and gaseous mixtures has tremendous potential in many application fields. This technology could revolutionize the biochemical, pharmaceutical and other chemical industries. It is worth attempting to develop thin membranes from SBR/EVA and to examine their efficiency for the separation of many industrially important liquid and gaseous mixtures, particularly by using the pervaporation technique.

9.2.4 Controlled Drug Delivery

The capability of small molecules to diffuse through SBR/EVA blends can make it useful in controlled drug delivery. An investigation into the efficiency of SBR/EVA blends for their applications in drug delivery can be done in future.